CR 151256

51SX

FINAL REPORT

APOLLO SERVICE PROPULSION SYSTEM ROCKET ENGINE OPTIMIZED SPS INJECTOR DEVELOPMENT AND VERIFICATION PROGRAM

Prepared Under
Contract NAS 9-8285

for

Manned Spacecraft Center
National Aeronautics and Space Administration
Houston, Texas

Report NASA 108581 March 1971

MSC-14076

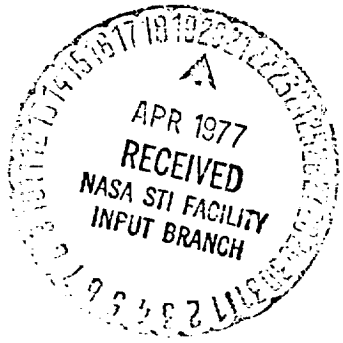

AEROJET LIQUID ROCKET COMPANY
A DIVISION OF AEROJET-GENERAL
SACRAMENTO, CALIFORNIA

AL 33X

Report NASA 108581

Final Report

Apollo Service Propulsion System Rocket Engine
Optimized SPS Injector
Development and Verification Program

Prepared Under

Contract NAS 9-8285

For

Manned Spacecraft Center
National Aeronautics and Space Administration
Houston, Texas

AEROJET LIQUID ROCKET COMPANY
A Division of Aerojet-General Corporation
Sacramento, California

Report NASA 108581

TABLE OF CONTENTS

		Page
I.	Foreword	1
II.	Introduction	2
III.	Summary	3
IV.	Work Accomplished	8
	A. Storable Propellants	8
	1. Program	8
	2. Single Element Tests	9
	3. Injector SN 149	11
	4. Injector SN 135	12
	a. Test	13
	b. Problem Areas	14
	(1) Intermediate-Frequency Combustion Instability	14
	(2) High-Frequency Combustion Instability	16
	(3) Popping	18
	5. Fabrication	21
	6. Conclusions and Recommendations	23
	B. Cryogenic Propellants	26
	1. Program	26
	2. Injector	28
	a. Tradeoff Studies	28
	b. Design	30
	c. Fabrication	32
	d. Test	33
	3. Chamber	40
	a. Criteria	40
	b. Design	41
	c. Fabrication	42
	d. Test	46
	4. Conclusions and Recommendations	58
Appendix A	OMS Injector Development Test Procedure	

FIGURE LIST

	Figure
Plate 1XB, ΔP = 30 psi	1
Injector Element Test Program Plate or Element Identification	2
Injector Element Test Fixture Schematic	3
Plates 1XB and 2X	4
Plates 5XB and 6R	5
Design Rationale	6
Instrumentation Location Schematic	7
Engine Instrumentation Requirements	8
Injector Thermocouple Locations, IOS TCA Test	9
Workhorse Thrust Chamber	10
IOS Full-Scale Injector Test Summary	11
IOS Injector	12
SPS MOD IV Injector	13
Workhorse Resonator, Design A	14
Proposed and Slotted Workhorse Resonator	15
Nominal Operating Conditions - Without Resonator	16
Nominal Operating Conditions - With Resonator	17
Low P_c - Low MR - With Resonator	18
Low P_c - Nominal MR - With Resonator	19
Effect of Element Spacing on Blastwave Coupling	20
Mach 1 Radii Layout - IOS Injector	21
Plugged Orifices within Injector Hub	22
Injector Face with Plugged Orifices	23
Tube Injector	24
Coaxial Injector	25
Injector Design Information	26
Injector Face after Element Braze	27
Injector Backside after Element Braze	28
Injector Oxidizer Manifold with Elements	29
Elements Installed and Elements Staked	30

FIGURE LIST (cont.)

	Figure
Coaxial Injector Element Side	31
Coaxial Injector Element End	32
Coaxial Injector Element After Braze	33
Normalized Fuel Distribution	34
Normalized Oxidizer Distribution	35
Mixture Ratio Distribution	36
ERE Derivation	37
Test Stand	38
Workhorse Thrust Chamber Assembly	39
Igniter	40
Igniter Schematic	41
Injector Test Summary	42
Injector Face Prefire 2K-2-108	43
Injector Face Postfire 2K-2-108	44
Close-up of Injector Face Postfire 2K-2-108	45
Oscillograph Record Test 115	46
Copper Thrust Chamber	47
Inside Contour Machining	48
Coolant Passage Machining	49
Chamber after Machining	50
Braze Samples	51
Outlet Manifold	52
Inlet Manifold Machining	53
OME Thrust Chamber Cold Flow Test	54
Results of OME Combustion Chamber Gas Flow Tests	55
Combustion Chamber with Manifolds Brazed in Position	56
Combustion Chamber After Wire Wrap	57
TCA Instrumentation Location	58
TCA Instrumentation	59

FIGURE LIST (cont.)

	Figure
OME TCA on Test Stand	60
OME TCA on Test Stand	61
OME TCA on Test Stand	62
OMS TCA Post Fire	63
OMS TCA Post Fire	64
OMS TCA Post Fire	65
Oscillograph Record of Test 5K-3-102	66
Test 5K-3-103 Chamber Wall Temperature vs Time (Forward Section)	67
Test 5K-3-103 Chamber Wall Temperature vs Time (Center Section)	68
Test 5K-3-103 Chamber Wall Temperature vs Time (Aft Section)	69
OMS Cooled Chamber Performance Summary	70
OMS Cooled Chamber Data Summary	71
Summary of Tests with Regeneratively Cooled Combustion Chamber	72

I. FOREWORD

This is the final report of the Optimized Service Propulsion System Injector Development and Verification Program sponsored by the National Aeronautics and Space Administration, Manned Spacecraft Center. It is submitted in accordance with Appendix I in partial fulfillment of Contract NAS 9-8285. This report summarizes all of the work accomplished under this contract. Primary emphasis has been placed upon Phase II of the Program which included all work with cryogenic propellants. A more detailed description of the work accomplished during Phase I of the Program with storable propellants may be found in Phase I Interim Report No. 8285-P1 of June 1970.

The program was administered from the ALRC Apollo Department under the direction of C. E. Teague.

II. INTRODUCTION

Contract NAS 9-8285 started in July 1968 as an uninterrupted follow-on to Contract NAS 9-6925. The basic program objective of these contracts was to improve the performance of the Service Propulsion System (SPS) injector.

The program progressed to a point at which all the purely technical objectives were realized when the success of the Apollo flights made it apparent that the replacement of the SPS injector was becoming increasingly remote. Consequently, it was decided to direct the remainder of the contract to a technology-type effort with oxygen and hydrogen propellants.

Phase II, the oxygen-hydrogen portion of the contract, started in January 1970 and was extended to the end of the contract in March 1971. Approximately 25% of the program funding was expended during Phase II.

One injector and one regeneratively cooled combustion chamber were designed, fabricated, and tested during Phase II.

III. SUMMARY

The initial program plan of Contract NAS 9-8285 divided the work to be accomplished into two phases. Phase I was to be a development type of effort, and Phase II was to verify the results of Phase I.

The scope of Phase I included a continuation of testing with injector SN 135, available from a previous NASA sponsored contract, as well as the design, fabrication and testing of one additional injector. During Phase II another injector, incorporating the most desirable features of the injectors developed in Phase I, would be fabricated and subjected to pre-qualification type testing. A limited number of single-element tests were also scheduled for Phase I.

The design of the additional injector was started shortly after the start of the program. The pattern of the injector designated POUL 41-63, had a coarser matrix than the SN 135 pattern; however, the contoured orifices were maintained. This design was reviewed at NASA/MSC on 31 October 1968 and fabrication was initiated immediately thereafter.

The single-element portion of the program was also started immediately. This program consisted of numerous cold flow tests of single-orifice elements. The test series was completed in April 1969 with the conclusion that manufacturing anomalies with contoured inlets exercised little effect on the effluent stream discharge coefficient although they did affect the nature of the stream. Additionally, contouring from the face side of the injector was feasible but required considerable additional effort to develop an acceptable production technique.

At approximately the same time, all work on the second injector was placed on hold because recent information made it appear probable that this pattern would "pop" (spontaneous combustion chamber pressure perturbations). Consequently, the major emphasis was placed upon the continued development of injector SN 135.

III, Summary (cont.)

The three problems affecting injector SN 135 were intermediate frequency combustion instability at the low chamber pressure limit, dynamic (i.e., pulse charge initiated) high-frequency combustion instability, and pops.

A series of injector test firings with the first modifications of injector SN 135 were disappointing because there was no improvement in either the intermediate frequency instability problem or in the popping problem; however, during May and June 1969, tests with injector SN 135 and an uncooled acoustic resonator were encouraging because there was a marked improvement in the high-frequency combustion instability with recovery from pulse charges demonstrated for all conditions except helium-conditioned propellants.

Despite the encouraging results obtained with the multiorifice resonator and also with an ablative combustion chamber, the intermediate combustion frequency instability and the pops were still present.

At this time, it was decided to modify the injector pattern in accordance with the results of the pop investigation study. Test results were extremely encouraging because both the pops and the intermediate frequency stability were eliminated.

Consequently, the only task remaining was the elimination of the pulse-charge-initiated, high-frequency instability which occurred with the use of propellant conditioned with helium. Based upon tests with the multiorifice acoustic resonator, it was calculated that this task could be accomplished by increasing the resonator volume by approximately 20%.

In summary, the purely technical objectives of the program were realized and the remaining task, consisting of the design and fabrication of an injector with an integral resonator having the increased volume, presented a challenge with respect to the perfection of fabrication techniques but would not contribute to the technical state of the art.

III, Summary (cont.)

The technical status, as described above, when considered in conjunction with increasingly remote possibility of a new SPS injector design being incorporated in the engine, led to the conclusion that it would be more beneficial to expend the funds remaining under the contract on a technology-type effort directed toward the use of oxygen and hydrogen. All work with storable propellants was terminated at this time.

The program for Phase II was designed to remain within the existing fiscal limitations and to make maximum utilization of other related technology programs at Aerojet. The plan called for a tradeoff study to define the configuration of the first test injector. The selected injector and an uncooled heat sink chamber would then be committed to fabrication and test. The test results were then to be compared with those obtained from similar tests with other injectors at AGC and a final design selection made. This design would then be fabricated and delivered to NASA. In addition, the design of a water-cooled chamber would be delivered to NASA at this time.

Work on Phase II started in February 1970 with a series of injector tradeoff studies. These studies were based upon nominal operating conditions of 500 psia chamber pressure, 5000 lb thrust and mixture ratio of 6.0:1 O/F.

The results of the tradeoff studies indicated that three concepts showed the most promise for this application. These were the platelet, the micro-coaxial or swirl cup, and the conventional coaxial. Because the two former concepts were already being tested at ALRC, it was decided that the first injector fabricated under this program should be a coaxial design using gaseous propellants.

The injector consisted of 74 coaxial elements (68 lb of thrust per element) feeding through a rigimesh face plate.

III, Summary (cont.)

Twenty-three injector test firings were conducted in July 1970. The tests demonstrated that a combustion chamber length of 8 in. (16 in. L*) was required to assure stable combustion. Other characteristics were high performance (99% of ERE) stable operation over a mixture ratio range of from 5 to 7, at chamber pressures over a range of 300 to 700 psia and recovery from pulse induced over pressures of 1000 psi in 0.006 sec. Compatibility indications were promising although firing durations were limited to 0.5 sec due to the uncooled copper combustion chamber.

In early August 1970, the program was re-evaluated and it was decided to place emphasis upon the development of a hydrogen-cooled combustion chamber instead of an additional injector as had been originally planned. This change of plans was implemented because the success of the injector made additional injector development unnecessary at that time.

Several manufacturing techniques and two materials were considered before making the final combustion chamber design selection. The final selection for this particular application was a chamber with single pass longitudinal cooling passages milled in an OFHC copper shell. The passages were closed by furnace brazed square copper wire covers. Hoop strength was provided by a Hastelloy X square wire overwrap.

Fabrication was completed in early January 1971. The first tests were on 3 March 1971. Propellant inlet temperature was maintained at approximately 200°R which was representative of the temperature which could be expected at an expansion ratio of 6:1 (the inlet of the chamber being evaluated) because on a flight unit the propellants would be introduced at an expansion ratio of 20:1. Results of the tests showed gas side wall temperatures of approximately 400 and 500°F for the throat and injector, respectively. These values would normally be considered entirely acceptable. However, they may be marginal with respect to

III, Summary (cont.)

the life cycle criterion of 10,000 cycles. Consequently, it is recommended that additional testing be conducted to obtain empirical data on this parameter.

All testing was terminated during the second week of March 1971 and inventory contract closeout procedures were initiated immediately thereafter.

IV. WORK ACCOMPLISHED

A. STORABLE PROPELLANTS

1. Program

The work accomplished during the storable propellant phase of the contract was a continuation of work originally started under Contract NAS 9-6925. The objective of this contract was to improve the performance of the Apollo SPS injector through a better understanding of the mechanics of short tube flow.

A comprehensive test program was conducted with orifice test plates or elements to evaluate flow characteristics. These tests demonstrated that orifices with contoured inlets had more repeatable flow characteristics than those formed by conventional drilling. The test results also supported an extensive analytical effort which resulted in the deviation of expressions defining orifice flow with respect to injector inlet conditions including angle and manifold cross velocity.

The knowledge gained from the orifice flow portion of the contract was then extended to the design of an Apollo SPS size injector designated SN 135. The injector was designed to be physically and functionally interchangeable with the production injector, the primary difference being that SN 135 had a finer pattern and contoured inlet orifices.

Test firings with SN 135 demonstrated improved performance and good compatibility; however, the injector was not dynamically stable.

The experience gained on Contract NAS 9-6925 with injector SN 135 formed the baseline for contract NAS 9-8285. The various program elements were all interrelated and were conducted concurrently; however, for the purpose of clarity, each of the elements is reported as a separate entity in this report.

IV, A, Storable Propellants (cont.)

2. Single Element Tests

The work with single-orifice elements of the type shown in Figure 1 had two primary objectives: (1) to investigate the effects of the orifice surface on hydraulic flow, and (2) to establish the feasibility of manufacturing an injector with contoured orifice inlets by an etching.

The knowledge from these tests was applicable to injector design in two ways: (1) the results of the surface effect evaluation would be used as a basis for deciding if the development of a more sophisticated method of orifice fabrication was warranted, and (2) the development of an efficient method of contouring injector orifice inlets from the outlet side would overcome two of the major disadvantages of this type of orifice, i.e., the loss of the capability to make pattern modifications subsequent to manifold welding, and the common oxidizer and fuel manifold welds which result if contouring is accomplished by machining from the back.

These test conditions were orifice length-to-diameter ratio 3, common orifice diameter (0.0512 in.), orifice axis perpendicular to axis of supply manifold, and no manifold cross velocity other than the velocity incident to the flow through the orifice. Test data included photographs of the orifice and of the effluent stream and plots of the discharge coefficient for various pressure differentials. The various configurations tested are listed in Figure 2.

a. Test Setup

The single-element tests were conducted on the same setup that had been used on the preceding program (NAS 9-6925). The test fixture was designed and fabricated to accommodate interchangeable orifice plates and to allow for testing under a wide variety of conditions. Figure 3 gives a schematic

IV, A, Storable Propellants (cont.)

representation of the test fixture, whose design criteria included visibility of the effluent flow stream, easy interchangeability of orifice plates, propellant compatibility, and a design pressure capability of 500 psi, except for window strength.

b. Tests

(1) Manufacturing Extremes on Contoured Inlets

Tests were conducted on a contoured orifice in which the entrance contour was purposely scored. This entrance (plate IXB) compared with a smooth entrance (plate 2X) is shown in Figure 4.

Results indicated that variations of the type to be expected from normal machining processes will exert a minor influence as long as sufficient back pressure is maintained to prevent cavitation (back pressure equal to or greater than the sum of the vapor pressure of the flow medium and the pressure differential across the orifice).

(2) Manufacturing Extremes on Sharp-Edged Inlets

Similar results were obtained with sharp-edged orifices with respect to the coefficient of discharge; however, there is a marked difference in the character of the effluent streams. A perfect sharp-edged orifice has a well defined stream and a burred orifice a pronounced bushiness. Plates 5XB and 6R (Figure 5) represent the manufacturing extremes.

IV, A, Storable Propellants (cont.)

One plate was manufactured by drilling, plugging the outlet with wax, and then etching the inlet for approximately 3 hr. This process resulted in a tapered orifice having an inlet of 0.0586 in. and an outlet of 0.0524 in. The results closely approximated those of the machined orifice and it appears feasible to obtain flow characteristics that are approximately those of a machine-contoured orifice by etching. Two major problems must be resolved before it would be advisable to apply this technique to an injector. These are repeatability, and the tendency of the etchant to enlarge small imperfections within the propellant passages.

3. Injector SN 149 (Pattern POUL 41-63)

a. Design

Work on the design of an entirely new injector, designated SN 149, commenced shortly after the start of the program. The basic design philosophy was to eliminate or reduce some of the characteristics which were considered contributory to the instability of injector SN 135 with a minimum sacrifice of performance and compatibility.

The primary reason the SN 135 injector was thought to have high-frequency instability was that the pattern was finer than the pattern on the production injector. Therefore, the backup approach to achieve stability was dependent upon reducing the number of elements. However, a stable injector achieved with a coarse pattern would be useless unless it were also at least as compatible and significantly higher in performance than the current production injector. A comparison of the design features of injectors SN 135 and POUL 41-63 is shown in Figure 6.

IV, A, Storable Propellants (cont.)

b. Subscale Test Program

This test series was designed specifically to support the performance analysis of the POUL 41-63 pattern to be incorporated in injector SN 149 and also to provide better visibility as to the cause of the "pop" experienced during the initial test firings of injector SN 135 during Contract NAS 9-6925.

The basic approach involved the test firing of subscale injectors in a 6-in. L* combustion chamber.

The subscale test results tended to substantiate the analytical performance predictions and also supplied data for the "pop" investigation.

c. Fabrication

Fabrication of injector SN 149 was started and operations completed through the point at which the pattern was to be committed. A hold was placed on fabrication at this time pending a resolution of the popping problem.

4. Injector SN 135

As has been previously mentioned, SN 135 injector (pattern POUL 21-5) had excellent performance and compatibility but it also had three problem areas. These were intermediate frequency combustion instability at low chamber pressure, dynamic high-frequency combustion instability and spontaneous chamber pressure perturbations or pops.

IV, A, Storable Propellants (cont.)

All of the work accomplished with injector SN 135 was directed toward the elimination of these problems.

a. Test

(1) Test Setup

All tests were conducted at sea-level conditions at the Aerojet Liquid Rocket Company in Sacramento, California. Two test stands, both of which test the engine in the vertical attitude, were used. Stand C-3 was used for the majority of test firings. This stand is of the usual type and is not designed to simulate any particular feed system. Stand C-11 was used for a minimum number of tests. This stand was designed specifically to simulate the SPS feed and propellant supply system.

Figure 7 is an instrumentation schematic of stand C-3.

The instrumentation requirements are tabulated in Figure 8. The locations at which the various functions were recorded are shown in Figures 9 and 10 for the injector and combustion chamber, respectively.

(2) Procedure

Two procedures may be considered somewhat unique to SPS-type tests and warrant additional discussion:

(a) Pulse Charge or Bomb

Each firing, so designated, utilized three pulse charges consisting of a 13.5 grain, center-mounted thermal pulse and two 6.5 grain,

IV, A, Storable Propellants (cont.)

chamber-wall-mounted electrically detonated pulses. The 13.5-grain pulse charge was installed in the center of the injector as shown in Figure 9. The 6.5-grain pulses were installed in ports B-1 and B-2 as shown in Figure 10. The 6.5-grain pulse located at B-1 location was installed in the inserted position and was initiated at 1.0 $\pm$ 0.2 sec after FS_1. The second 6.5-grain pulse charge was initiated at 2.6 $\pm$ 0.2 sec after FS_1. Pulse actuation for the B-2 location consisted of a pneumatic (200-psig maximum pressure) system with associated sequence and firing circuitry. The pulse charge was initiated 0.5 $\pm$ 0.3 sec after insertion.

(b) Helium Conditioning of Propellants

Helium conditioning of propellants was accomplished by bubbling helium gas through a 1/4-in. fitting near each tank bottom until the tanks were overpressurized to 265 psi. Tank pressures were then allowed to decay to the required run pressure.

It should be noted that this procedure differed from that employed by the SPS Program which recirculated helium until the propellants were saturated. This deviation was made in the interest of economy. Figure 11 summarizes all of the test firings conducted with injector SN 135 in support of that work, and the following paragraphs discuss the work accomplished in these problem areas.

b. Problem Areas

(1) Intermediate-Frequency Combustion Instability

The SN 135 injector, pattern designation POUL 21-5, first demonstrated combustion instability in the 800 to 900 Hz range when operated

IV, A, Storable Propellants (cont.)

at chamber pressures below 80 psia during the injector orifice study, IOS Contract NAS 9-6925; consequently, one of the primary objectives of the follow-on contract, NAS 9-8285, was the elimination of that instability.

The SN 135 injector envelope is identical to the Service Propulsion System (SPS) Mod IV injector. Since the SPS injector has stable combustion characteristics, the analysis concentrated on the areas in which the IOS injector differed from the SPS injector. These were:

(a) Oxidizer distribution plates within the oxidizer manifold;
(b) Contoured orifices; and,
(c) A much finer pattern matrix involving approximately twice the number of orifices.

Items (a) and (b) are shown in Figures 12 and 13.

An early analysis showed that the addition of the thermal barrier plates could be introducing enough phase shift into the system to cause an instability coupled with the injector. However, the analysis of the thermal barrier plates was subsequently proved in error in the manner in which it treated the contribution of the fuel feed system to the instability because after modification of the injector to remove the plates, further testing determined that the intermediate-frequency instability still existed.

After the failure of the modification, a more extensive analytical effort was initiated including a mathematical model for the contoured orifice and further analysis involving power spectral density functions.

Pursuant to the recommendations resulting from the analysis, a series of test firings was conducted on test stand C-11 which is

IV, A, Storable Propellants (cont.)

nearly identical to the flight feed system. Tests, Runs 1.2-18-DAJ-025 through 029, showed little or no improvement, and as a consequence, it was concluded that the only recourse was the inclusion of Helmholtz resonators or inline accumulators.

After this series of tests, the injector pattern was modified to evaluate a theory for the elimination of pops.

Results of these tests were extremely encouraging because not only were the pops eliminated, but the intermediate-frequency instability as well, e.g., run 029 vs 032 and 033.

These results strongly indicate that the spatial orientation of the elements exert a stronger influence upon combustion instabilities of the nonacoustic mode than was expected and that the conventional lumped parameter model is severely hampered by this assumption.

The program was redirected at this point and as a consequence it was not possible to pursue this theory.

(2) High-Frequency Combustion Instability

It will be recalled that the SN 135 injector had experienced pulse-charge-induced, high-frequency instability (5 to 7000 cps) although it was not spontaneously unstable.

To damp or overcome the instability, it was decided to investigate an acoustic resonator.

The selected test approach was based upon the use of resonator rings bolted between the injector and combustion chamber flanges.

IV, A, Storable Propellants (cont.)

Two resonator inserts were designed and fabricated as shown in Figures 14 and 15. In the first insert, the apertures consisted of drilled holes from the combustion chamber to the resonator cavity. This design was preferred because of its broadband operating capability but it was thought that it might be prone to the accumulation of residual propellants. In recognition of this problem, a slotted design with improved draining capability but a more narrow band of efficient operation was also fabricated.

The first test with the multiorifice configuration insert (Test 1.2-18-016) was disappointing because it resulted in a CSM shutdown. However, the result was not totally unexpected because the baffle tip clearance was approximately 0.25 in., which was considered excessive by some of the design personnel. The baffle tips were then built up with weld to reduce the clearance to approximately 0.020 in. and testing was resumed.

Subsequent test results were very encouraging because complete recovery was experienced in every instance except in those cases in which helium-conditioned propellants were used. In addition, the intermediate-frequency oscillations were damped although not to an acceptable level. Figure 16 is a representative record of the chamber pressures without the resonator insert. Figures 17 through 19 compare the SN 135 injector and resonator combination with the SPS injector without a resonator.

Following the test series with the multiorifice resonator, the slotted configuration was tested. Tests 1.2-18-DAJ-025 through 029 showed no improvement over the tests with the multiorifice resonator with respect to the high-frequency instability because recovery from pulse change detonations with helium-conditioned propellants was still not effected.

IV, A, Storable Propellants (cont.)

As a result of these tests, it was concluded that the "tuning" of the multiorifice resonator was more appropriate for the combustion process existing within the combustion chamber but that approximately 20% additional back volume was required to increase the capacitance sufficiently to overcome the effect of helium-conditioned propellants.

(3) Popping

The occurrence of popping in injector SN 135 was unexpected because this injector was designed specifically to prevent pop triggers. The design was based upon the results of a previous study which seemed to indicate that the pop triggers were caused by hydraulically unstable propellant streams. Using these criteria, injector SN 135 was designed with contoured inlet orifices to ensure stable propellant streams. The continued occurrence of popping (although of low amplitude) indicated that the unstable streams or hydraulic flip were not the only causes of pop triggers.

Parallel and concurrent analytical and experimental programs were initiated with the objective of developing design criteria by which the occurrence of popping could be controlled.

The first experiments investigated some of the more obvious possibilities. The theory that pops were caused by drops forming at orifice exits and running into adjacent streams was disproved in subscale tests when the orifices were spot-faced to dam droplets and the pops persisted.

Efforts to relate the pops to a specific section of the injector face were also unsuccessful when high-speed motion pictures taken of the injector face while firing were not conclusive when correlated with the high-frequency records.

IV, A, Storable Propellants (cont.)

The analytical portion of the program was aimed at development of a pop model which could be used to correlate engine pop data. The analytical model was developed by modifying an existing hypergolic stream impingement model in conjunction with both engine pop data and the results of 188 subscale tests performed during the experimental portion of the program. The objective of the experimental portion of the program was to verify the pop model and to define the design and operating conditions that produce pop triggers.

The engine pop data used to make the correlations were obtained from several sources. Data from the lunar module ascent engine injectors were obtained through personal visits, arranged by the NASA Technical Monitor, to Rocketdyne, TRW, and Bell. Pop data for the SPS engine Mod II and Mod IV injectors and the IOS injector were supplied by Aerojet. Finally, pop data obtained with a combustion research engine were supplied by JPL.

(a) Model Development

The model is based on the assumption that the transient pressure and accelerometer disturbance (pops) observed in rocket engines are the result of a spray detonation which is triggered by a blastwave generated by small explosions associated with hypergolic stream impingement. The first step in developing the model was to verify the occurrence of the impingement explosions with N_2O_4/AeroZINE 50 at engine operating pressures since they had only been observed previously with N_2O_4/N_2H_4 at atmospheric pressure. Verification of these trigger sources was accomplished photographically during the experimental phase of the program using special techniques which represent an advancement in the state-of-the-art of high-speed movie taking.

IV, A, Storable Propellants (cont.)

A hypergolic stream impingement model was used to define three regimes of injector element operation: mixing, impingement explosion, and separation in terms of the fuel orifice diameter and velocity, impingement angle, and fuel temperature. The element operating regime is defined by a separation number, S, which is determined by the parameters listed above.

The element mixing efficiency, E_M, as defined by the Rupe mixing uniformity criteria was found to affect the occurrence of the impingement explosions. Also, it was found that stream quality as determined by the orifice L/D exerts a strong influence upon the impingement explosions presumably due to a modification of the mixing efficiency and separation parameter.

The final step was to define a coupling mechanism between the impingement explosions and the spray detonation which was done by making the assumption that the explosions emit a spherical blastwave which can grow into a detonation wave if it passes through an adjacent element spray with a Mach number greater than one. Existing blastwave theory was then used to define the pressure and velocity field associated with the impingement explosion from which a detonation coupling parameter, D, was derived. D is affected by the chamber pressure, fuel orifice size, and spacing between elements. Spacing of adjacent elements closer than a critical value as defined by D can cause engine popping if the elements are operating within the impingement explosion regime as shown in Figure 20.

The experimental engine data correlations indicate that, for injectors having well defined propellant streams (L/D > 2), the occurrence of engine popping is defined by the following three conditions.

IV, A, Storable Propellants (cont.)

Pop	No Pop
$0.03 < S < 1.0$	$1.0 < S < 0.03$
$1.2 < D$	$D < 1.2$
$0.5 < E_M$	$E_M < 0.5$

All three pop conditions must be met to produce engine popping; however, only one of the three no-pop conditions is required to prevent popping. Injectors having L/Ds less than two produce bushy streams which promote stream separation (i.e., S < 1) and, therefore, are not likely to pop. The data also indicate that placing elements too near the chamber or baffle walls promotes coupling of the impingement explosion blastwave with adjacent sprays through shock wave reflections. A complete derivation of this theory is contained in AGC Report TCER 9642:0106, Rocket Engine Pop Design Criteria.

(b) Test Verification

Design criteria obtained from the above described work were used to recommend modifications to the SN 135 pattern to eliminate the popping problem. Specifically, the pattern modification recommended was to increase the spacing between elements in rows 2 and 7 so that D would be less than 1.2 as shown in Figure 21. Figures 22 and 23 show the injector after the orifices were plugged. A total of eight test firings (Tests 1.2-18-DAJ-030 through 037) were made with orifices which had been plugged with an aluminum lithium silicate compound. Results of these tests substantiated the pop theory.

5. Fabrication

The original program plan called for the fabrication of three injectors, four ablative combustion chambers and two resonators.

IV, A, Storable Propellants (cont.)

At the beginning of the program, permission was obtained to procure long-lead material and subcomponents to support these needs. However, as the program developed, it became obvious that more effort would be required in analysis and less in fabrication, and therefore, the fabrication effort was scaled down from the original requirements.

No major problem was encountered with respect to fabrication other than that logistic planning became increasingly difficult because of the phasing out of the SPS program which in some instances, particularly in the case of the combustion chamber, made it necessary to commit to fabrication based upon the imminent shutdown of a production line rather than immediate need.

The components fabricated or procured were:

Part Name	PN	SN	Status
Ablative Chamber	1123011-1	376	Complete except for hydro-test
Ablative Chamber	1123011-1	377	Through asbestos over-wrap machining
Resonator Ring	1158622-3	001	Complete
Resonator Ring	1157642-8	001	Complete
Injector	Component Level	149	Subcomponent Level
Miscellaneous forgings, baffles, etc.			Subcomponent Level

IV, A, Storable Propellants (cont.)

6. Conclusions and Recommendations

a. Conclusions

At the time the program was redirected, the SN 135 and resonator combination had demonstrated compliance with the program objectives; therefore, the major conclusion is that the technology is now available to increase the SPS engine performance by 5 to 6 sec I_s should the need arise.

The conclusions to be inferred in the various operating parameters are:

(1) Performance

Techniques used to predict performance are adequate because an increase in performance was realized.

(2) Compatibility

The technique is satisfactory as confirmed by excellent test results.

(3) Contoured Orifices

(a) Provide steady, predictable streams over a wide range of operating conditions.

(b) The machined orifices tested had inlet radii twice that of the orifice radius; however, very similar results were obtained with orifices which had etched inlets in which the entrance was slightly broken;

IV, A, Storable Propellants (cont.)

consequently, it is concluded that it is possible to manufacture contoured orifices from the fuel side of the injector although controls and inspection techniques would be difficult.

(c) Contoured orifices are relatively insensitive to manufacturing anomalies (burrs, gouges, etc.).

(4) Intermediate-Frequency Instability

Existing analytical techniques are inadequate probably because of the treatment of the combustion process. The elimination of the intermediate frequency over the entire operating range of the injector after effecting a minor pattern change suggests that the pattern rather than the feed system alone has a strong influence. This experience was not confined to this contract because inquiries both within and outside of Aerojet relative to experience with intermediate frequency resulted in the comment that numerous changes were incorporated in the feed system but that the problem finally "went away" coincident with a pattern change. Consequently, it is strongly recommended that the possibilities suggested by these results be more thoroughly investigated.

Another conclusion with respect to the elimination of intermediate-frequency combustion instability is that an acoustic resonator could in all probability be designed to eliminate this problem as shown by the reduction in the 900 cps instability amplitude when the multiorifice resonator insert was used.

(5) High-Frequency Combustion Instability

It is concluded that the techniques currently in use are satisfactory.

IV, A, Storable Propellants (cont.)

(6) Pops

(a) A photographic tech[illegible] was developed which allows observation of hypergolic stream impingement [illegible]esses at rocket engine operating conditions. This accomplishment is consi[illegible] to be an advancement in the state-of-the-art.

(b) A rocket engine pop[illegible]el was developed by which experimental engine data were correlated and [illegible]n criteria obtained.

Although design cri[illegible] obtained from these correlations provide useful guidelines for preventi[illegible]cket engine popping, there are several items that require research and v[illegible]cation. They are:

1 Effect of bush[illegible]reams on hypergolic stream impingement.

2 Effect of mixi[illegible]fficiency on impingement explosion energy.

3 Effect of mixi[illegible]fficiency on spray susceptibility to detonation.

4 Effect of impi[illegible]ent explosion and solid wall interactions.

IV, Work Accomplished (cont.)

B. CRYOGENIC PROPELLANTS

1. Program

Upon the completion of Phase I, the hypergolic propellant portion of the program, planning for Phase II was started. Phase II was to concentrate upon hydrogen and oxygen propellants and was to remain within the existing fiscal limitations.

The resulting program plan was designed to make maximum utilization of other technology programs at ALRC as well as another NASA sponsored contract, NAS 9-8317, a valve development contract, which had also been redirected to the use of cryogenic propellants.

The program planning criteria were:

a. Maximum technology yield.

b. Components fabricated must be capable of integrated workhorse engine test firings.

c. Program elements must be independent to the extent that failure of one portion would not jeopardize the other portions.

The original program plan devoted the first month of the phase to tradeoff studies. The purpose of these studies was to define the optimum injector configuration with respect to satisfying the program criterion enumerated in the preceding paragraph.

During the next four program months, the selected injector configuration and an uncooled combustion chamber were to be fabricated and tested.

IV, B, Cryogenic Propellants (cont.)

The results of the tests were then to be compared with the results of similar tests conducted with other candidate configurations being evaluated under ALRC sponsored programs. This comparative analysis would establish the configuration of a second injector which would be fabricated and delivered to NASA.

The original program plan was followed through the fabrication and test of the first injector. Test results were extremely encouraging with all the objectives satisfied. Consequently, a "second try" injector was not required.

As a result of a design review held at NASA/MSC on 5, 6, August 1970, it was decided to place program emphasis upon the development of a regeneratively cooled combustion chamber instead of pursuing the original plan. This decision was based upon two factors:

(1) The excellent performance demonstrated in short duration test firings did not make another design iteration necessary at that time.

(2) The design and fabrication of a regeneratively cooled combustion chamber would allow longer injector test durations and also provide valuable insight into the problems associated with chambers of this type.

In consonance with this decision, a combustion chamber was designed and fabricated. Testing with the injector was accomplished during January 1971 immediately prior to the end of the program.

The various technical elements of the program are discussed in the following paragraphs.

IV, B, Cryogenic Propellants (cont.)

2. Injector

a. Tradeoff Studies

The first program task was a tradeoff study to select the basic injector configuration. The basic operating parameters for the study were:

(1) Operating Parameters

(a) Thrust: 5K to 10K
(b) P_c: 1 psi chamber pressure for 10 lb of thrust
(c) MR: 5.0 to 7.0 O/F, 6.0 nominal
(d) O_2, H_2
(e) I_s: 450 to 460 sec
(f) ε: 300:1
(g) Design Life: 10 Starts/Mission, 100 Missions

Several injector element concepts were reviewed in the tradeoff study to determine their relative applicability for this program. The coaxial, platelet, triplet, and LO_2 doublet/fuel showerhead elements were each considered. The study considered the relative performance, design simplicity, compatibility, and combustion stability (where known) of each of the various injector element types. From this study, two injector types appeared most promising; the coaxial element and a platelet type element. The coaxial element was suited for this application because of its excellent compatibility and stability with LO_2/GH_2 propellants. It also possessed design simplicity and could easily be modified during a development program. Its major disadvantage was that in short chambers it was lower performing than several other element designs. The platelet injector, on the other hand, provided a high performance potential in short chambers. Its design, however, was more complex than that of the coaxial and probably would require greater development effort.

IV, B, Cryogenic Propellants (cont.)

The results of the engine and injector tradeoff studies were presented and discussed in a working session at MSC on Friday, 6 March 1970. As a result of these studies and subsequent coordination, the following basic design ground rules were established:

(2) Injector Design Ground Rules

(a) The initial injector would be of a coaxial element configuration.

(b) The design nominal operating conditions for the injector would be as follows:

1. Chamber Pressure, P_c = 500 psia (nom)
2. Thrust, F = 5000 lb (nom)
3. Mixture Ratio, O/F = 6.0:1 (nom)
4. Gaseous Oxygen and Hydrogen Operation
   T_o = 460°R entering injector
   T_f = 430°R entering injector
5. Specific Impulse, I_s = 450 to 460 sec
6. Expansion Ratio, ε: approximately 230:1 considering 40.0 in. exit diameter constraint
7. Engine Cycle: gas generator

Both of the foregoing decisions were tempered by the practical aspects of available funding, potential application, and existing programs.

One of the primary factors affecting the injector selection was the ease of fabrication of the coaxial element. This consideration was of paramount importance in this program because of the requirement to have an operating unit in "one try" with no contingency for fabrication or other types of failures.

IV, B, Cryogenic Propellants (cont.)

(3) Engine Cycle Selection

The selection of the engine cycle was affected by two factors:

(a) OMS engine cycle was not firm, consequently, representative values were the best available at the time.

(b) Desirability of keeping within the approximate chamber pressure of the high pressure APS system being evaluated at ALRC at the same time to enhance technology interchange.

b. Design

The injector design effort included the design of the injector and two supporting components, the igniter, and the heat sink combustion chamber.

The igniter design was identical to that used on an ALRC sponsored program, and as a consequence, design effort under this contract was confined to attach brackets and modifications to the igniter propellant valves.

The copper heat sink combustion chamber was also similar to that used on other programs and the only new designs generated were two cylindrical L* sections to permit this parameter to be varied during testing.

The major design effort was directed to the injector. The detail design was, as is normal to all new design efforts, the result of numerous tradeoffs.

IV, B, Cryogenic Propellants (cont.)

Once the desirability of an injector with coaxial elements had been established, the first decision to be made was the number of elements.

The diameter and available face area of the injector were already established because of the desirability of using the existing combustion chamber and igniter. A preliminary system study indicated injector pressure differentials on the order of 50 psi for the oxidizer circuit and 100 psi for the fuel circuit. A review of similar injector designs showed that approximately 5% of the fuel flow should be allocated to face cooling. These factors, in addition to the already established propellant flow rate, mixture ratio, and densities, made it possible to calculate the total injector flow area required.

Once the total area was established, the next step was to determine the optimum number of elements which could be accommodated within the face of the injector. This involved a tradeoff between fabrication complexity and performance. Generally, the finer the pattern, i.e., the more elements, the higher the performance. The potential performance gains to be realized by a fine pattern with small elements must be weighed against the problems associated with the manufacture of very small elements. The results of a tradeoff study showed 74 elements with 68 lb thrust per element as being the most desirable compromise. This element has a 0.014 in. fuel annulus (approaching the lower practical machining limit), and a 150 diameter oxidizer passage.

The elements have two unique design features. Contoured inlets have been provided in an attempt to ensure predictable flow, and flared outlets are provided to enhance mixing. A drawing of the element is included in Figure 24.

The manifold designs were also influenced by prior experience on other ALRC programs. Propellant distribution difficulties had been experienced with manifolds in which the propellant lines discharged directly into

IV, B, Cryogenic Propellants (cont.)

the manifold because elements under the discharge received a disproportionate share of the propellant. In order to eliminate this problem, a primary collector manifold was provided in both fuel and oxidizer circuits. To further enhance even propellant distribution, the fuel manifold was designed with a variable cross section to minimize variation in fuel velocity.

A schematic drawing of the injector is shown in Figure 25 and the significant operating parameters of the injector are tabulated in Figure 26.

c. Fabrication

The injector fabrication was accomplished with no difficulties. Figures 27 through 30 show the injector after the elements had been brazed and before the back manifold was welded in position or the igniter boss machined.

All components were fabricated from type 304 SS because of its good brazing characteristics.

The basic fabrication sequence consisted of the following:

a. Component fabrication
b. Fuel and oxidizer manifold subassembly
c. Braze elements in place
d. Oxidizer closure weld

A unique feature of the injector was the fabrication of the elements. The elements are of one piece construction manufactured by EDM machining. This technique has resulted in the elimination of an intermediate

IV, B, Cryogenic Propellants (cont.)

step which is normally required to attach a sleeve to the basic element to form the annulus. In addition, this technique provides superior control of both annulus width and concentricity. (See Figures 31, 32 and 33).

Element installation was accomplished by inserting the elements from the back side through the holes in the oxidizer manifold bulkhead and into the rigimesh. The elements were then staked in place (see Figure 30) and the body inverted or placed in the face-up position. A retention collar (see Figures 25 and 31) was then placed over the end of each element and seated in the register of the rigimesh face. The body was then placed in the brazing furnace where both the element to manifold and element to retention collar braze were accomplished simultaneously.

d. Test

(1) Cold Flow

When injector fabrication was completed, a flow test was conducted to determine manifold distribution. The information from these tests was desired to assist in "trouble shooting" in the event that performance anomalies developed during the subsequent hot test series.

The testing was conducted in the ALRC Aerophysics Laboratory. Both the oxidizer and fuel propellants were simulated with gaseous N_2, maintaining Mach No. similarity by flowing at design circuit pressure ratio. Individual element flow rates were determined by routing the element flow through a rotameter.

The results of this testing are graphically depicted in Figures 34, 35, and 36. Referring to Figure 34, one notes that the fuel distribution normalizes uniformly about one, with a data band width of $\pm$ 10%.

IV, B, Cryogenic Propellants (cont.)

It can also be observed that the outside row of elements (Row A) is slightly deficient in flow (2.4% low). The oxidizer flow is biased high under the injector (Figure 35) inlet resulting in a mixture ratio distribution that is high under the oxidizer inlet and low opposite the inlet. (See Figure 36).

(2) Hot Fire

Twenty-three injector test firings were conducted. These tests demonstrated that a combustion chamber length of 8 in. (16 in. L*) was required to assure stable combustion. Other characteristics were high performance (99% of energy release efficiency ERE); see Figure 37 for derivation of ERE, stable operation over a M.R. range of 5 - 7, and chamber pressure over a range of 300 to 700 psia and recovery from pulse induced over pressures of 1000 psi. Compatibility indications were promising although firing durations were limited to 0.5 sec by the uncooled copper chamber.

Appendix A describes the test procedures and instrumentation used during the tests. All of the tests were conducted in the horizontal attitude on the stand shown in Figure 38 located in Bay 7 of the ALRC Research Physics Laboratory.

A photograph of the workhorse thrust chamber assembly with two cylindrical L* chamber inserts is included in Figure 39. One of the inserts is two inches long and the other is four inches long. The convergent - divergent section of the chamber is four inches from the forward flange to the plane of the throat. Consequently, it was possible to vary chamber L' from four inches to ten inches.

Figure 40 shows the igniter and igniter valves that were used for all tests. This assembly is identical to that employed on other programs at ALRC and was used on this program because of its ready availability.

IV, B, Cryogenic Propellants (cont.)

Modifications to this concept would be required for a flight configuration of the workhorse engine developed under this contract. A schematic of the test igniter is shown in Figure 41. The igniter is centrally mounted in the injector with the igniter tip flush with the injector face. The engine firing sequence (see Appendix A) involves energizing the aircraft spark plug and igniter propellant valves approximately 20 M.S. prior to initiation of main propellant valve opening. The igniter valves admit all of the oxidizer and some of the fuel to the torch chamber where they are ignited by the spark plug. The remaining fuel cools the barrel until it is dumped down stream in the main combustion chamber where it raises the torch temperature. All the tests are tabulated in Figure 42.

The purpose and results of tests are summarized in the following paragraphs:

(1) Tests 5K-2-101 through -103

The first three tests were conducted with a 6 in. L' combustion chamber. The purpose of the tests was to check out the test setup and to determine the operating characteristics with the 6 in. combustion chamber. All of the tests resulted in a CSM (combustion stability monitor) induced shutdown at approximately 0.2 sec due to 800 cycle combustion instability. There was also some evidence of "spiking" or popping within the igniter.

(2) Test 5K-2-104

Test 104 was conducted at a mixture ratio (O/F) of approximately 10 rather than the nominal of 6 which had been used in the previous three tests. The purpose of the test was to ascertain if the increased oxidizer pressure drop occasioned by the increased oxidizer flow would inhibit the combustion stability. Results were positive in that there was no evidence of either combustion instability or igniter spiking.

IV, B, Cryogenic Propellants (cont.)

(3) Test 5K-2-105

The chamber length was increased to 8 in. for Test 105. In all other respects it was similar to Test 104. The purpose of the test was to determine the effect of the increased chamber length upon performance. The test resulted in stable operation and showed a performance increase of approximately 0.5% ERE over Test 104.

(4) Test 5K-2-106

The purpose of Test 106 was to evaluate the operating characteristics of the injector when fired in a 8 in. combustion chamber at nominal conditions, MR(O/F) = 6 and chamber pressure P_c = 500 psia. Results were excellent because combustion was stable, performance was approximately 98.5% ERE and there were no hardware anomalies. The only undesirable feature was the presence of igniter spikes.

As a result of Test 106, the chamber L' of 8 in. was established as the preferred length and all subsequent tests were conducted with this chamber length.

(5) Tests 5K-2-107 and -108

Tests 107 and 108 were conducted at conditions similar to those of Test 106; however, the igniter flow rate was increased by a factor of 1.5. It was believed that the increased flow and resulting higher igniter chamber pressure would eliminate the spiking which was thought to be a result of an interaction between the igniter and main chamber pressures. The increased igniter chamber pressure did eliminate the spiking on Run 107; however, after Run 108, the surface of the injector and chamber were found to have a

IV, B, Cryogenic Propellants (cont.)

black deposit on their interior surfaces and the end of the igniter was found to be completely burned away. Figures 43, 44, and 45 are before and after photographs of the injector face.

The igniter assembly was removed from the injector and the barrel or wall of the igniter chamber was found to be completely burned through from a plane approximately midway to the exit. Subsequent thermal analysis and flow testing demonstrated that the explanation for the failure was the radial thermal expansion of the igniter barrel which reduced the clearance or flow passage between the OD of the igniter barrel and the ID of the igniter boss.

The foregoing failure was experienced during steady-state operating conditions in which both the igniter and main combustion chamber were operating simultaneously. This operating mode is the standard practice followed on other programs at ALRC; however, this engine had no requirement for parallel operation. Consequently, the procedure for this contract was modified to terminate the igniter oxidizer flow and igniter combustion approximately 0.030 sec after main chamber steady-state combustion was achieved. Igniter fuel flow was then maintained throughout the run to provide igniter cooling.

(6) Tests 5K-2-009 through -114

This series of tests was conducted to evaluate operational characteristics at off-nominal conditions. The lower operational limit was established as 300 psia chamber pressure at a mixture ratio of 5. Posttest examination of the elements showed a slight increase in the minor erosion on the trailing edge of the oxidizer tube. This erosion is predominate in the central hub location and, when first noted after Run 008, had been associated with the faulty igniter operation experienced during the two previous tests.

IV, B, Cryogenic Propellants (cont.)

(7) Tests 5K-2-115 and -116

Both of these tests were conducted at nominal conditions with a 6.5 grain side-mounted pulse charge ignited approximately halfway through the test. Over pressures of approximately 1000 psi resulted from the pulse charges. In both tests, complete recovery was experienced within 0.006 sec. Figure 46 is a reproduction of the oscillograph record.

During the posttest examination of the injector after Test 116, damage to several elements in the form of deflected oxidizer tubes and minor shrapnel pitting was noted. Since this damage was confined to the pulse charge location, it has been attributed to the detonation blastwave.

Since the dynamic stability had already been established, the one remaining scheduled pulse test was canceled. A blueing of the rigimesh around the periphery of the igniter boss was also noted during posttest examination. Test records indicate that the main oxidizer propellant valve opened abnormally fast during Run 116. The fast opening may have resulted in main oxidizer flow combining with the igniter fuel coolant which in turn would result in combustion adjacent to the igniter prior to the establishment of cooling fuel flow through the rigimesh.

To evaluate this possibility, the igniter rigimesh face was instrumented with two thermocouples near the igniter port, and two igniter tests were conducted that simulated the previous start condition. The first test was conducted with the combustion chamber detached and a complete TCA assembly was used for the second test. The results of the tests were inconclusive because no temperature rise of the rigimesh face was evidenced during either test.

IV, B, Cryogenic Propellants (cont.)

Consequently, the precise cause and nature of the blueing of the rigimesh and minor erosion on the trailing edge of some of the oxidizer tubes has not been definitely established; however, it appears to have been associated with the fast opening of the oxidizer valve because there were no anomalies on succeeding tests.

(8) Tests 5K-2-117 through -120

This series of four tests was conducted to evaluate operational characteristics at off-nominal mixture ratios and high chamber pressure conditions with ambient propellant inlet temperatures. The test, 5K-2-117, conducted at the lowest mixture ratio, 4.5, resulted in a CSM (combustion stability monitor) induced shutdown at approximately 0.23 sec due to the 800 cycle combustion instability. The remaining three tests were conducted at mixture ratios above 5.0 and resulted in excellent performance and stable combustion. Posttest examination of the elements and rigimesh showed no evidence of additional erosion on the trailing edge of the oxidizer tube or increased blueing of the rigimesh face. As previously described, the igniter oxidizer flow and igniter combustion were terminated approximately 0.030 sec after main chamber steady-state combustion was achieved. Igniter fuel flow was maintained throughout the run to provide igniter cooling. Visual inspection of the igniter assembly revealed no visible defects.

(9) Tests 5K-2-121 through -123

This series of tests was conducted to evaluate operational characteristics at off-nominal high mixture ratios and nominal chamber pressure conditions at low propellant inlet temperatures. Results of these tests were excellent because combustion was stable, performance was approximately 100.0% ERE, and there were no hardware anomalies. The igniter firing sequence utilized was the same as in previous tests.

IV, B, Cryogenic Propellants (cont.)

This series concluded the injector test plan portion of the program. The major effort during the remaining portion of the program was devoted to the design, fabrication, and test of the fuel-cooled copper chamber.

3. Chamber

a. Criteria

The primary objective of the combustion chamber fabrication phase of the program was to provide a chamber capable of supporting long-duration test firings with the injector fabricated during the first portion of the program. The secondary objective was to obtain insight into the various factors that affect the design and fabrication of a flight-weight regeneratively cooled chamber. It was of paramount importance that all of these objectives be satisfied with a very limited budget.

The design criteria established to satisfy these requirements were:

(1) Nominal operating conditions - same as injector, i.e., P_c = 500, MR = 6.0:1.

(2) Sufficient service life to evaluate nominal and off limit operating conditions.

(3) Coolant inlet temperature 215°R - representative temperature range expected at ε = 6:1 also within existing test stand capability.

IV, B, Cryogenic Propellants (cont.)

(4) Pressure drop ≈ 300 psi - representative of engine system and within test stand capability.

(5) Design to minimize fabrication risk and use of readily available materials whenever possible.

b. Design

Several methods of fabrication and two material types were considered before making the final selections. The fabrication methods were concentric shell, tube bundle, milled slots with electro-deposit back covers, and milled slots with brazed cover plates. Although all of the techniques offered certain advantages, the milled slot with brazed covers was selected as the best for this particular application. The advantages were: straightforward fabrication techniques, ease of inspection, schedule and cost.

The same general philosophy dictated the selection of OFHC copper instead of the zirconium copper alloy. The zirconium alloy had somewhat better structural properties; however, braze techniques were not as well established as were those with OFHC and lead time and cost were approximately twice that of OFHC.

The selected chamber configuration (see Figure 47) was based upon the foregoing considerations, the results of the tests with the uncooled chamber, and an extensive thermal analysis. The specific features are:

(1) L* 16 in. - L' 8 in.

(2) ε 7:1

(3) 100 milled slots 0.040 in. wide

(4) Slot spacing 0.100 in. at injector end, 0.040 in. at throat and 0.200 at the exit

IV, B, Cryogenic Propellants (cont.)

(5) Constant wall 0.040 in. thick

(6) Brazed channel covers with square wire overwrap for hoop strength

The thermal and pressure characteristics of the chamber are also summarized in Figure 47. A service life of approximately 1100 cycles and 10 hr is expected at a thrust level of 5000 lb or 500 cycles and 10 hr at 8000 lb thrust.

c. Fabrication

The basic fabrication sequence was:

(1) Mandrel fabrication
(2) Template fabrication
(3) Inside chamber contour machine
(4) Outside chamber contour machine
(5) Manifold assembly fabrication
(6) Cooling passage machining
(7) Cooling passage cover installation
(8) Cold flow
(9) Manifold installation
(10) Wire overwrap installation
(11) Finish machine
(12) Instrumentation installation

Work was accomplished as follows:

(1) Chamber Shell

The chamber was fabricated from solid OFHC copper forging, 8.5 in. dia by 13.0 in. long. The billet was machined in an as-received

IV, B, Cryogenic Propellants (cont.)

condition and was not subjected to a stress-relieve or anneal cycle. An internal stainless-steel mandrel was made to support the chamber during external machining. The inside chamber contour and the mating mandrel surfaces were match-machined using a numerical tape-controlled machine. Machining of the chamber inside contour is shown in Figure 48. The outside chamber contouring was accomplished on a tracing lathe using specially fabricated contour template.

Cooling passages were then machined on a three-dimensional duplicating mill using carbide-type slitting saws.

One of the most critical mileposts was machining of the coolant passages. There are 100 full length passages, 0.040 in. wide, equally spaced around the periphery of the chamber. The channels have a variable depth starting with 0.200 in. at the injector interface, decreasing to 0.071 in. at the throat, and increasing to 0.400 in. at 6:1 expansion area ratio. A constant gas wall of 0.040 in. is maintained and the web between adjacent passages varies from 0.10 in. at the injector to 0.040 in. at the throat and to 0.20 in. at the exit.

Coolant passage depth was controlled during machining by templates. Two passes were made for each passage. The first pass was made with a 0.051 in. wide cutter to provide a register for the coolant passage covers and the second pass, which formed the actual coolant passage, was made with a 0.039 in. wide cutter. See View AA of Figure 47. The machining of the channels is shown in Figure 49. Figure 50 is a photograph of the chamber shell after machining.

Several braze samples were made to evaluate the braze technique which was used to braze the rectangular wire coolant passage covers in position. The samples were sectioned with the result that an excellent braze joint was indicated and the passages were free of any obstruction from the braze material. Figure 51 is a photograph of the specimens.

IV, B, Cryogenic Propellants (cont.)

The electroless nickel-plated OFHC copper wire coolant passage covers were installed and furnace brazed at 1780°F for 30 min. With one exception, the results were excellent; the exception being that some braze material (NICROBRAZ), which is applied to the exterior of the chamber prior to placing the chamber in the furnace, ran down the chamber while in the molten state, partially obstructing the entrance slots. Clean-up was accomplished by EDC machining.

(2) Manifolds

Figures 52 and 53 depict the manifolds during fabrication. Figure 52 shows the outlet manifold assembled for TIG welding of the cylindrical section to the flange. Machining of the coolant passages in the inlet manifold subassembly is shown in Figure 53. The outlet manifold, which has a variable flow cross-section, is fabricated from CRES 304 type steel. It is fabricated by welding two subcomponents: the slotted cylindrical section (there are 100 slots, 0.062 in. wide and 0.50 in. long, equally spaced around the circumference); and the flange/manifold cavity section. The manifold cavity which has a variable circular cross-section was produced by off-center machining.

The inlet manifold, which is also fabricated from CRES 304 type steel, has a constant cross-section. The two major subcomponents of this assembly are a slotted conical section (100 slots, 0.062 in. wide and 0.60 in. long), and a manifold cavity. The manifold cavity is a toroid of constant semicircular cross-section.

IV, B, Cryogenic Propellants (cont.)

(3) Cold Flow

After the machining operation a water flow test was conducted in an attempt to determine if the flow emitted from the coolant passage was uniform. This test (Figure 54) was not successful because the flow was not well enough defined. Consequently, the chamber was moved to the Aerophysics Laboratory where it was flow tested with gaseous nitrogen, maintaining Mach No. similarity by flowing at design circuit, flow rate, temperature and pressure ratio. Individual passage flow rates were determined by routing the passage flow through a rotameter.

The results of the testing are graphically depicted in Figure 55. The results of the test were satisfactory because they demonstrated flow uniformity within $\pm$ 5% around the periphery of the chamber.

(4) Manifold Installation

The next step in fabrication procedure was the brazing of the inlet and outlet manifolds in position as shown in Figure 56. The initial results of this operation were disappointing because upon removal from the brazing furnace it was found that the inlet manifold was cocked or inclined off the longitudinal axis by approximately 0.060 in. The outlet manifold was satisfactorily brazed.

In an attempt to bring the manifold to the proper position the assembly was reinstalled in the brazing furnace with weights applied to the high side of the manifold. The results were not satisfactory.

The cocked or inclined-off-the-longitudinal axis condition of the inlet chamber manifold was repaired utilizing an additional rebraze cycle at a lower temperature. This repair consisted of brazing the

IV, B, Cryogenic Propellants (cont.)

circumferential closure ring over the mismatch area at the aft manifold end, and filling the gap at the forward end with 20 mils copper and stainless steel wires prior to braze. Upon completion of the repair braze cycle, the chamber coolant passages and manifolds were pressurized with GN_2 at 200 psi and checked for leakage; no leakage was noted.

Remaining steps of the chamber fabrication consisted of Hastelloy wire hoop wrap and braze, and final machining of the interfaces and instrumentation ports. No problems were encountered during these steps of fabrication.

The chamber configuration after the wire wrap and braze is shown in Figure 57.

d. Hot Fire Test

(1) Set Up

Four OMS TCA test firings were conducted. One test was conducted for 0.5 seconds duration and the remaining three were conducted for about 5 seconds duration each. The test plan called for all tests to be conducted at nominal conditions (MR = 6, P_c = 500 psi and propellant inlet temperature of around 215°R); however, test stand problems resulted in all of the tests being conducted at a MR of between 5.0 and 6.0. These tests demonstrated stable combustion and excellent compatibility. The other characteristic was the verification of previously demonstrated high performance (99% of energy efficiency ERE).

Figures 58 and 59 describe the test and instrumentation used during the tests. All of the tests were conducted in the horizontal attitude on the stand shown in Figures 60, 61 and 62, located in Bay 7 of the ALRC Research Physics Laboratory.

IV, B, Cryogenic Propellants (cont.)

Post test condition of the chamber and injector is depicted in Figures 63 through 65.

Post test examination of the hardware indicated excellent compatibility. Although there was evidence of minor streaking in the chamber portion, no evidence of erosion was noted. No blueing of the injector regimes or erosion on the trailing edge of some of the oxidizer tubes (observed during the initial injector tests) were noted during these tests.

Oscillograph record of test 5K-3-102, Figure 66, shows typical start and steady-state characteristics during these tests.

The igniter and igniter valves shown in Figure 40 were used during these tests. Operating characteristics of these components were presented earlier in this report under the injector testing.

The purpose and results of each test are summarized in the following paragraphs.

(a) Test 5K-3-101

The purpose of this test was to checkout the test setup and to determine the operating characteristics and sequencing. Results were positive with stable combustion, excellent compatibility and no evidence of anomalies. Near steady-state conditions were achieved.

(b) Tests 5K-3-102 Through 104

This series of tests was conducted to demonstrate longer duration firings which achieved steady-state conditions and to evaluate performance characteristics at nominal conditions. (MR = 6.0 and

IV, B, Cryogenic Propellants (cont.)

P_c = 500 psi), also to verify predicted chamber wall temperatures. Results of these tests were excellent because combustion was stable, chamber wall temperatures were below the predicted values, performance was 99% ERE and higher, and there were no hardware anomalies.

This series concluded the TCA test plan portion of the Phase II program. Remaining portion of the program was devoted to preparation of the final report.

The chamber wall temperature plots at various locations along the chamber are shown in Figures 67 through 69. Location of the thermocouples is shown in Figure 58. The temperature measurements were taken about 0.050-in. back from the inside chamber contour and in a band between coolant passages. The chamber gas-side wall temperatures will be about 130°F higher. The temperature plot shown is for the highest temperatures recorded during Test 5K-3-103. Chamber manifold inlet fuel temperature is shown in Figure 68 for comparison.

(2) Performance

The OMS performance data were evaluated using the performance model recommended by the JANNAF Performance Standardization Working Group. The OMS energy release model for gaseous hydrogen/gaseous oxygen was modified for a mixing limited mechanism since the JANNAF methodology is incomplete in modeling the combustion process of gas/gas injectors.

The technique used for evaluation and prediction of performance considers the one dimensional equilibrium (ODE) flow condition to be the base case. All performance losses are then subtracted from the base case. Five primary sources of specific impulse losses due to (1) nozzle divergence, (2) nozzle kinetic (expansion), (3) thrust chamber boundary layer,

IV, B, Cryogenic Propellants (cont.)

(4) mixture ratio maldistribution and (5) energy release performance losses were considered in this analysis.

(a) Theoretical Thermochemical Performance

Theoretical thermochemical $I_{sp_{vac}}$ and c* were calculated from the ODE option of the improved TDK computer program. Nominal propellant enthalpies were based upon 100% pure gaseous para-H_2 at 200°R for fuel and 537°R ambient temperature gaseous oxidizer consisting of 99.389% mole fraction O_2 + 0.549% Argon + 0.053% N_2. Nominal P_c = 500 psia. The magnitude of the Argon contaminant loss at ε = 7.38 is approximately 0.4 sec. From these nominal base performances which were derived in the O/F range from 4 to 8, corrections in theoretical performance were made for individual test $T_o \neq 537°R$ and $T_f \neq 200°R$ by correcting inlet propellant enthalpy by the amount

$$\delta H_{tot} = (O/F)\ C_{pO_2}\ (TOV - 537°R) + C_{P_{H_2}}\ (TFV - 200°R)$$

and correcting test $P_c \neq 500$ psia by

$$I_{sp}\ (P_c) = I_{sp}\ (P_c = 500) + \left[\frac{d\ I_{sp}}{d\ P_c}\right]_{P_c = 500} (P_c - 500\ \text{psia})$$

$$c^*\ (P_c) = c^*\ (P_c = 500) + \left[\frac{dc^*}{d\ P_c}\right]_{P_c = 500} (P_c - 500\ \text{psia})$$

(b) Nozzle Curvature-Divergence Efficiency

The two-dimensional nozzle curvature divergence efficiency was calculated using the ideal gas (method-of-characteristics) expansion option of TDK at average gas properties corresponding to 5.0 and 6.0 injector mixture ratio and comparing the results with the one dimensional

IV, B, Cryogenic Propellants (cont.)

ideal expansion performance calculated on the GE-235 timeshare computer for identical corresponding gas properties. The nozzle contour has a 37° 16' conical divergence angle with both the upstream and downstream throat radii of curvature equal to the throat radius. The nozzle exit area ratio is truncated at $\epsilon = 7.38$. Results of both the one-dimensional (1-D) and two-dimensional (2-D) nozzle analyses at O/F = 5 and 6 are tabulated below.

Mixture Ratio	5.0		6.0	
Analysis	1-D	2-D	1-D	2-D
Gas Temperature, °R	5946	5946	6236	6236
Molecular Weight	12.0	12.0	13.8	13.8
Gamma	1.193	1.193	1.150	1.150
Chamber Pressure, psia	500	500	500	500
Thrust Coef., C_F	1.7057	1.5021	1.7283	1.5227
Curv., - Div. Eff., η_{CD}	1.0000	0.8806	1.0000	1.8810

The cooled chamber nozzle curvature-divergence performance loss was calculated to vary between 48.1 to 49.2 sec depending upon mixture ratio and delivered performance using the following relationship.

$$\Delta_{CDL} = \left[\frac{1 - \eta_{CD}}{\eta_{CD}}\right] I_{sp,vac,\ delivered}$$

(c) Nozzle Kinetic Loss

The nozzle kinetic performance loss was evaluated by using the one-dimensional kinetic (ODK) option of the TDK computer program and comparing its results versus the ODE equilibrium performance for the same mixture ratio and P_c. The 37° 16' conical nozzle contour to $\epsilon = 7.38$ was used to determine the kinetic expansion rate. The kinetic loss was adjusted for each test data summary period for $P_c \neq 500$ psia by the following relationship.

IV, B, Cryogenic Propellants (cont.)

$$\Delta KL\ (P_c,\ O/F) = \Delta KL\ (500\ psia,\ O/F) + \left[\frac{d\ (\Delta KL)}{d\ P_c}\right]_{P_c = 500} (P_c - 500)$$

(d) Boundary Layer Loss

The thrust chamber boundary layer loss results from both thermal heat loss and viscous drag at the thrust chamber wall. With the regenerative hydrogen cooled thrust chamber, however, the thermal energy loss is transferred to the fuel coolant thereby increasing the fuel propellant enthalpy which effectively recovers the performance degradation due to thermal loss. The thermocouple instrumentation on the copper regeneratively cooled chamber is buried approximately 0.050 in. from the internal chamber surface. Based upon the measured average chamber heat flux and thermal conductivity of copper, it was estimated that the gas-side wall temperature was approximately 300°F hotter than the measured 200°F average buried wall temperature. The gross boundary layer performance decrement resulting from combined thermal and viscous losses was calculated using the TBL-Chart Program which is based upon the results from the JANNAF Turbulent Boundary Layer Program for an estimated 500°F steady state average gas side wall temperature. The transient wall temperature during the first data summary (0.7 to 0.8 sec) period was estimated at 340°F. The gross TBL loss ranged between 4.3 to 5.0 sec depending upon the wall temperature and mixture ratio. This loss was offset by an increase in fuel propellant enthalpy which was calculated from the measured fuel coolant flowrate and measured bulk temperature rise across the chamber. The thermal enthalpy recovery resulted in 2.1 to 3.1 sec performance recovery between the 5.0 to 6.0 O/F range. Therefore, the net boundary layer performance loss for the cooled chamber is only 1.3 to 2.0 sec as tabulated in Figure 70. Measured pressure and temperature data for all tests are summarized in Figure 71.

IV, B, Cryogenic Propellants (cont.)

(e) Mixture Ratio Maldistribution Loss

The mixture ratio maldistribution loss (MRMDL) on the OMS injector occurs as a result of two separate effects. The first effect is due primarily to a non-uniform flow distribution near the oxidizer inlet. The mixture ratio non-uniformity measured during cold flow testing of the injector in the Aerophysics Laboratory is calculated to contribute 0.3 to 0.5 sec performance loss at $\varepsilon = 7.38$.

The second source of MRMDL is due to igniter fuel cooling. To extend useful igniter life, the oxidizer flow to the igniter is terminated after injector ignition is accomplished. The fuel flowrate continues at full flow throughout the test duration to keep the igniter cool. This unreacted fuel coolant results in a performance loss by (1) shifting the core mixture ratio to a higher O/F decreasing the core I_{sp}, (2) reducing the thermal energy of the core by the amount of enthalpy required to heat the fuel coolant, and (3) increasing the kinetic loss of the core due to its higher O/F. The magnitude of the igniter fuel coolant loss is approximately 0.2 sec for the 0.7 to 0.8% fuel coolant flow rates utilized by the OMS igniter.

(f) Energy Release Loss

For conventional liquid propellant rocket injectors the energy release loss is attributed to a combined mass and enthalpy reduction from the completely vaporized and chemically reacted exhaust gas products. The JANNAF Distributed Energy Release (DER) computer program calculates the percent of fuel and oxidizer vaporized in each stream tube at the nozzle throat plane. The unvaporized propellant droplets at the throat plane are assumed to be unavailable to do gas expansion work in the nozzle and are assumed to contribute zero thrust. Furthermore, the enthalpy release due to combustion is based upon the vaporized mixture ratio instead of the injected mixture ratio.

IV, B, Cryogenic Propellants (cont.)

For the gaseous hydrogen - gaseous oxygen OMS injector, the incoming propellants are already completely vaporized, and it is not possible to incur a gas phase mass reduction as with liquid propellant injectors. Therefore, gaseous propellant energy release performance losses can only be attributed to an enthalpy reduction which differs from the JANNAF methodology.

If the local injection mixture ratio everywhere within the combustor were completely uniform and homogeneous in pressure, temperature and chemical species, the enthalpy reduction could only occur due to chemical reaction rate limitations. However, chemical reaction rates of gaseous hydrogen - gaseous oxygen are sufficiently fast above 4500°F ($3 < O/F < 30$) that this would be a second order effect. On the other hand, deviations in local mixture ratio from the overall injection mixture ratio would result in incomplete combustion enthalpy release, added thermal dissociation, and non-optimum chemistry so that the mass weighted sum of the enthalpies of all stream tubes is less than the enthalpy which would result from a homogeneous mixture. Thus, a local micro-scale mixture ratio non-uniformity has a first-order effect on gaseous hydrogen - gaseous oxygen energy release efficiency and is considered to be the rate controlling energy release mechanism for the OMS injector.

Because of the complexity of the energy release process, no analytical model is currently available which will reliably predict gas/gas energy release efficiency from design and operation conditions without empirical data. Therefore, the empirical energy release loss (ERL) of the OMS injector is determined by subtracting all of the above calculated losses from the difference between theoretical thermochemical and delivered specific impulse.

$$\Delta ERL = [I_{sp,\ ODE} - I_{sp,\ del}] - \Delta CDL - \Delta KL - \Delta BLL - \Delta MRMDL$$

IV, B, Cryogenic Propellants (cont.)

The absolute magnitude of steady state ERL (neglecting the first data summary period) for the three 5 sec duration tests was between 2.3 to 4.6 sec. The earliest data summary period is unreliable because of transient thermal losses to the copper chamber which are not accurately reflected in the boundary layer loss and because of variable fuel density and variable fuel capacitance in the series regen chamber volume which makes the injected fuel flow rate at the injector face differ from the measured fuel flow rate at the venturi due to varying hydrogen temperature.

The injection element mixing efficiency can be characterized by the parameters, E_m, which is a measure of the mass weighted average micro-scale mixture ratio deviation from the mean injection O/F. A simplified energy release mechanism can be postulated by assuming the injector is divided into two discrete stream tubes. One stream tube is assumed to be lower than the uniform overall injection mixture ratio by the factor E_m; the other stream tube is assumed to be higher than the nominal O/F by the reciprocal of E_m. Using this simplified model, the element mixing efficiency of the OMS injector is 0.84 at the cooled chamber nozzle exit area ratio, $\varepsilon = 7.38$. This agrees almost identically to the mixing efficiency derived from previous copper heat sink chamber testing at $\varepsilon = 2.7$. If the effects of the oxidizer manifold injection mixture ratio maldistribution and igniter fuel coolant maldistributions are combined with the ERL, the overall injector mixing efficiency is reduced to $E_m = 0.82$.

(g) Extrapolated (ε = 240:1) Performance

A performance extrapolation was made for nominal design P_c = 500 psia, O/F = 6.0, ε = 240:1 (Rao), and fuel and oxidizer inlet propellant temperatures at their respective saturated liquid normal boiling points. For these conditions the cooled chamber performance data extrapolation suggests that a realistic nominal performance for vacuum flight conditions

IV, B, Cryogenic Propellants (cont.)

is 455 lb_f-sec/lb_m I_{sp}. This value is unchanged from the earlier results of the uncooled copper heat sink chamber performance data extrapolation. In the earlier performance extrapolation, the $\varepsilon = 240$ nozzle kinetic loss was evaluated at the core mixture ratio and the % ERL at $\varepsilon = 240$ was assumed equal to the % ERL at $\varepsilon = 2.7$. However, in view of the constant mixing efficiency extrapolation for ERE, the % ERL will be lower at $\varepsilon = 240$ than at $\varepsilon = 2.7$ due to the shift in the maximum I_{sp} versus O/F to higher mixture ratio resulting from added nozzle recombination effects. However, the improvement in predicted flight ERE is offset by a higher two stream tube kinetic loss which is in consonance with the E_m mixing model. The net effect is that both effects nearly cancel each other at O/F = 6. The $\varepsilon = 240$ performance extrapolation will be slightly higher at O/F = 5.0, but predicted performance will be lower at O/F = 7. The exact magnitude of the differences in method of extrapolation will require additional analysis. The results of the cooled chamber tests are summarized in Figure 72.

(3) Thermal Data

As has been stated previously the copper heat sink chamber with surface thermocouples was used to obtain heat flux data for the design of the regeneratively cooled chamber. It was found in this work that the experimentally determined heat flux agreed very well with the currently used prediction techniques. The throat heat flux, for a 1000°F wall, was found to be 29 Btu/$in.^2$-sec under the same wall conditions. These data then were used for the design of the regeneratively cooled chamber.

It was necessary to assume that the heat flux in the chamber was a constant since there was no copper data taken in the cylindrical section. Obviously, this is a conservative assumption since it is well known that the heat flux near the injector will be less than near the convergent section of a nozzle.

IV, B, Cryogenic Propellants (cont.)

The OMS test program consisted of four test firings at or near the nominal conditions of 500 psi and MR = 6. The durations of these tests were approximately 0.5 sec for test 101 and 5 sec for tests 102, 103 and 104. In each of these tests the data indicated that the chamber was operating near steady-state conditions at the end of the test. The test conditions are summarized as follows:

Test No.	P_c psia	MR	W_{ox}, lb/sec	W_f, lb/sec	P_{inlet}, psi	T_{inlet}, °R	P_{inlet}, psi	T_{inlet}, °R
5K-3-101	537	5.08	9.36	1.83	1160	196	585	-
5K-3-102	531	4.94	9.13	1.84	1145	178	574	493
5K-3-103	496	5.85	0.05	1.53	1059	238	542	495
5K-3-104	499	5.322	8.83	1.65	1082	213	540	495

Each of the parameters listed above were, of course, recorded continuously during the test. In addition to these parameters there were thermocouples imbedded 0.050 in. to 0.060 in. below the gas-side surface between channels.

A comparison of important parameters between predicted and test is shown in the following.

Parameter	Prediction	Data			
		101	102	103	104
Pressure Drop	251.3*	493	479	445	459
Bulk Temperature Rise	420.7	269	290	316	302

*Total Pressure Loss

IV, B, Cryogenic Propellants (cont.)

Two things become apparent from this table; first the test pressure drop is higher than predicted and secondly the bulk temperature rise is lower. The latter effect is not altogether surprising in light of the conservative assumptions with regard to the heat flux discussed above. However, the pressure drop does cause some concern.

Cause of the excessive pressure drop is, at this time not definitely established. It is possible that the geometry of the channels was altered during the braze cycle as has been experienced on other programs at ALRC. It is also possible that the surface roughness is higher than expected. However, visual inspection of fabrication samples tend to discount these two possibilities.

A possible explanation for the excessive pressure drop being experienced is that the flow in the channels is experiencing local areas of Mach 1 caused by small disturbances in the surface such as a metal chip or other particle. This could cause essentially a choking of flow even though the predicted maximum mach number is 0.430. This same effect may be occurring in the cold flow testing. In this case the maximum mach number was predicted to be 0.487.

Wall surface thermocouples exhibited readings that were generally lower than were predicted before the firings. This is attributed to both the lower than expected heat flux in the chamber and the higher than expected channel velocities due to the higher than expected ΔP.

Conclusions and recommendations: The following conclusions were reached.

(a) The assumption of a constant heat flux in the cylindrical chamber is conservative.

IV, B, Cryogenic Propellants (cont.)

(b) Test pressure drops are higher than predicted. The reason is not apparent but may possibly be attributed to local regions having Mach 1 flow.

(c) Work should be continued to understand the reason for the high ΔP.

4. Conclusions and Recommendations

a. Conclusions

The basic conclusion derived from the Phase II portion of the program is that the techniques used both in performance prediction and component design were generally adequate. Consequently, future programs embodying similar design concepts may be planned with a high degree of confidence.

Although all of the program objectives were achieved, a comparative analysis of test results with respect to prediction indicates that some of the techniques are more precise than others. A qualitative assessment is as follows:

(1) Performance - Good

Injector performance was predicated to be 98% of ERE and test results indicate 99%.

(2) Compatibility - Good

Prediction agrees with test results.

IV, B, Cryogenic Propellants (cont.)

(3) Stability - Good

Injector demonstrated stable operation over operating range of MR 5.0 to 7.0. Instability at lower MRs may be due to low pressure differential across oxidizer elements.

(4) Heat Transfer - Fair

Pressure drop higher than predicted.

(5) Design and Fabrication - Good

Successful completion of both injector and chamber on "first try" with no scrappage attests to adequacy of design and fabrication techniques developed under this contract.

b. Recommendations

Recommendations are divided into two general categories.

(1) Those which are directly related to the work accomplished under this contract and would have been accomplished if funding had permitted and (2) work related to follow on effort which would apply to the technology required for an engine system.

Examples of the former are:

(1) Continuation of regeneratively cooled chamber and injector tests at design MR of 6 and at off MR conditions. These tests were planned for the program but were not conducted because of funding limitations.

IV, B, Cryogenic Propellants (cont.)

(2) Life cycle testing with objective of establishing chamber life capability with respect to chamber wall temperature.

(3) Extensive flow testing, and if necessary, sectioning of regeneratively cooled combustion chamber to definitely establish the cause of the high pressure drop. Manufacture and test of one additional chamber were based upon results of this investigation.

Additional effort falling in the latter category is:

(1) Development of an igniter capable of being used with the OMS injector with a low (20 psia) propellant supply pressure.

(2) Design, fabrication and test of a regeneratively cooled combustion chamber/injector which eliminates forward manifold, i.e., feeds directly into injector.

(3) Design, fabricate, and test oxidizer regeneratively cooled expansion skirt section.

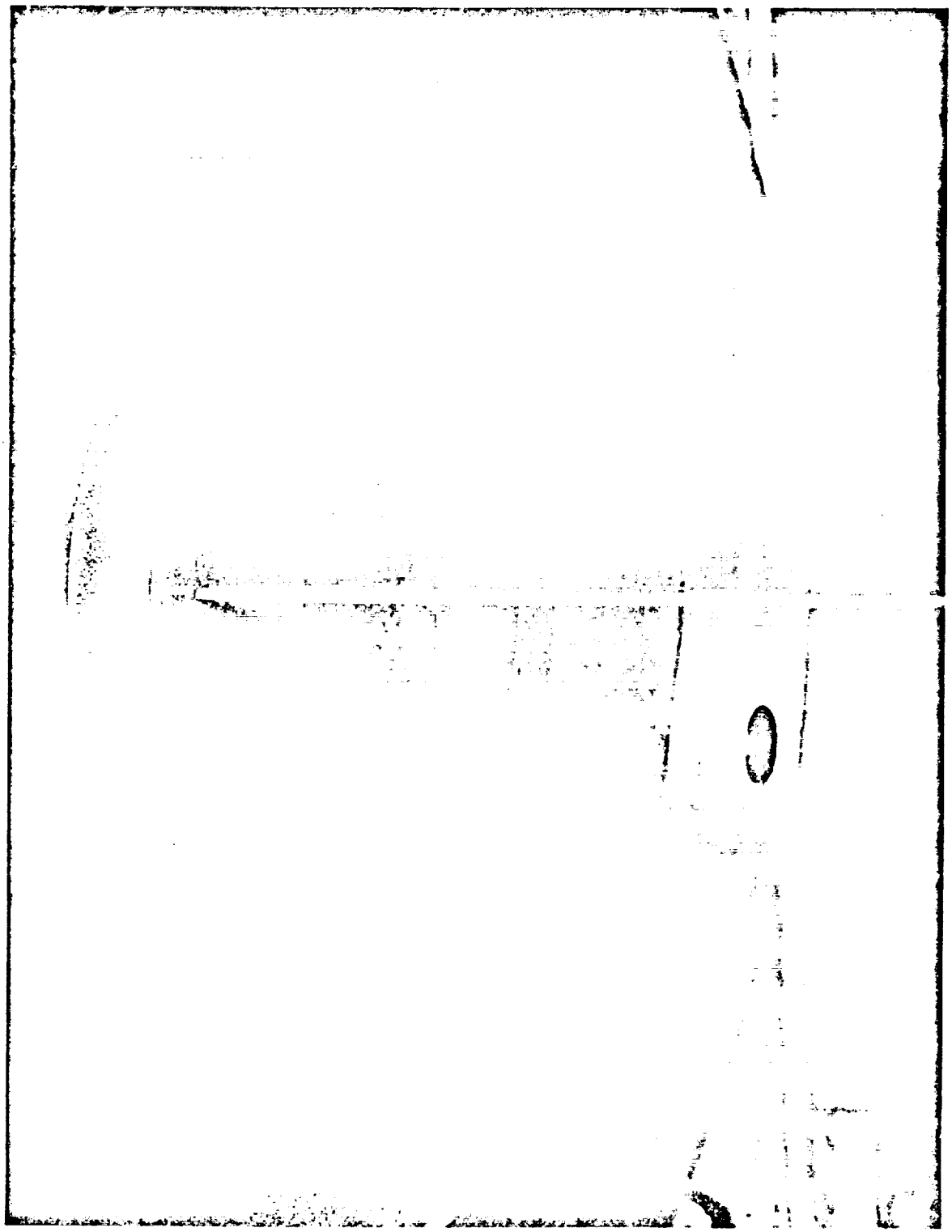

Plate 1XB, ΔP = 30 psi

Figure 1

Element or Plate	L/D	Diameter, in.	Configuration and Manufacturing Technique
1X	3	0.0528	Contoured inlet (inlet radius at least twice orifice radius). Drilled using slow feed and high speed (best machining practice).
2X	3	0.0521	Same configuration but manufactured using fast feed low tool speed (worst machining practice)
3X	3	0.0532	Same configuration and manufactured same as 1X but made under size and then etched to proper diameter.
4X	3	0.0533	Same as 3X except machining operation conducted with fast feed slow speed.
5X	3	0.0515	Sharp-edged inlet drilled with a slow feed and high tool speed.
5X1	3	0.0514	Same except drilled with a high feed and slow drill speed.
5XB	3	0.0513	Same hole as 5X except purposely scored after drilling.
6X	3	0.0537	Drilled undersize with slow feed and high tool speed, then etched to proper diameter.
7X	3	0.0523	Same as 6X except drilled using fast feed and slow tool speed.
8X	3	0.0508	Eloxed using Aerojet-General equipment.
9X	3	0.0531	Eloxed undersize and then etched to proper diameter.
10X	3	Outlet 0.0530 Inlet 0.0558	Eloxed to proper diameter, plugged from outlet side with wax and inlet etched.
6R	1.4	0.0575	Eloxed, manufactured by NASA.
8R	1.6	0.0497	Eloxed, manufactured by NASA.
10R	1.6	0.0450	Eloxed, manufactured by NASA.
1XB	3	0.0528	Same as 1X except scored after drilling.
3XA	3	Outlet 0.0524 Inlet 0.0544	Same as 10X except longer etch period.
7XA	3	Outlet 0.0524 Inlet 0.0586	Same as 3XA except longer etch period.

Injector Element Test Program Plate or Element Identification

Figure 2

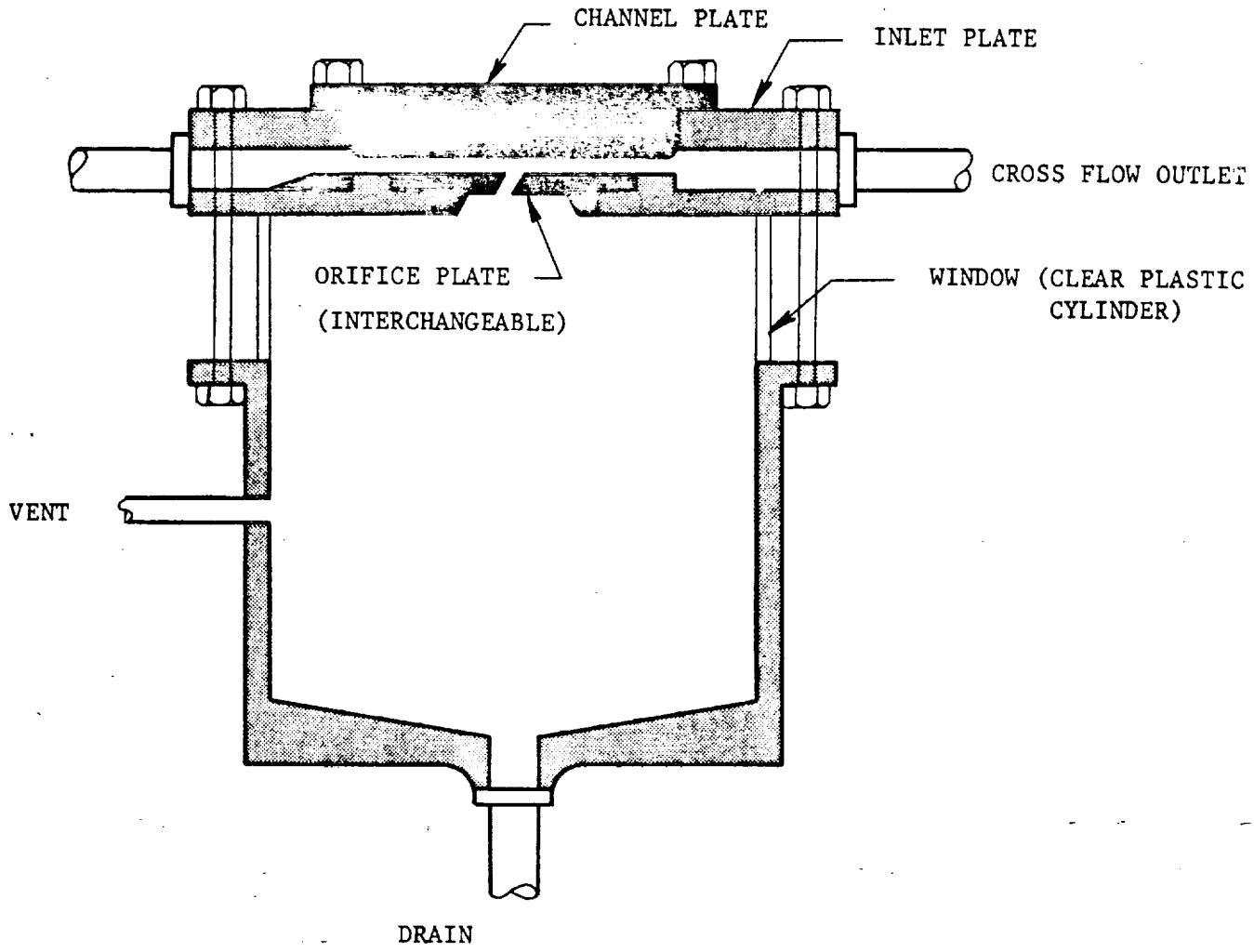

Injector Element Test Fixture Schematic

Figure 3

PLATE 1XB

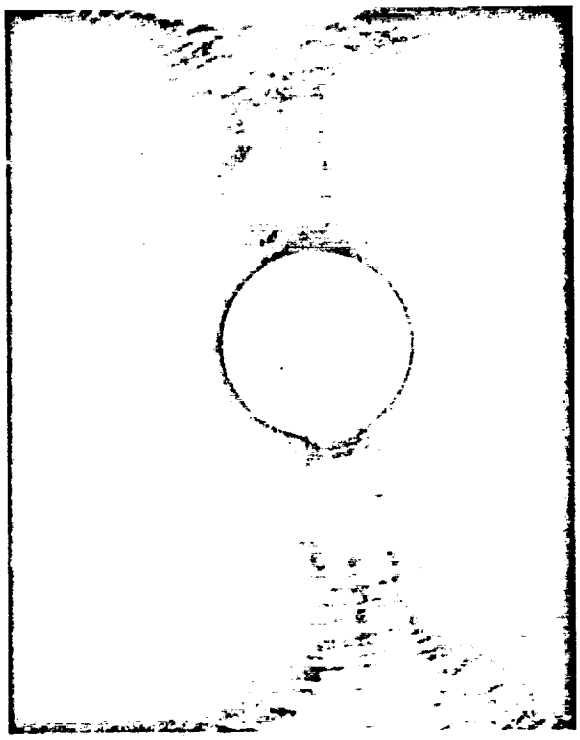

PLATE 2X

Plates 1XB and 2X

Figure 4

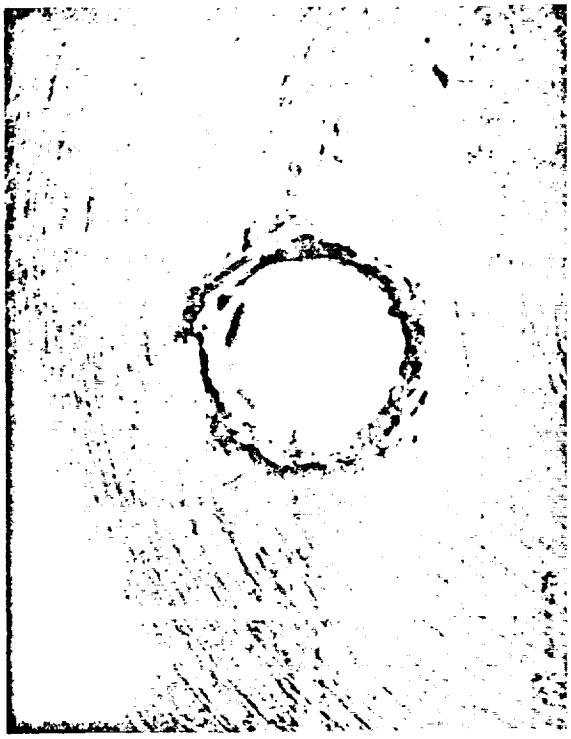

PLATE 5XB

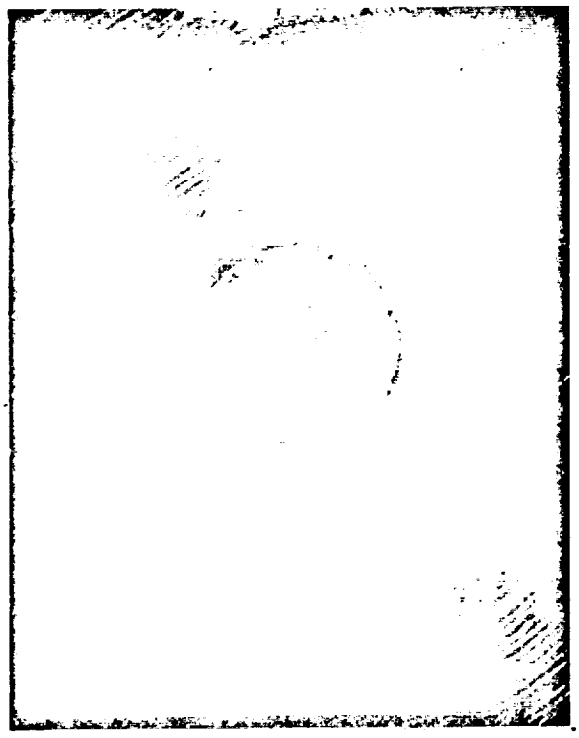

PLATE 6R

Plates 5XB and 6R

Figure 5

IOS (SN 135) OPERATING CHARACTERISTIC	PROBABLE CAUSE	PLANNED MODIFICATIONS IOS, POUL 21-5	PLANNED MODIFICATIONS POUL 41-63
1. HIGH PERFORMANCE (319 ± 2 SEC I_S VS 313 FOR SPS)	(A) FINE PATTERN, 955 ELEMENTS. (B) SPRAY OVERLAP. (C) MIXTURE RATIO DISTRIBUTION. (D) CONTOURED INLET OF ORIFICES.	NONE	(A) COARSER PATTERN TO IMPROVE STABILITY INDEX. 610 ELEMENTS. SAME % SPRAY OVERLAP, MRD AND ORIFICES. PREDICTED PERFORMANCE 317 ± 1 SEC I_S.
2. GOOD COMPATIBILITY INDICATIONS	(A) 5% FILM COOLING (B) BARRIER OF OUTER ELEMENTS	NONE	(A) FUEL RICH SIDE OF OUTER ELEMENT STREAM TUBES ADJACENT TO WALL. (B) REDUCED DYNAMIC FORCES AGAINST BAFFLES. (C) SAME % FILM COOLANT.
3. ROUGH START	OXIDIZER FLOW DISTRIBUTION PLATES	REMOVE	REMOVE
4. INTERMEDIATE FREQUENCY (850 - 1200 CPS) COMBUSTION INSTABILITY	OXIDIZER FLOW DISTRIBUTION PLATES	REMOVE	REMOVE
5. HIGH FREQUENCY (5000 - 7000 CPS) COMBUSTION INSTABILITY INDUCED FROM SIDE BOMB AND INTERMEDIATE FREQUENCY.	INSTABILITY FREQUENCY BEYOND DAMPING CAPABILITY OF BAFFLES AND INJECTION DISTRIBUTION.	ACOUSTIC RESONATOR	LOWER SENSITIVE TIME LAG AND COMBUSTION FREQUENCY BY COARSER PATTERN. SAME BAFFLE ASSEMBLY AND INJECTION DISTRIBUTION.
6. POPS - LOW AMPLITUDE << 25 PSI AT A HIGH FREQUENCY ≈ 1/SEC.	LOW AMPLITUDE MAY BE A RESULT OF IMPROVED MIXING. TRIGGER NOT KNOWN.	REMOVE DISTR. PLATES, SPOT FACE ORIFICE.	REMOVE OX. DISTR. PLATES, SPOT FACE ORIFICE.

Figure 6

Report NASA 108581

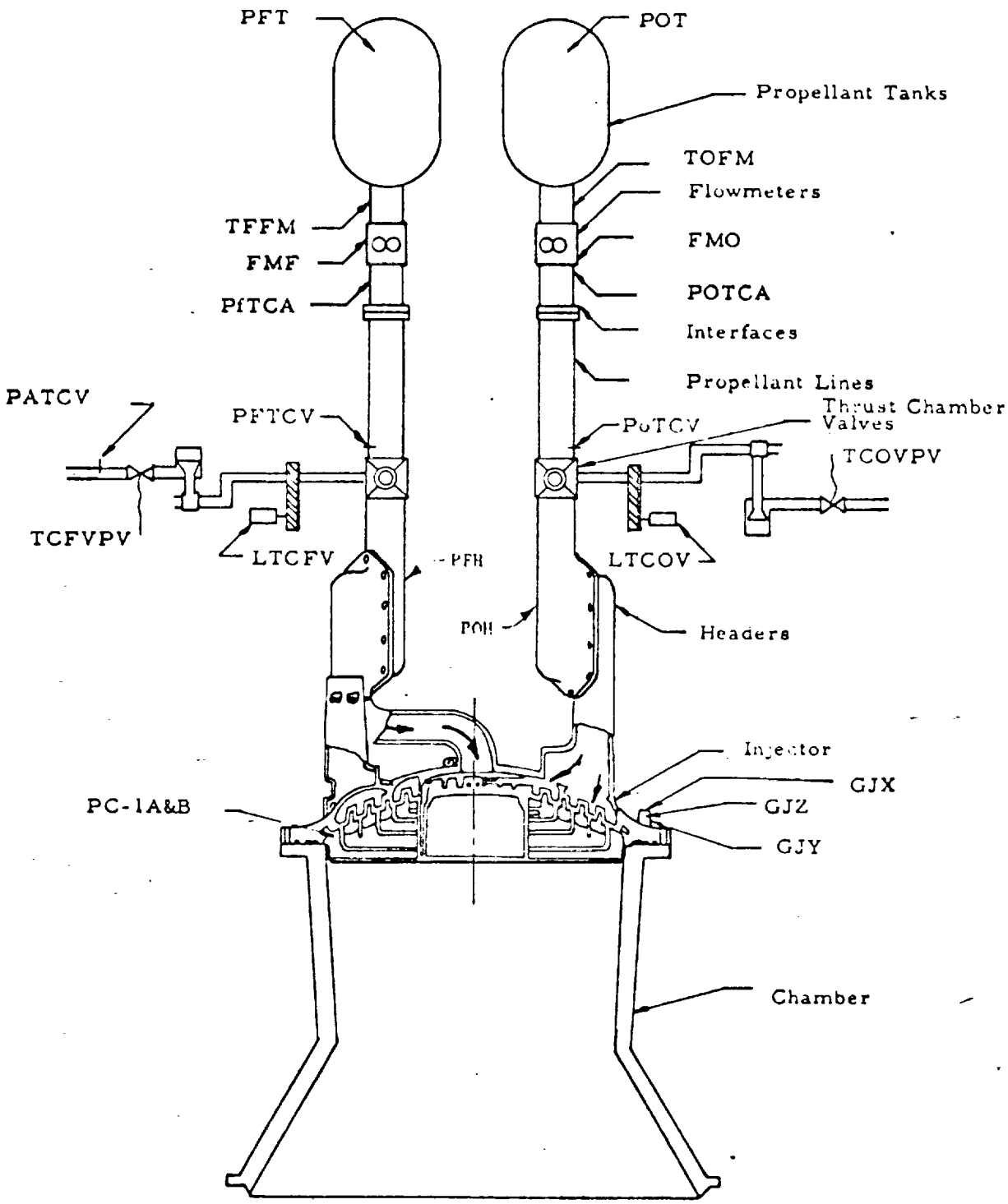

Instrumentation Location Schematic

Parameter	Symbol	Transducer	Oscillograph	Strip Chart	ADC	Magnetic Tape	Suggested System Range	Frequency Response, cps	*System Recording Accuarcy (1σ)
Thrust, A	FA	Strain Gage, Force	X	X	X		0-20K-lb	0-100	± 0.19%
Thrust, B	FB	Strain Gage, Force	X		X		0-20K-lb	0-100	
Chamber Pressure, A	PC-1A	Strain Gage, Pressure	X	X	RS	X	0-100 psig	0-400	± 0.1%
Chamber Pressure, B	PC-1B	Strain Gage, Pressure	X	X	RS		0-100 psig	0-400	
Chamber Pressure High Frequency	P_c-5P-1 thru P_c-5P-7	Photocon				X	0-500 psig	0-10,000	± 5.0%
Fuel, Interface Pressure, Downstream	PFTCA-2M	Micro Systems				X	0-500 psig	0-20,000	± 3.0%
Oxidizer, Interface Pressure, Downstream	POTCA-2M	Micro Systems				X	0-500 psig	0-20,000	± 3.0%
Oxidizer, Interface Pressure, Upstream	POTCA-1M	Micro Systems				X	0-500 psig	0-20,000	± 3.0%
Fuel, Interface Pressure, Upstream	PFTCA-1M	Micro Systems				X	0-500 psig	0-20,000	± 3.0%
Oxidizer, Interface Pressure, Upstream	POTCA-1A	Strain Gage, Pressure	X	X	X		0-250 psig	0-400	± 0.1%
Oxidizer, Interface Pressure, Upstream	POTCA-1B	Strain Gage, Pressure	X	X	X		0-250 psig	0-400	
Fuel, Interface Pressure, Upstream	PFTCA-1A	Strain Gage, Pressure	X	X	X		0-250 psig	0-400	± 0.1%
Fuel, Interface Pressure, Upstream	PFTCA-1B	Strain Gage, Pressure	X	X	X		0-250 psig	0-400	

Engine Instrumentation Requirements

Figure 8, Sheet 1 of 6)

Report NASA 108581

Parameter	Symbol	Transducer	Oscillograph	Strip Chart	ADC	Magnetic Tape	Suggested System Range	Frequency Response, cps	*System Recording Accuracy (1σ)
Oxidizer Tank Pressure	POT	Strain Gage, Pressure	X	X	X		0-250 psig	0-400	± 1.0%
Fuel Tank Pressure	PFT	Strain Gage, Pressure	X	X	X		0-250 psig	0-400	± 1.0%
Oxidizer, Flow Rate	FMO	Flow Meter, Turbine 2-1/2 in.	X	X	X		0-250 lb-sec		± 0.28%
Fuel, Flow Rate	FMF	Flow Meter, Turbine 2-1/2 in.	X	X	X		0-50 lb-sec		± 0.32%
Oxidizer Temperature Flowmeter	TOFM	Resistance Temperature Transducer (RTT)			X		0-200°F		± 0.2°F
Fuel Temperature Flowmeter	TFFM	Resistance Temperature Transducer (RTT)			X		0-200°F		± 0.2°F
Oxidizer, Bipropellant Valve Lower Bore Inlet Pressure	POTCV 1A(M)	Micro Systems				X	0-500 psig	0-10,000	± 0.25%
Oxidizer, Bipropellant Valve Upper Bore Inlet Pressure	POTCV 1B(M)	Micro Systems				X	0-500 psig	0-10,000	± 0.25%
Fuel, Bipropellant Valve Lower Bore Inlet Pressure	PFTCV 1A(M)	Micro Systems				X	0-500 psig	0-10,000	± 0.25%
Fuel, Bipropellant Valve Upper Bore Inlet Pressure	PFTCV 1B(M)	Micro Systems				X	0-500 psig	0-10,000	± 0.25%

Engine Instrumentation Requirements

Figure 8, Sheet 2 of 6

Parameter	Symbol	Transducer	Oscillograph	Strip Chart	ADC	Magnetic Tape	Suggested System Range	Frequency Response, cps	*System Recording Accuracy (1σ)
Fuel Manifold Pressure	P_{fj}-1	Strain Gage, Pressure	X		X		0-250 psig	0-400	± 1.0%
Fuel Manifold Pressure	P_{fj}M-1	Micro Systems				X	0-500 psig	0-10,000	± 1.0%
Oxidizer Manifold Pressure (Outer)	P_{oj}-1	Strain Gage, Pressure	X		X		0-250 psig	0-400	± 1.0%
Oxidizer Manifold Pressure (Outer)	P_{oj}M-1	Micro Systems				X	0-500 psig	0-10,000	± 1.0%
Oxidizer Manifold Pressure (Inner)	P_{oj}-2	Strain Gage, Pressure	X		X		0-250 psig	0-400	± 1.0%
Oxidizer Manifold Pressure (Inner)	P_{oj}M-2	Micro Systems				X	0-500 psig	0-10,000	± 1.0%
Oxidizer Manifold Pressure (Outer)	P_{oj}-3	Strain Gage, Pressure	X		X		0-250 psig	0-400	± 1.0%
Oxidizer Manifold Pressure (Outer)	P_{oj}M-3	Micro System				X	0-500 psig	0-10,000	± 1.0%
Fuel Channel Pressure (opposite baffle)	P_{fj}-15A	Strain Gage, Pressure	X		X		0-250 psig	0-400	± 1.0%
Fuel Channel Pressure (between baffles)	P_{fj}-15B	Strain Gage, Pressure	X		X		0-250 psig	0-400	± 1.0%
Fuel Manifold Temperature	T_{fj}-1	Thermocouple			X		0-500°F	-	± 1°F
Oxidizer Manifold Temperature (Outer)	T_{oj}-1	Thermocouple			X		0-500°F	-	± 1°F

Engine Instrumentation Requirements

Figure 8, Sheet 3 of 6

Report NASA 108581

Parameter	Symbol	Transducer	Oscillograph	Strip Chart	ADC	Magnetic Tape	Suggested System Range	Frequency Response, cps	*System Recording Accuracy (1σ)
Oxidizer Manifold Temperature (Inner)	T_{oj}-2	Thermocouple			X		0-500°F	-	± 1°F
Oxidizer Manifold Temperature (Outer)	T_{oj}-3	Thermocouple			X		0-500°F	-	± 1°F
Fuel Channel Temperature (opposite baffle)	T_{fj}-15A	Thermocouple	X		X		0-500°F	-	± 1°F
Fuel Channel Temperature (between baffles)	T_{fj}-15B	Thermocouple	X		X		0-500°F	-	± 1°F
Chamber Temperature (Steel)	T_{cc}-1	Thermocouple		X	X		0-500°F	-	± 5°F
Resonator Ring Temperature	T_R-1 thru T_R-5	Thermocouple			X		Ambient to 2500°F	-	± 5°F
Resonator Ring Temperature	T_R-1	Thermocouple		X	X		Ambient to 2500°F	-	± 5°F
Pressure, Oxidizer Header	POH	Strain Gage, Pressure	X		X		0-250 psig	0-400	± 1.0%
Pressure, Fuel Header	PFH	Strain Gage, Pressure	X		X		0-250 psig	0-400	± 1.0%
Actuation Pressure, Bipropellant Valve, Source	PGAS-A, -B	Strain Gage, Pressure	X	X	X		0-3000 psig	0-400	± 1.0%

Engine Instrumentation Requirements

Figure 8, Sheet 4 of 6

Parameter	Symbol	Transducer	Oscillograph	Strip Chart	ADC	Magnetic Tape	Suggested System Range	Frequency Response cps	*System Recording Accuracy (1σ)
Actuation Pressure, Bipropellant Valve, Regulator Outlet	PGAR-A, -B	Strain Gage, Pressure	X		X		0-500 psig	0-400	± 1.0%
Pressure, Oxidizer Header	POH-M	Micro Systems				X	0-500 psig	0-10,000	± 1.0%
Pressure, Fuel Header	PFH-M	Micro Systems				X	0-500 psig	0-10,000	± 1.0%
Position Bipropellant Valve No. 1	LTCV-1, 1a	Potentiometer	X						± 1.0%
Position Bipropellant Valve No. 2	LTCV-2, 2a	Potentiometer	X						± 1.0%
Position Bipropellant Valve No. 3	LTCV-3, 3a	Potentiometer	X						± 1.0%
Position Bipropellant Valve No. 4	LTCV-4, 4a	Potentiometer	X						± 1.0%
Fire Switch Signal	FS	Direct	X	X	X	X			
Stability Monitor (GJY)	CSM	Direct	X	X	X	X			
Bipropellant Valve Pilot Current Trace	TCVPV B1 B2,B3,B4	Direct	X						
Injector Radial Acceleration	GJY-1	Accelerometer				X	0-500 RMS	0-10,000	± 2.0%
Injector Axial Acceleration	GJX-1	Accelerometer				X	0-500 RMS	0-10,000	± 2.0%

Engine Instrumentation Requirements

Parameter	Symbol	Transducer	Oscillograph	Strip Chart	ADC	Magnetic Tape	Suggested System Range	Frequency Response, cps	*System Recording Accuracy (σ)
Injector Tangential Acceleration	GJZ-1	Accelerometer				X	0-500 RMS	0-10,000	± 2.0%
Injector Radial Acceleration	GJY-2	Accelerometer				X			
	GJY-3	Accelerometer							
	GJY-4	Accelerometer				X			
Bipropellant Valve 2-Way Enable Valve Current Trace	TCVPV A1 & A2	Direct	X						
Bipropellant Valve Pilot Valve Voltage	EPV	Direct	X				0-30 VDC		± 1.0%
Bipropellant Valve Pilot Valve Current	IPV	Direct	X				0-10 AMPS		± 1.0%
Barometric Pressure	PA	Direct		X					± 0.2%
Temperature Ambient	TA	Direct		X					± 1°F

*Percent accuracy values are applied to the Suggested System Full Scale range only.

Engine Instrumentation Requirements

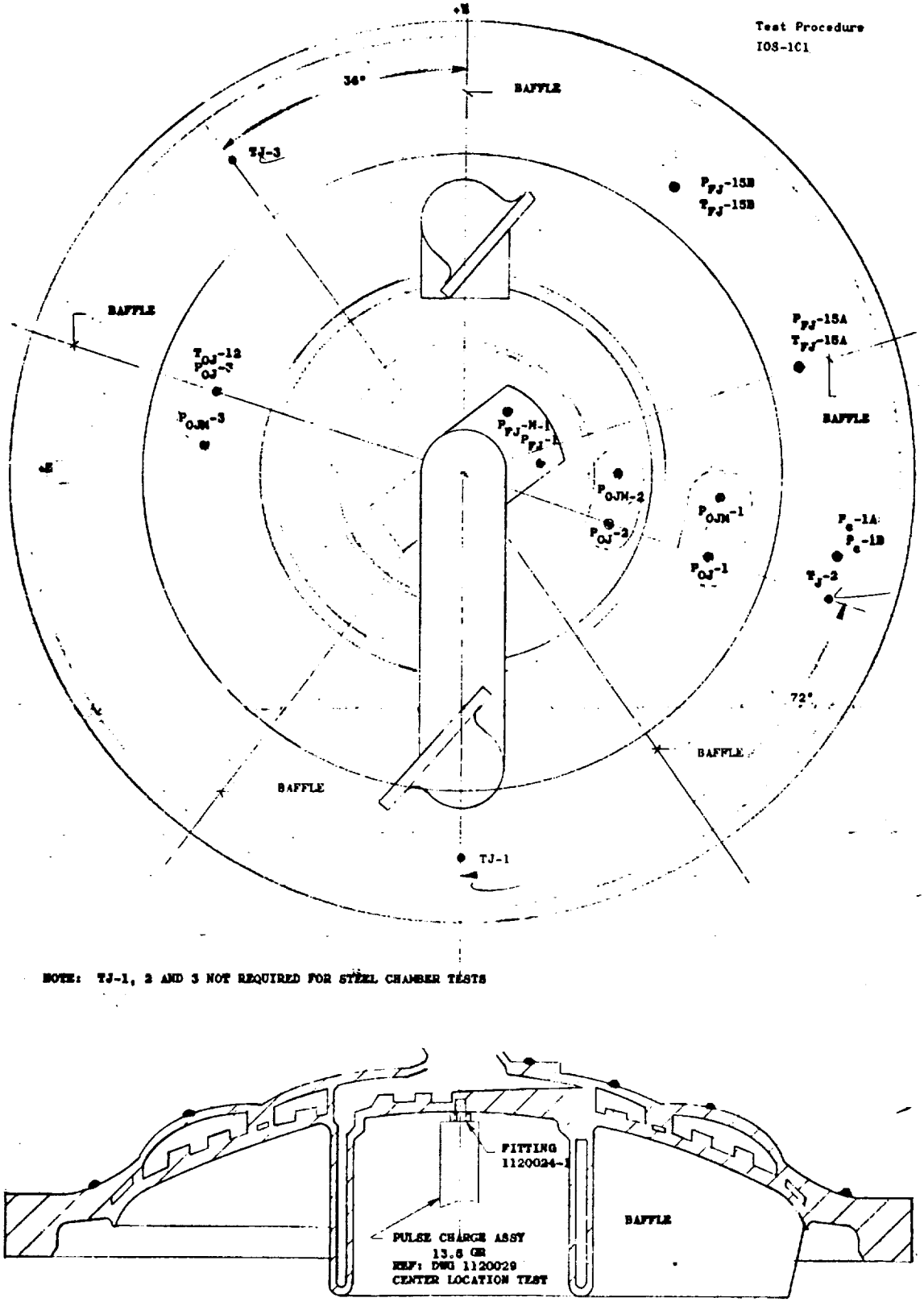

Injector Thermocouple Locations, IOS TCA Test

Figure 9

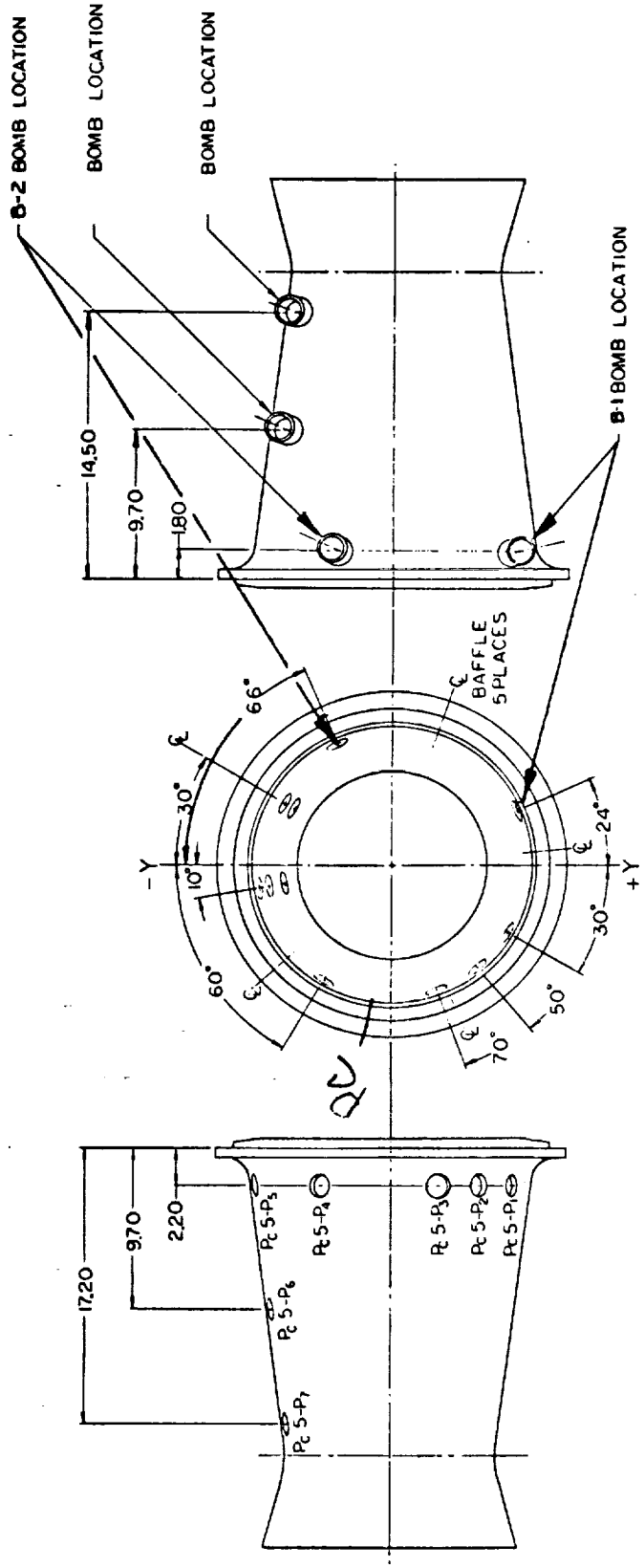

Workhorse Thrust Chamber

Figure 10

Test	Date	Duration	P_c	MR	T_o	T_F	No. Pops	Pops sec	Helium	Reson Ring	T.C.	Bombs	I_s	Remarks
1.2-18-DAJ-001	3/1/69	5.499	97.0	1.597	58.7	59.0	27	4.9	No	No	ST 003	No	319.97	First test after removing oxidizer distribution plates. Similar to previous tests. Intermediate frequency on start only.
-002	3/3/69	4.828	99.3	1.678	68.5	67.8	15	3.1	No	No		No	320.93	CSM caused by pop at 7000 cps. Same characteristics as Test 001
-003	3/5/69	5.612	98.3	1.601	78.3	78.4	28	5.0	Yes	No		No	319.78	Helium saturation by bubble through technique. Football throughout test.
-004	3/5/69	5.825	98.9	1.614	75.4	76.6	28	4.8	Yes	No	ST 003	No	319.28	No football final 2 sec. Repeat test may indicate bleed-in procedure 003 football related.
-005	3/11/69	2.223	99.5	1.602	72.1	70.6	9	4.1	No	No	ST 001	No	N/A	Baffle tip clearance reduced from ≈ 0.100 to ≈ 0.020. CSM at 7000 cps growing out of 850 cps.
-006	3/11/69	5.293	97.7	2.049	73.5	69.6	31	5.9	No	No		No		High MR test to evaluate pop rate. Rate slightly higher than at nominal conditions.
-007	3/11/69	5.397	75.0	1.579	73.8	70.7	58	10.7	No	No		No		Low P_c test to compare with NAS9-6925. Removal of oxidizer plates no improvement. 800 cps ± 15 psi throughout.
-008	3/13/69	1.292	99.2	1.587	71.9	71.1	1	0.8	No	No		No		CSM at 7000 cps growing out of 800 cps. 400/4000 frames/sec movie coverage. Pop origin not conclusive.
-009	3/13/69	3.317	96.2	2.526	73.6	71.8	0	0	No	No		No		High MR with movie coverage. No pops.
-010	3/13/69	1.333	100.4	1.636	68.5	69.5	1	0.8	No	No		No		CSM after pop. Movie coverage did not define pop origin.

IOS Full-Scale Injector Test Summary

Figure 11, Sheet 1 of 4

76

Report NASA 10851

Test	Date	Duration	P_c	MR	T_o	T_F	No. Pops	Pops sec	Helium	Reson Ring	T.C.	Bombs	I_s	Remarks
1.2-18-011-1	5/16/69	0.990	-	-	-	-	0	0	No	No	ST 001	Yes	N/A	CSM at 7000 cps with 6.5 grain side bomb. Suspect poor bleed-in.
1.2-18-011-2	5/16/69	2.639	99.3	1.623	78.8	78.7	4	1.5	No	No		Yes		CSM at 7000 cps with second 6.5 grain side bomb. Recovers from center but not side bombs.
1.2-18-011-3	5/16/69	5.314	99.5	1.630	79.1	81.2	6	1.1	No	No		No		Typical nominal condition test without bombs.
1.2-18-012	5/16/69	5.113	97.9	0.977	78.6	84.3	0	0	No	No		No		Low MR test with no pops. Tends to substantiate pop model.
1.2-18-013	5/16/69	5.523	97.2	1.602	102.7	103.8	2	0.4	No	No		No		High-temperature test. Two small pops.
1.2-18-014	5/16/69	0.991	Nom	Nom	-	-	1	1.0	No	No		Yes		Repeat of Test 011-1 because of reported poor bleed. CSM with first side bomb. Same results as 011-1.
1.2-18-015	5/19/69	5.404	99.3	1.634	48.7	46.9	0	0	No	No		No		Low-temperature test with no pops. Agrees with pop model.
1.2-18-016	5/22/69	1.1 CSM	-	-	-	-	-	-	No	Multiple Orifice		Yes		First test with resonator. CSM with first side bomb. Baffle tip clearance approximately 0.25 in.
1.2-18-017	6/11/69	5.131	97.0	1.577	64.5	63.8	1	0.2	No			Yes		Weld buildup resonator to reduce baffle tip clearance to 0.020. Recovery from all bombs (6.5, 13.0, 6.5).
1.2-18-DAJ-018	6/12/69	5.285	66.9	1.365	67.2	66.3	2	0.4	No			Yes		Low P_c, high MR test. Recovered from all pulse charges (3). Combustion oscillations at 750 cps $\pm$ 5 psi.
1.2-18-DAJ-019	6/12/69	5.528	73.8	1.580	71.0	71.5	7	1.3	No			Yes		Low P_c, nom MR test. Recovery from all bombs. 850 cps $\pm$ 4.5 psi oscillations. Apertures eroded.
-020	6/12/69	3.210	77.7	1.388	73.2	74.4	2	0.6	No	Multiple Orifice		Yes		Low P_c, low MR test. Recovery from all bombs. 850 cps $\pm$ 2.5 psi oscillations.

IOS Full-Scale Injector Test Summary

Figure 11, Sheet 2 of 4

Test	Date	Duration	P_c	MR	T_o	T_F	No. Pops	Pops sec	Helium	Reson Ring	T.C.	Bombs	I_s	Remarks
1.2-18-DAJ-021	6/12/69	2.352	74.4	1.424	63.7	69.0	-	-	Yes	Multiple Orifice	ST 001	Yes	N/A	Low P_c, low MR test. With helium sat. Recovery first bomb, CSM second (center bomb). No tape data.
-022	6/12/69	2.175	74.2	1.379	61.2	67.8	2	0.9	Yes	Multiple Orifice	ST 001	Yes		Repeat of Test 021. CSM with second pulse at 7000 cps. 400 cps ± 25 psi football throughout test.
1.2-18-DAJ-023	6/16/69	50.400	115.8	1.605	74.9	73.5	3	0.06	No	No	ABL-354	No		50-sec ablative test at high P_c. Slight streak in line with P_c pocket. Smooth combustion
-024	6/16/69	250.741	115.2	1.594	69.6	74.8	6	0.02	No	No	ABL-354	No		250-sec ablative test at high P_c. Streak increased to 1 in. deep. Small gouges. Plugged fuel orifice.
-025	10/29/69	3.208	99.0	1.690	61.1	61.7	5	1.6	No	Slotted	ST 001	Yes		First engine test on C-11. Slotted resonator. Recovered from all (3) pulse charges.
-026	10/29/69	1.194	99.0	1.589	70.8	70.0	1	0.8	Yes			Yes		Repeat of 025 with helium. CSM at 7000 cps with first bomb.
-027	10/30/69	3.501	73.5	1.406	63.5	63.4	9	2.6	No			Yes		Low P_c, low MR test; no helium. Recovered from all (3) pulse charges. 900 cps ± 30 psi oscillations.
-028	10/30/69	2.804	74.9	1.379	78.2	77.6	6	2.1	Yes			Yes		Same as 027 with helium. One side bomb at 2.6 sec caused CSM at 7000 cps. 900 cps sustained.
-029	10/30/69	3.381	77.4	1.614	77.4	77.0	14	4.1	No	Slotted	ST 001	No	N/A	Low P_c, nom MR, no bombs. 900 cps ± 30 psi, oscillations.
-030	12/30/69	5.366	102.0	1.607	47.5	48.0	0	0	No	No	ST 003	No	321.08	First test with modified pattern. No pops. Start oscillations still present otherwise smooth.
-031	12/31/69	5.430	100.8	1.594	68.6	68.3	0	0	No	No		No	319.98	Repeat of 031 with 70°F propellants. No pops. Same characteristics as 030.

IOS Full-Scale Injector Test Summary

Figure 11, Sheet 3 of 4

Report NASA 108581

Test	Date	Duration	P_c	MR	T_o	T_F	No. Pops	Pops sec	Helium	Reson Ring	T.C.	Bombs	I_s	Remarks
1.2-18-DAJ-032	12/31/69	6.118	77.0	1.55 EST	71.2	71.1	0	0	No	No	ST 003	No	N/A	No flow data. Low P_c, nom MR. No pops or intermediate frequency oscillations (steady-state).
-033	12/31/69	5.275	77.6	1.546	68.7	69.8	0	0	No	No	↓	No	319.62	Repeat of 032. No pops. Same characteristics.
-034	12/31/69	5.274	77.7	1.375	68.7	69.2	0	0	No	No	↓	No	319.07	Low P_c, low MR, no pops or cyclic oscillations.
-035	12/31/69	5.308	77.6	1.834	67.5	69.5	0	0	No	No	ST 003	No	319.57	Low P_c, high MR, no pops or cyclic oscillations.
-036	1/8/70	6.029	70.8	1.559	65.4	67.4	23	3.8	No	No	ABL 353	No	N/A	Checkout ablative test at 70 psia P_c. Many pops and severe IF oscillations. CSM at one oxidizer orifice Row 8B unplugged postfire. Photocon P_c.
-037	1/9/70	5.424	113.6	1.591	69.5	69.3	0	0	No	No	ABL 353	No	N/A	Test to evaluate popping at high P_c with unplugged orifice. No pops.

IOS Full-Scale Injector Test Summary

Figure 11, Sheet 4 of 4

Report NASA 108581

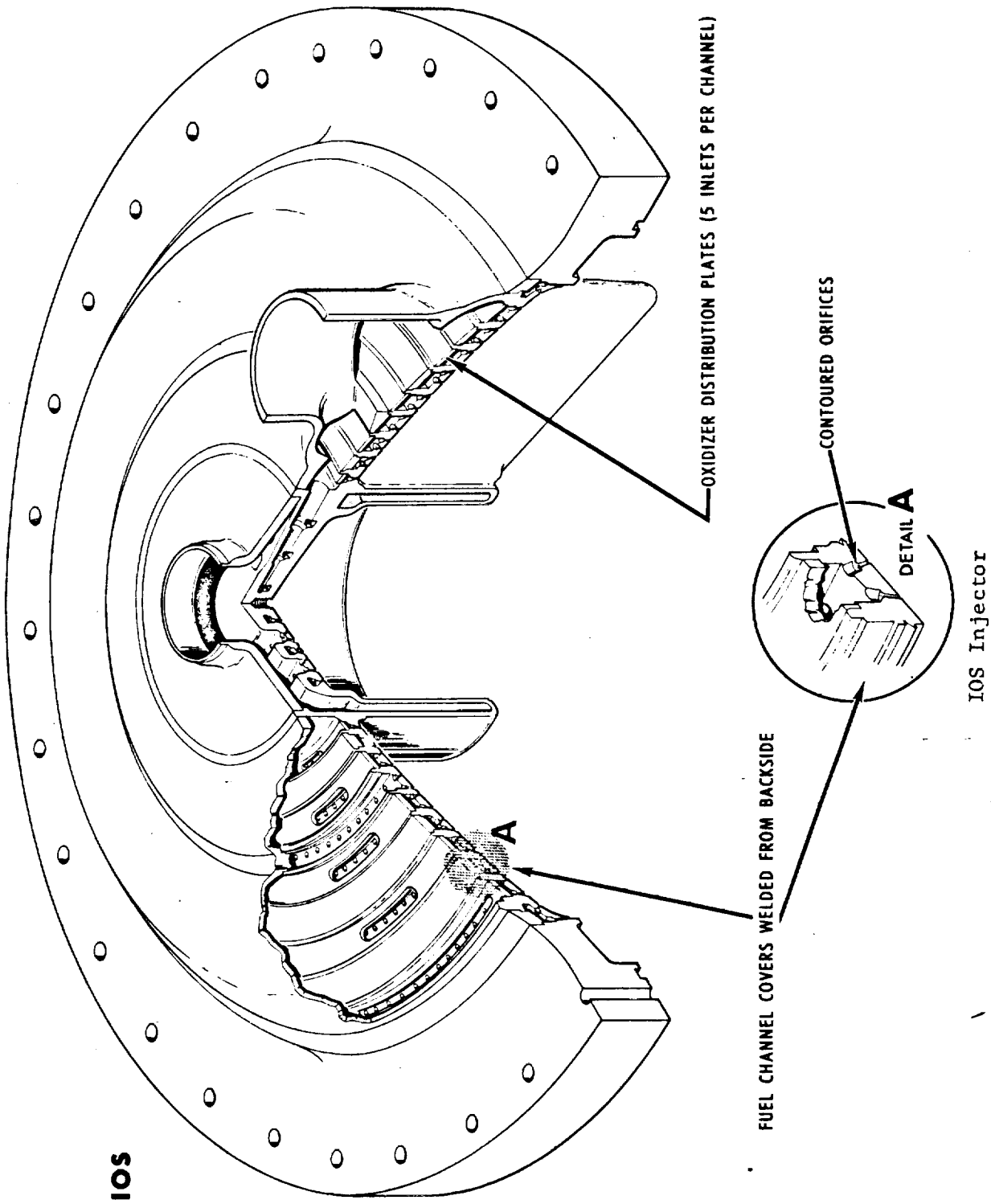
IOS
A
OXIDIZER DISTRIBUTION PLATES (5 INLETS PER CHANNEL)
FUEL CHANNEL COVERS WELDED FROM BACKSIDE
CONTOURED ORIFICES
DETAIL A
IOS Injector

Figure 12

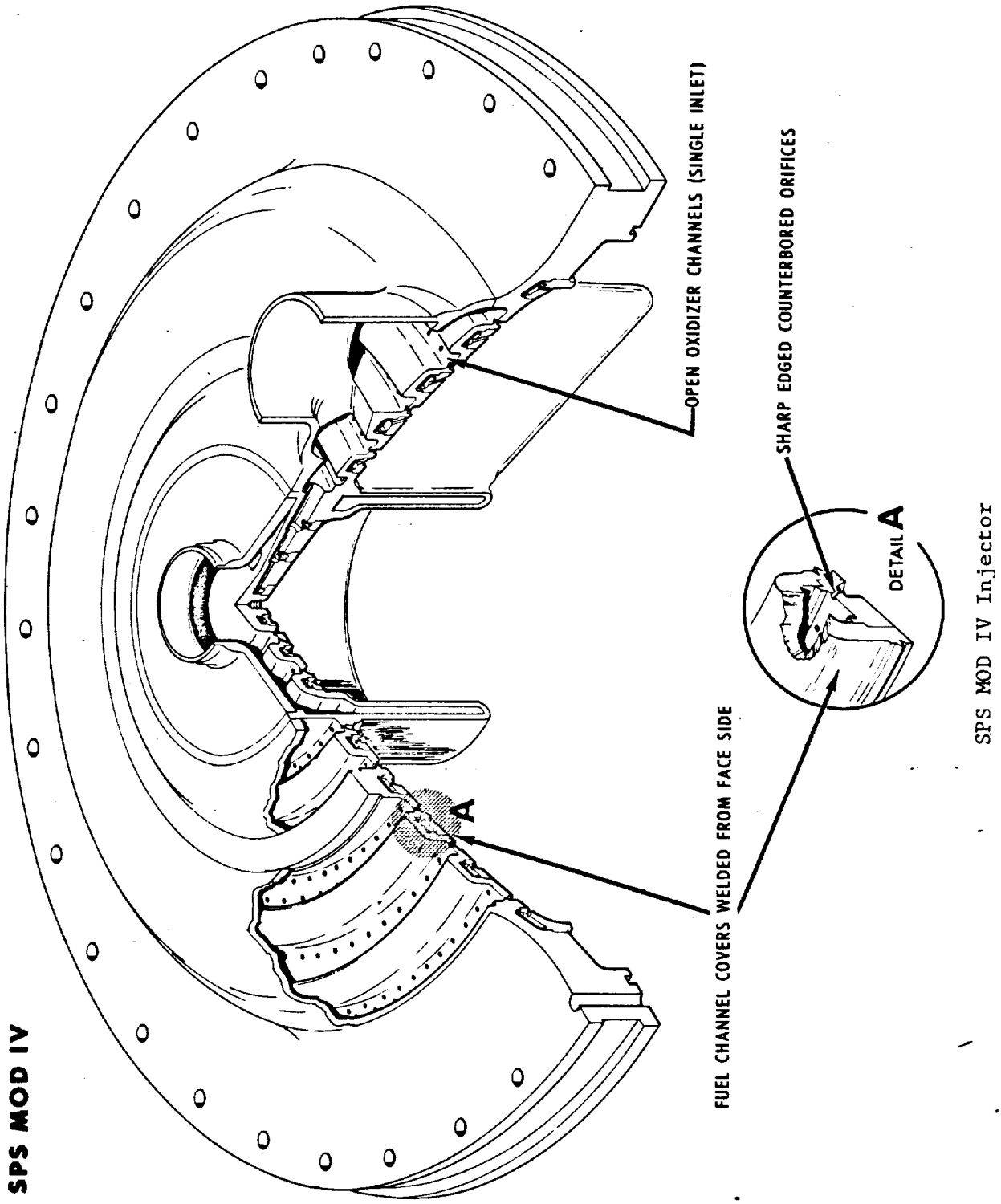

SPS MOD IV Injector

Figure 13

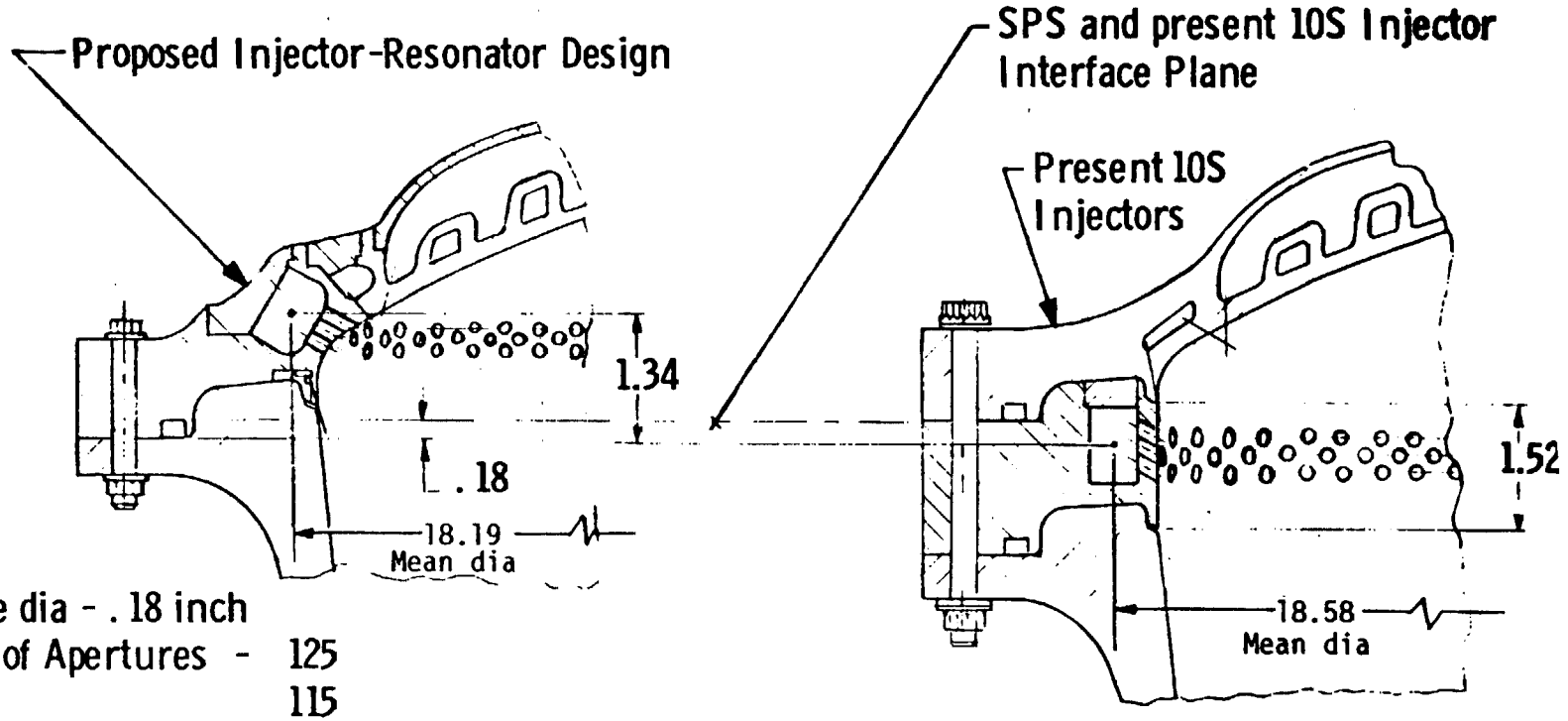

Aperture dia - .18 inch
Number of Apertures - 125
115
125
365

Cavity Volume - 30 in.^{3}
Cavity Temperature (assumed) - 2740°R
Cavity Temperature (actual) - 2210°R

Aperture Length - .25 inch

Aperture Area/Injector Face Area - 3.7%

Aperture Area/Cavity Back Surface Area - 26%

Workhorse Resonator, Design A

Figure 14

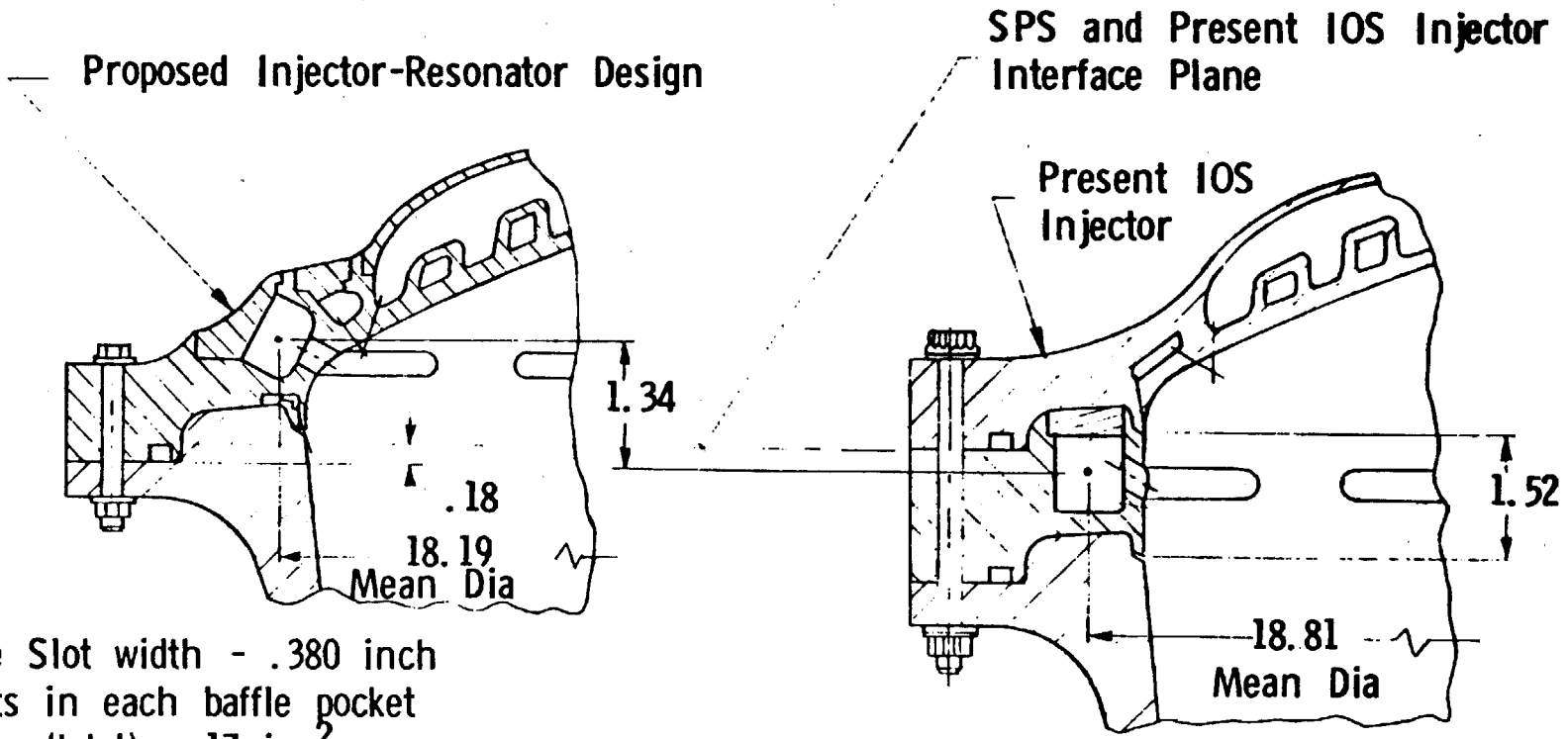

Aperture Slot width - .380 inch
Two Slots in each baffle pocket
Slot Area (total) - 17 $in.^2$
Cavity Volume - 43 $in.^3$
Cavity Temperature (L_o P_c & MR) - 2060°R

Slot Length - .25 inch

Aperture Area/Injector Face Area - 4.9%
Aperture Area/Cavity Back Surface Area - 31%

Figure 15

Report NASA 108581

Proposed and Slotted Workhorse Resonator

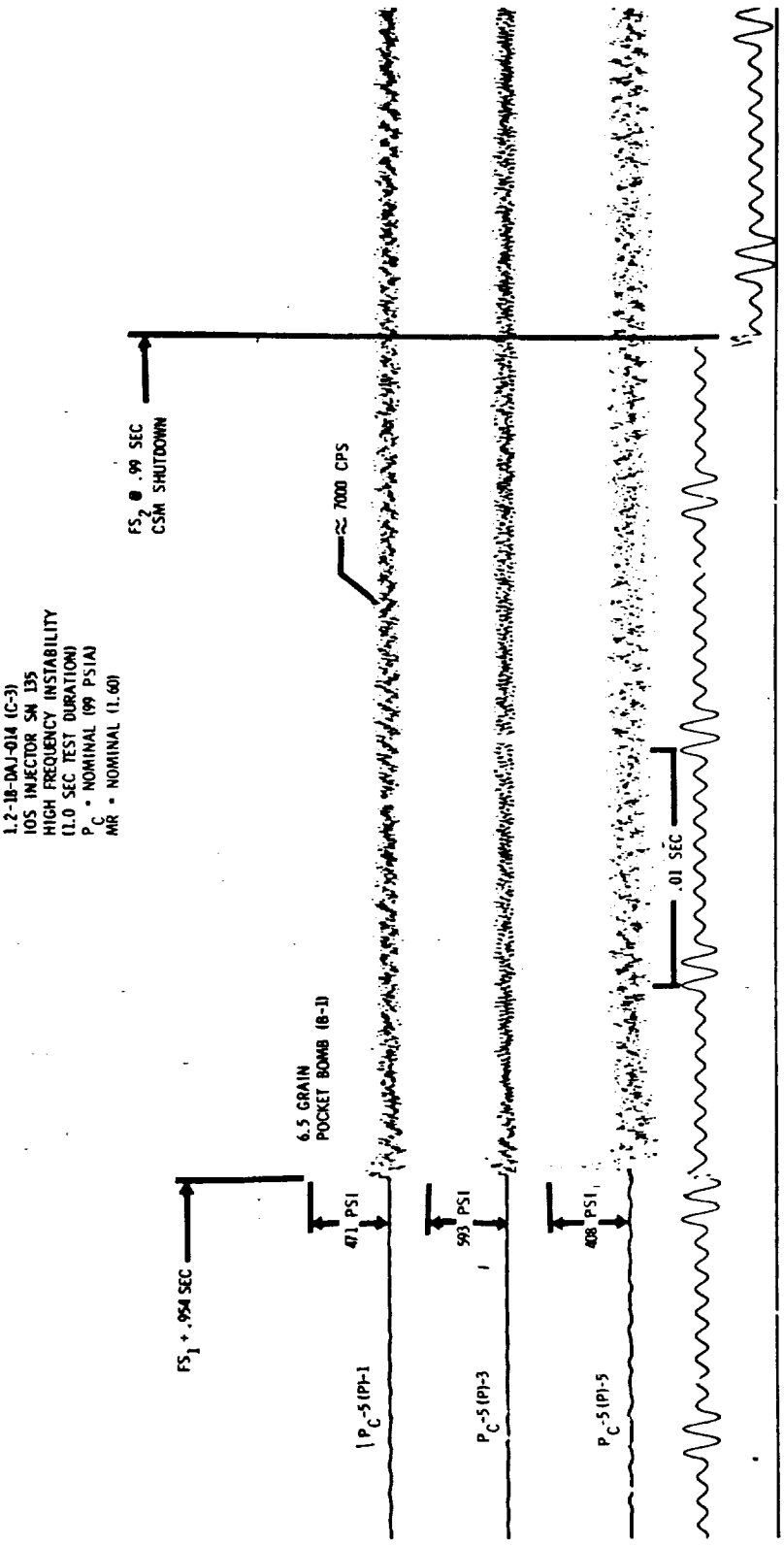

Nominal Operating Conditions - Without Resonator

Figure 16

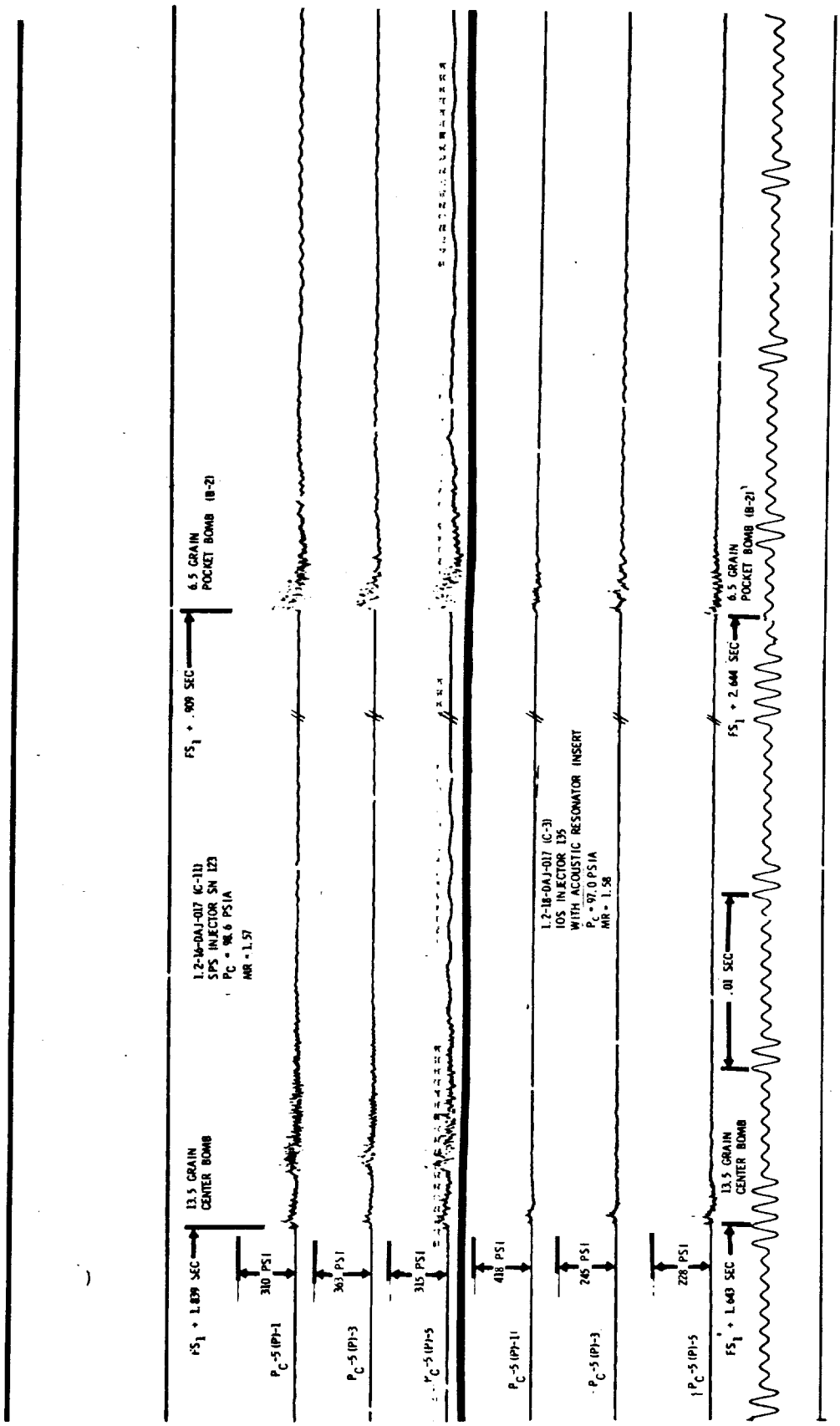

Nominal Operating Conditions - With Resonator

Figure 17

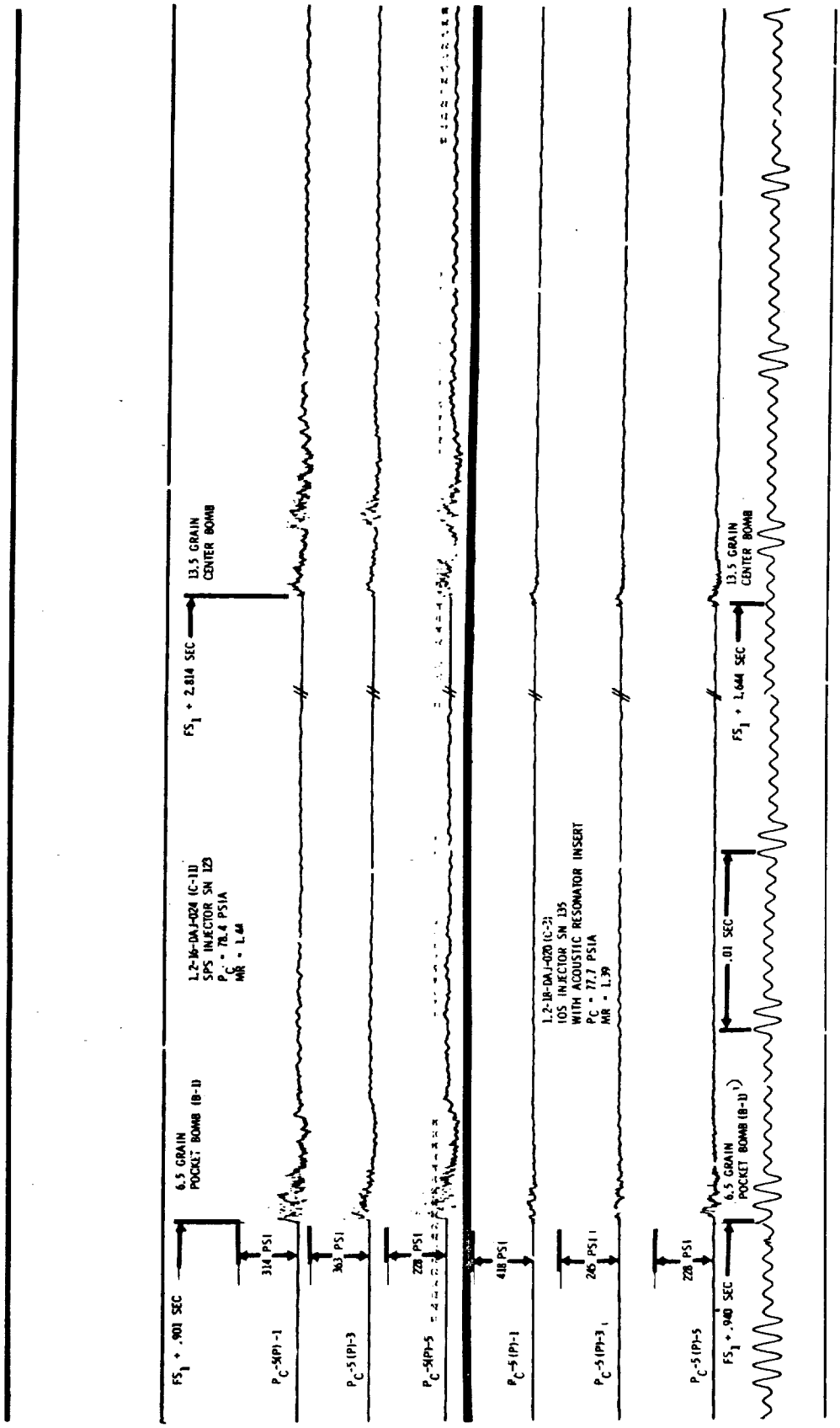

Low P_c - Low MR - With Resonator

Figure 18

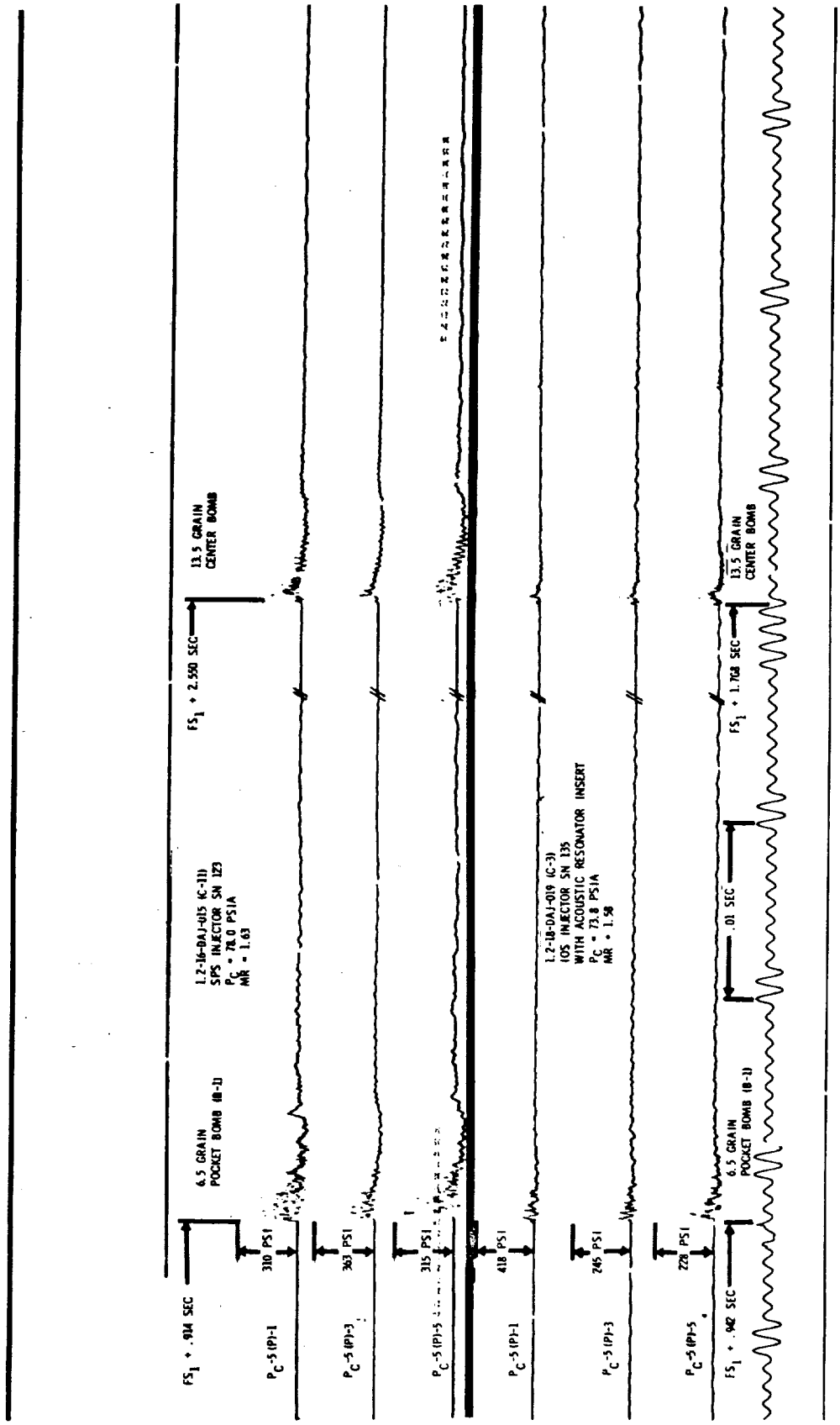

Low P_c - Nominal MR - With Resonator

Figure 19

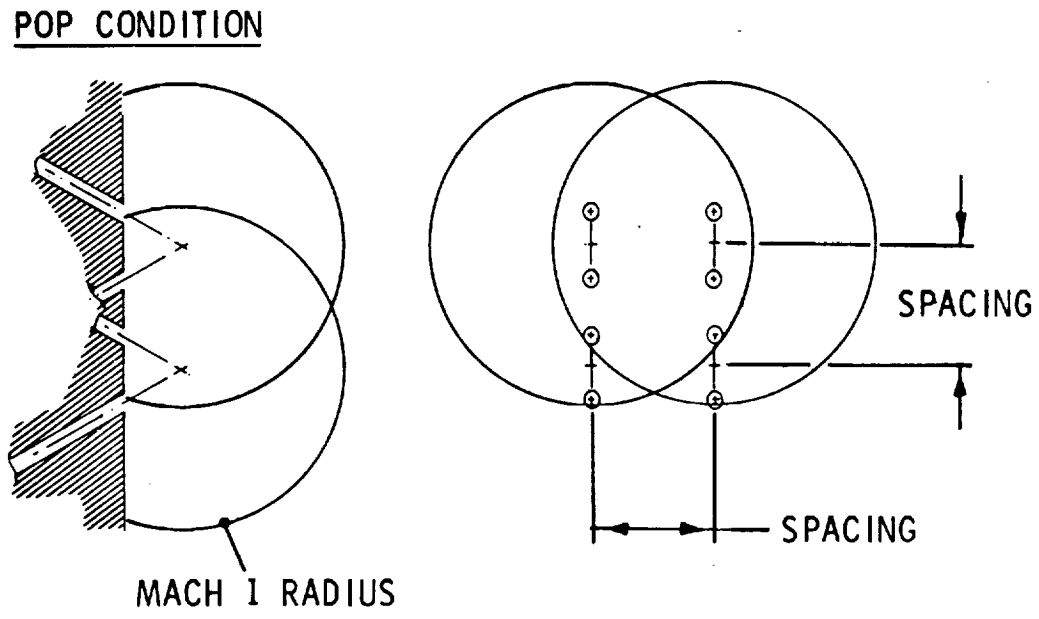

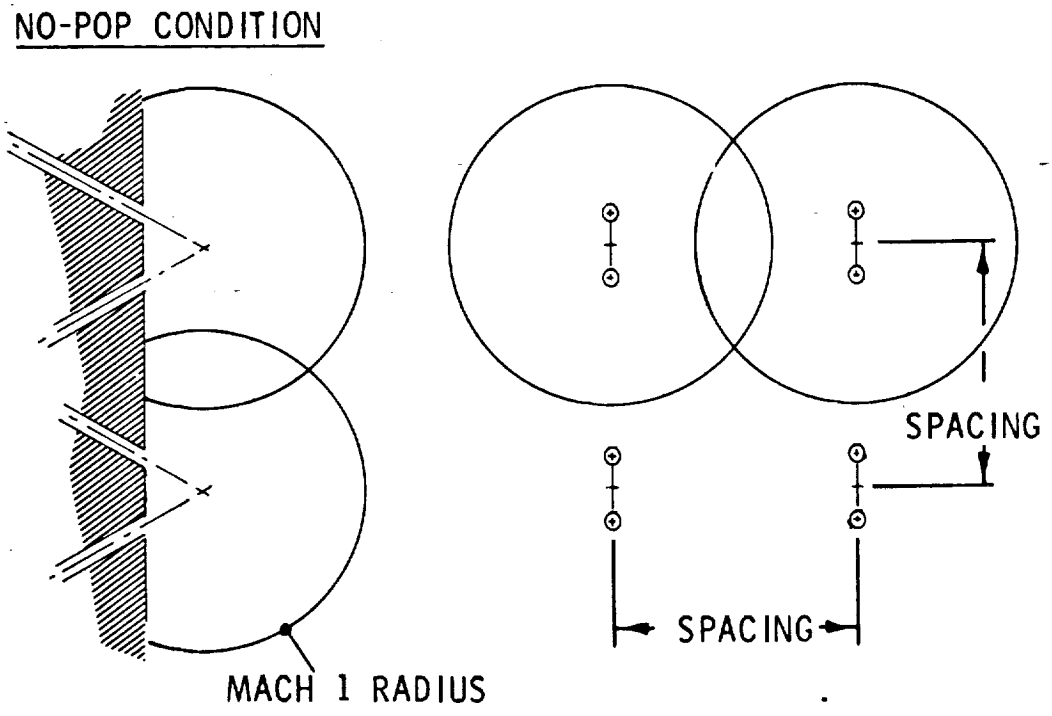

Effect of Element Spacing on Blastwave Coupling

Figure 20

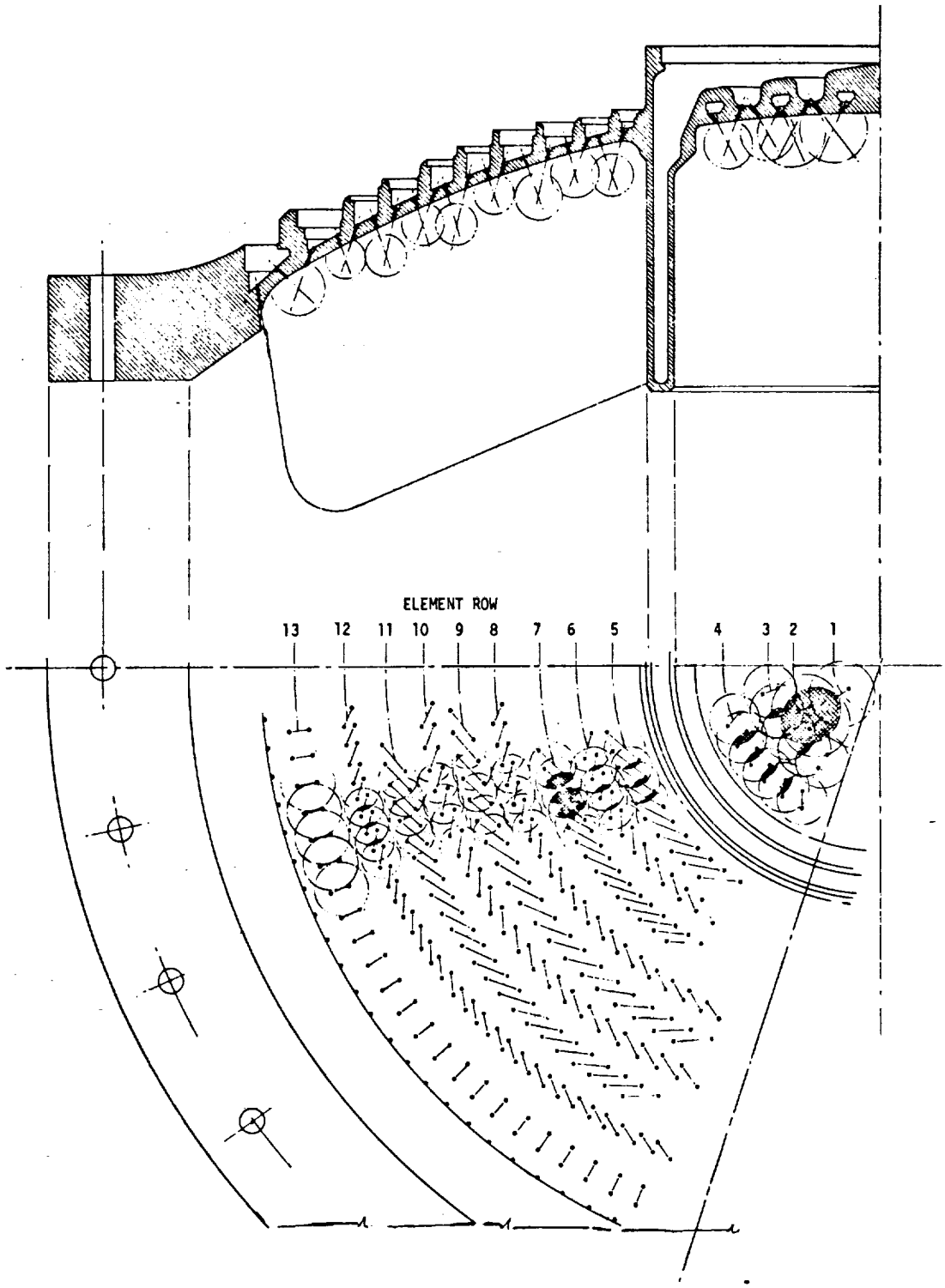

Mach 1 Radii Layout - IOS Injector

Figure 21

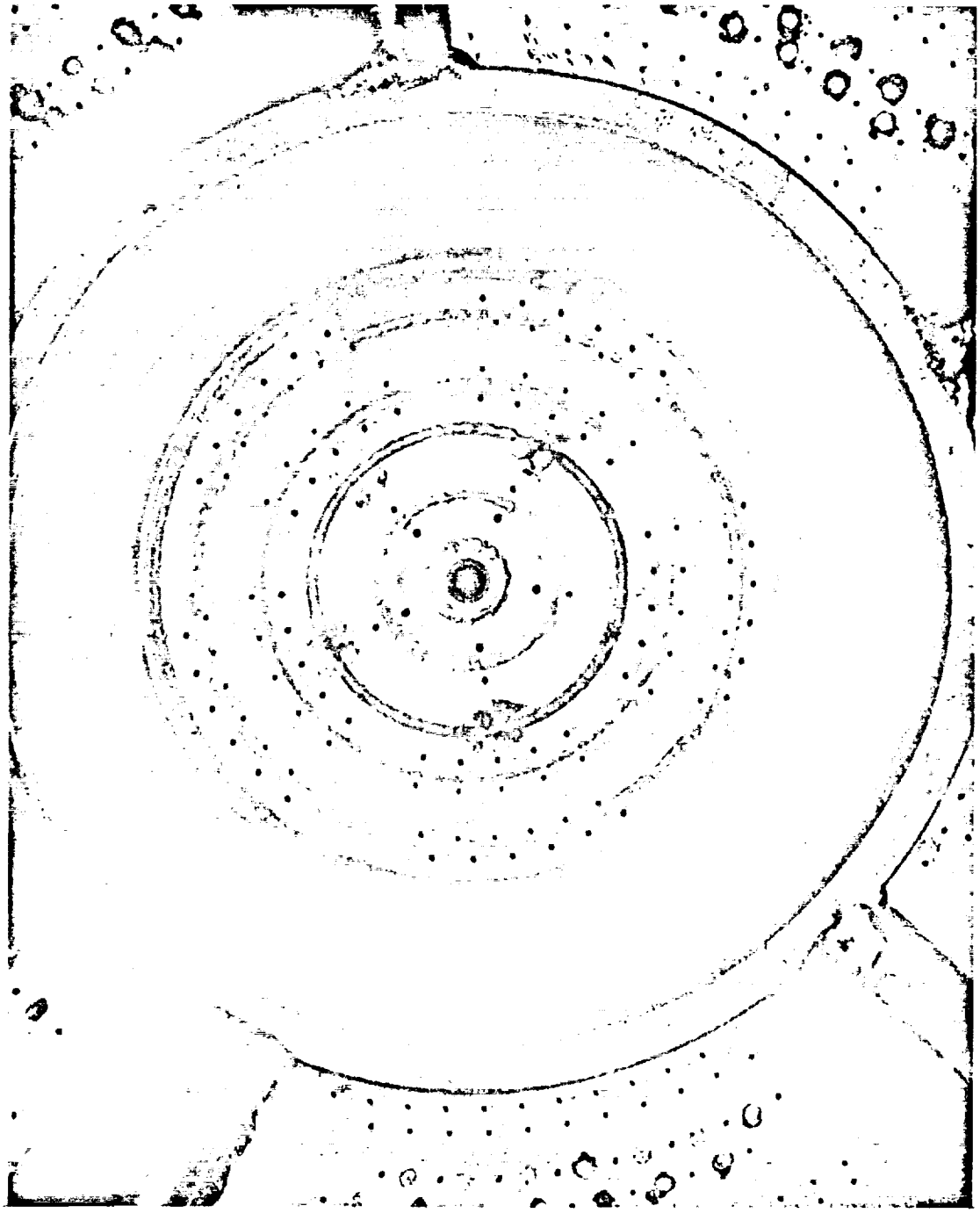

Plugged Orifices within Injector Hub

Figure 22

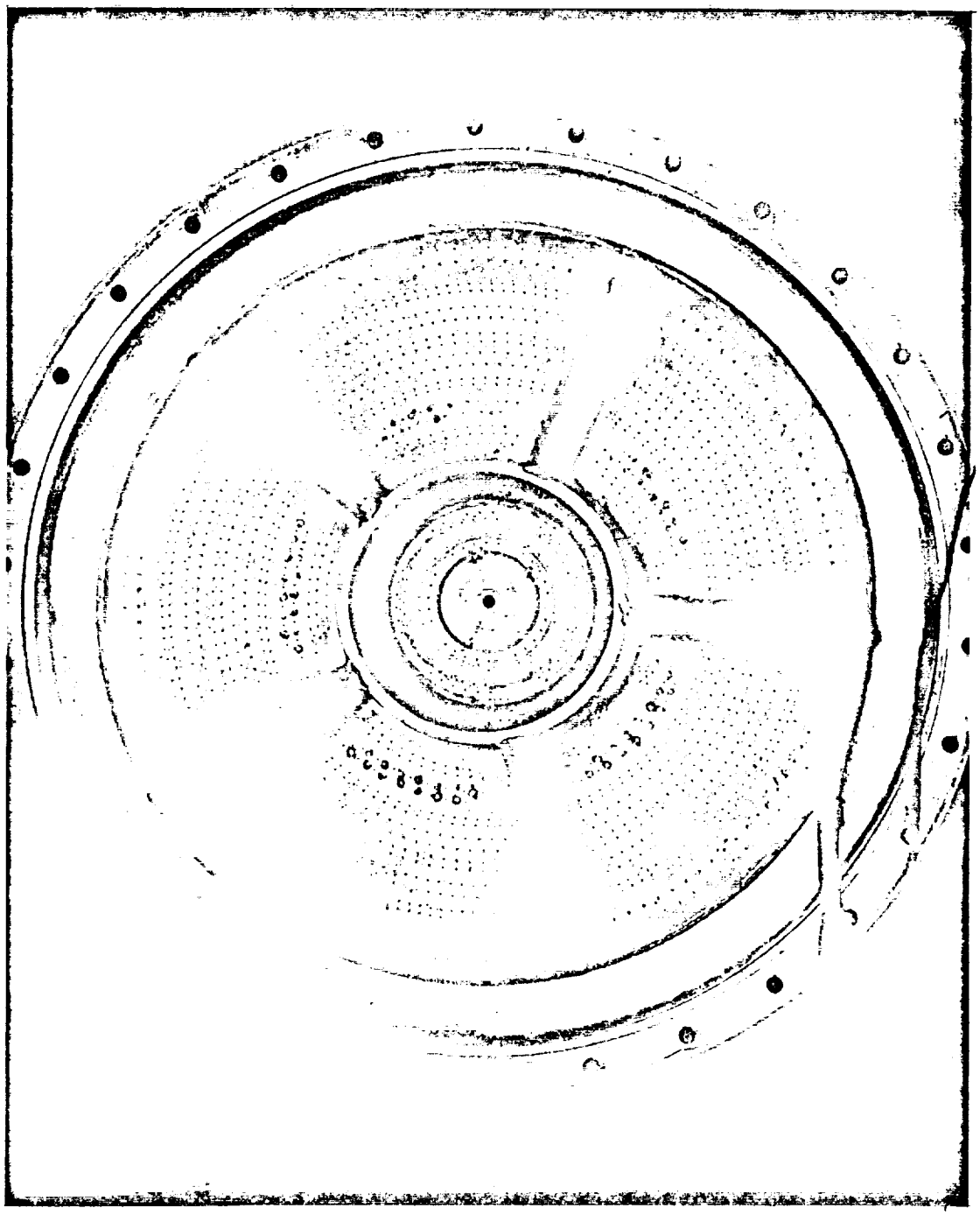

Injector Face with Plugged Orifices

Figure 23

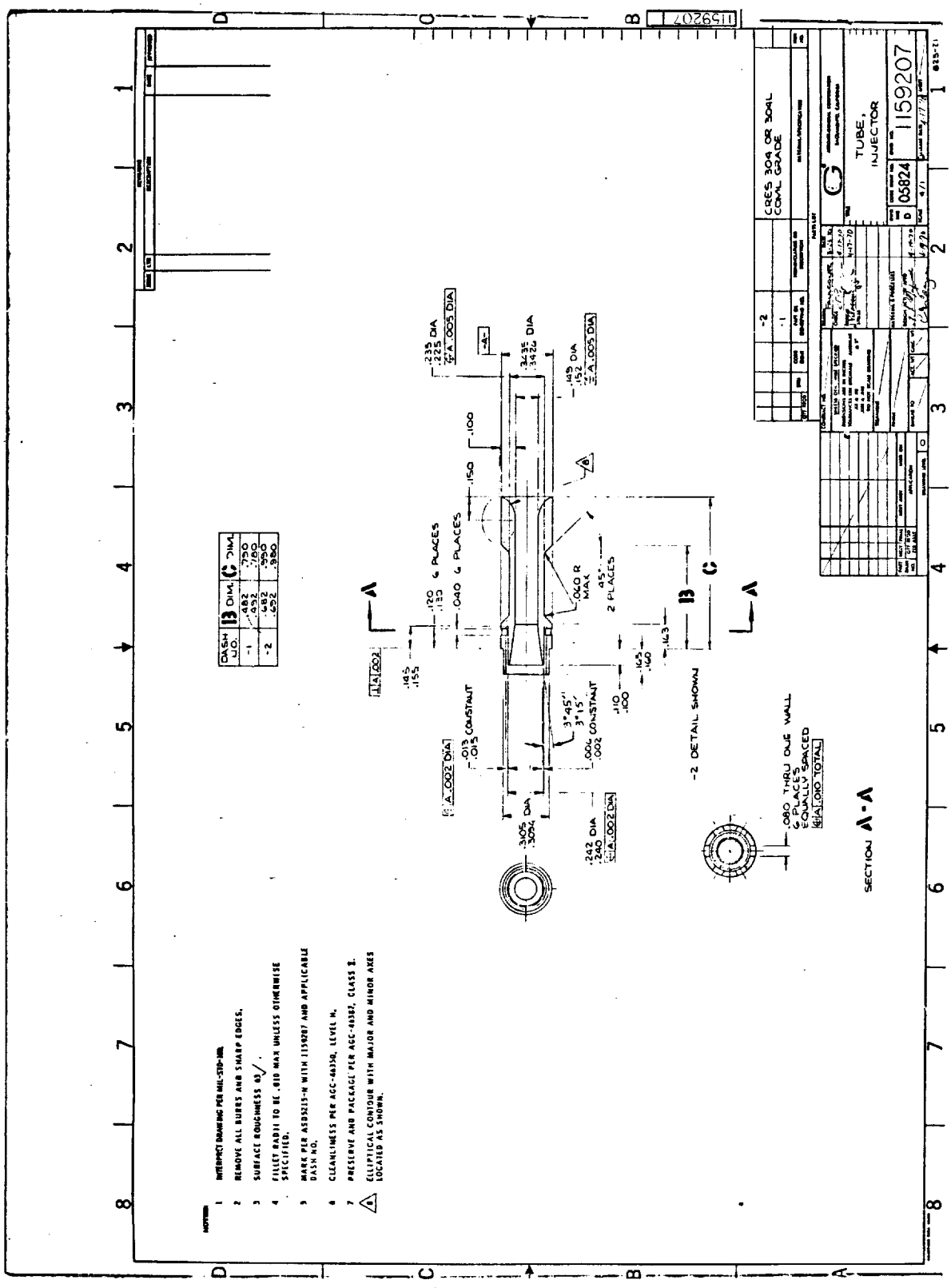

Figure 24

Tube Injector

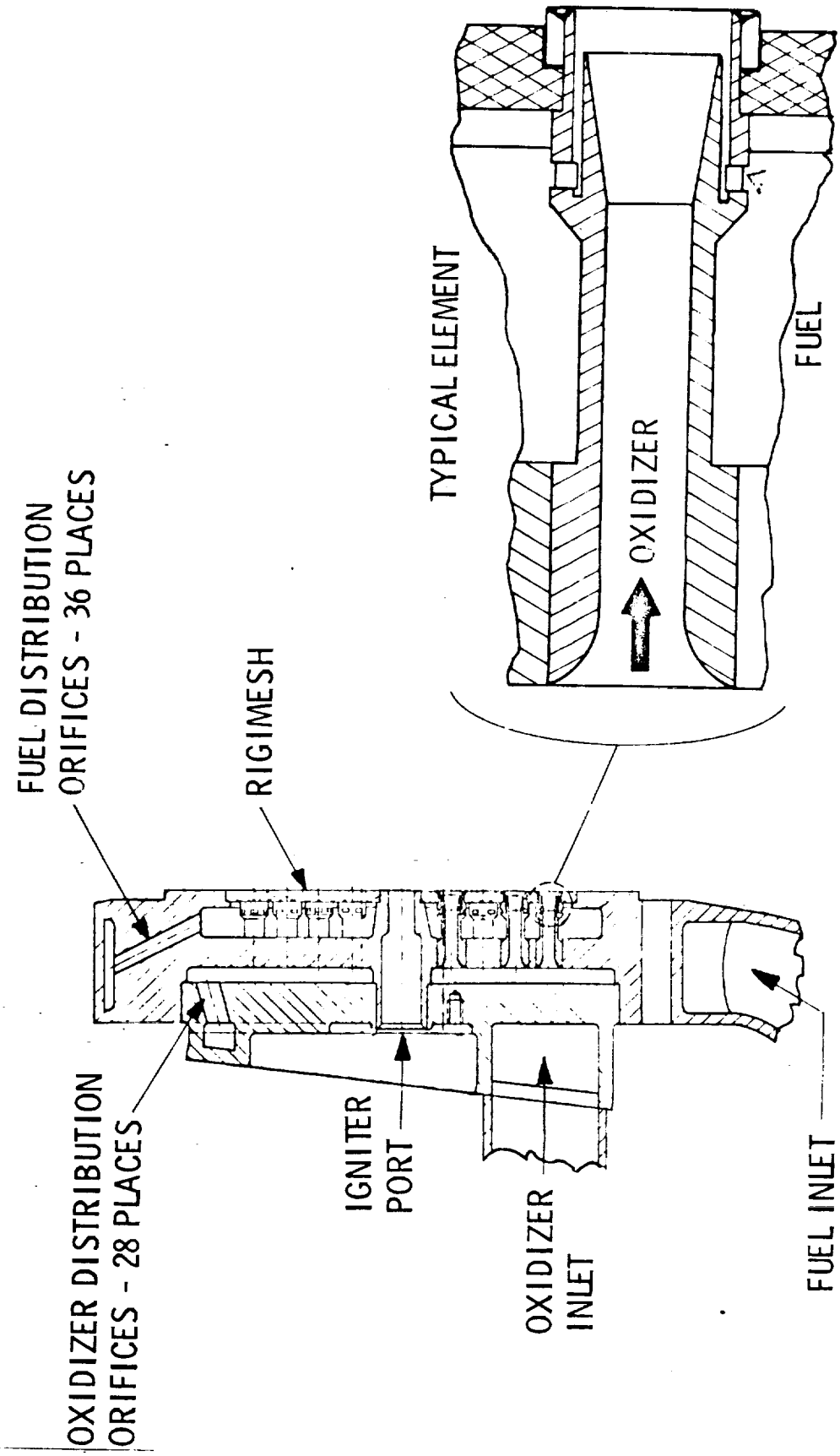

Coaxial Injector

Figure 25

Thrust	5000 lb (nom)
Chamber Pressure	500 psia (nom)
Mixture Ratio O/F	60:1

Propellants

Gaseous Oxygen at 460°R (Design)
Gaseous Hydrogen at 430°R (Design)

Specific Impulse: 445 sec (Target Vacuum at $\varepsilon = 240$)

Propellant Flow Rates

$\dot{w}_t$	10.990 lb/sec
$\dot{w}_{ox}$	9.420 lb/sec
w_f	1.570 lb/sec

Injector Pressure Drop

Oxidizer	60 psi
Fuel	95 psi

A_t 5.69 in.^{2}	D_t 2.69 in.
Contraction Ratio	2.5:1
Chamber Length	8 in.
Design Service Life	10 starts/mission for 100 missions
Number of Elements	74
Thrust/Element	68
Fuel Injection Velocity	900 fps
Oxidizer Injection Velocity	100 fps

Injector Design Information

Figure 26

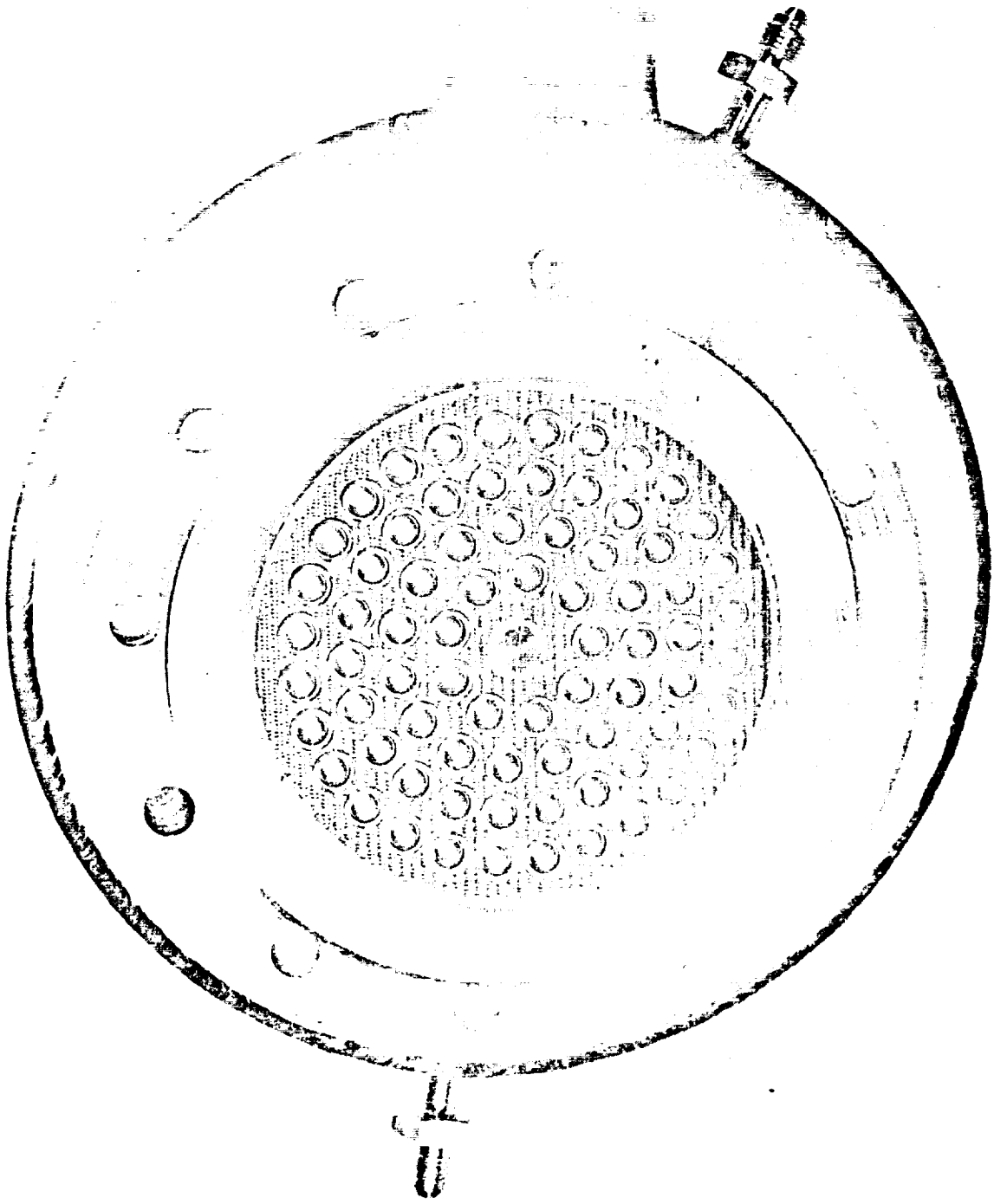

Injector Face after Element Braze

Figure 27

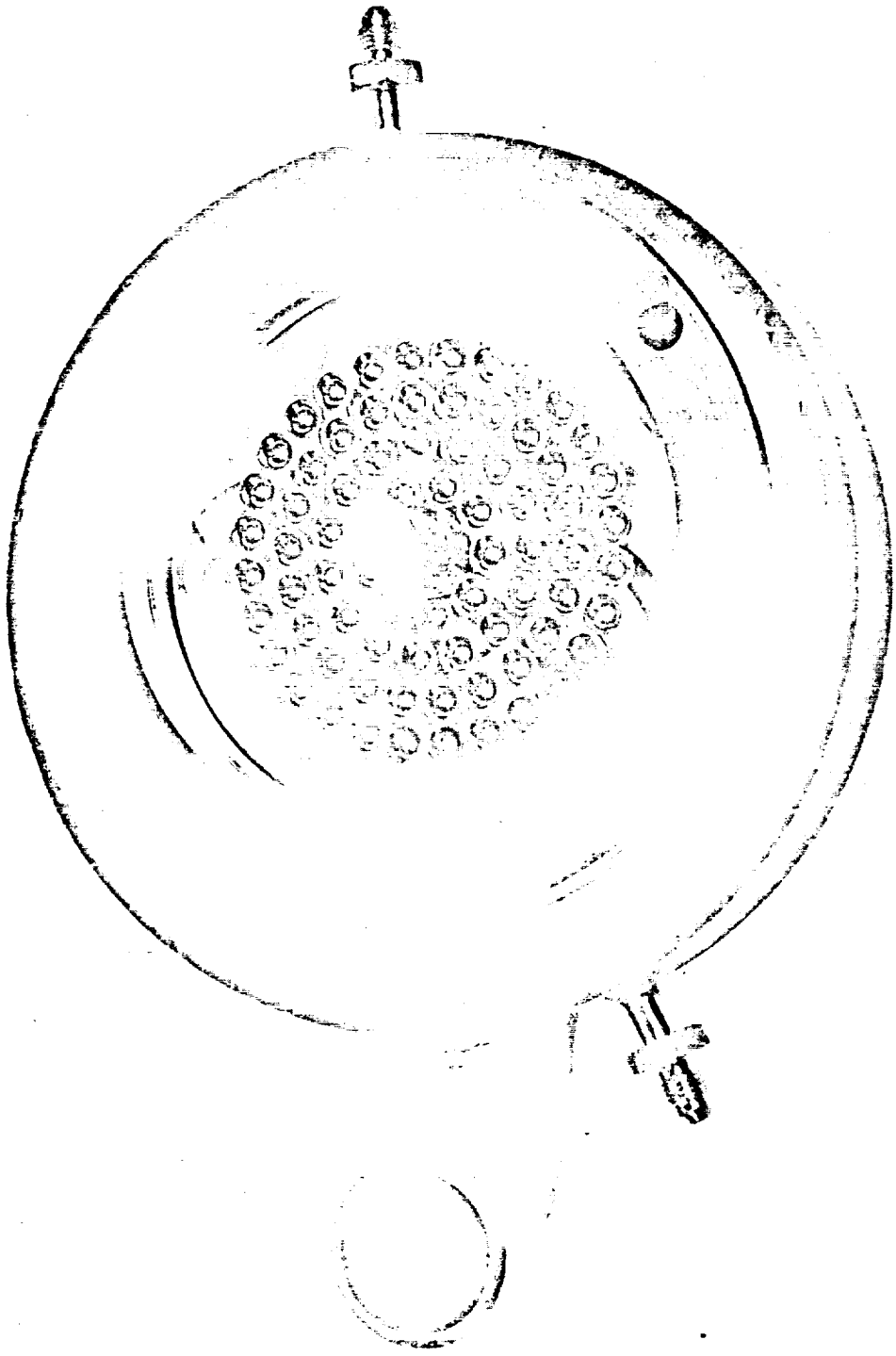

Injector Backside after Element Braze

Figure 28

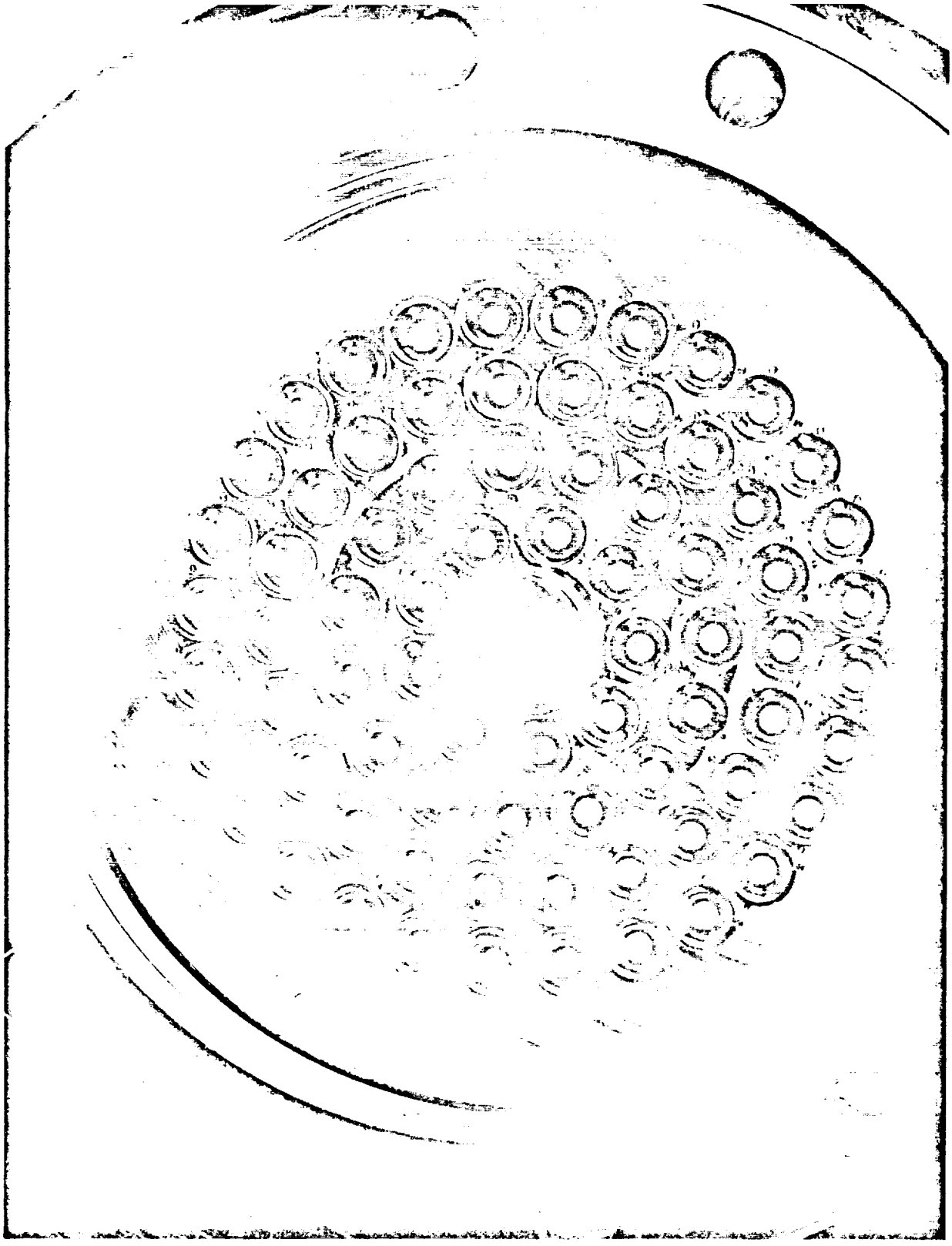

Injector Oxidizer Manifold with Elements

Figure 29

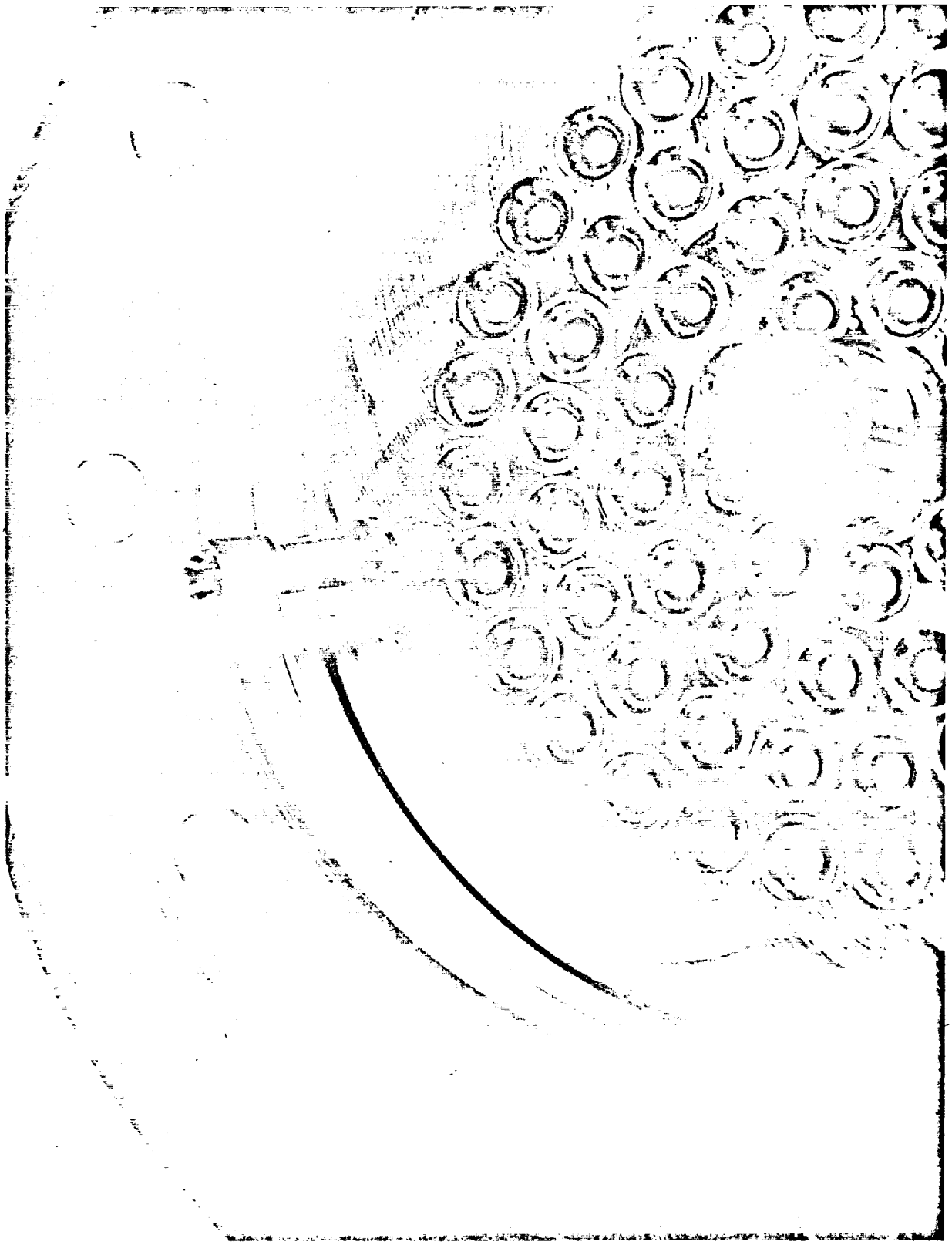

Elements Installed and Elements Staked

Figure 30

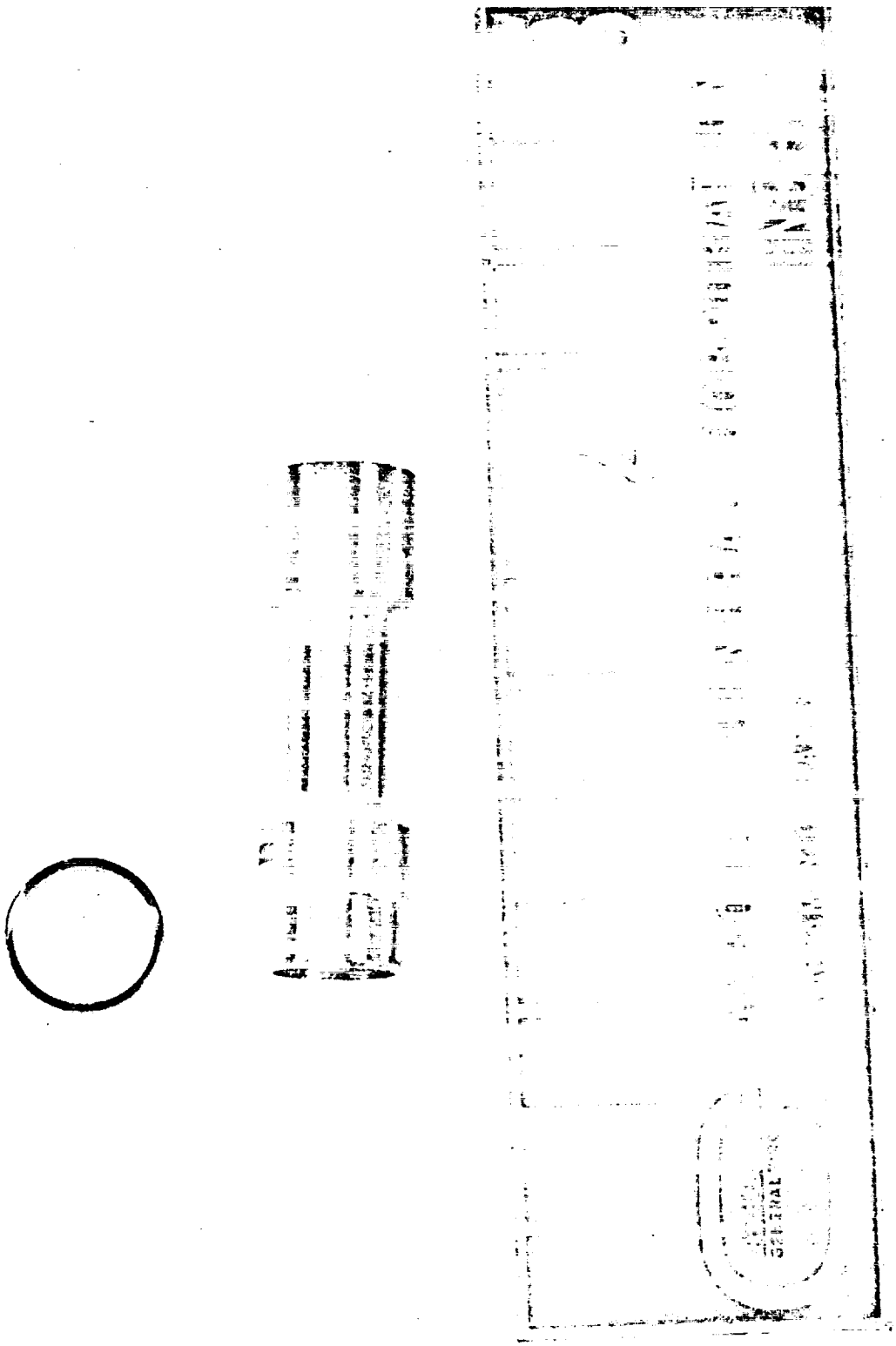

Coaxial Injector Element Side

Figure 31

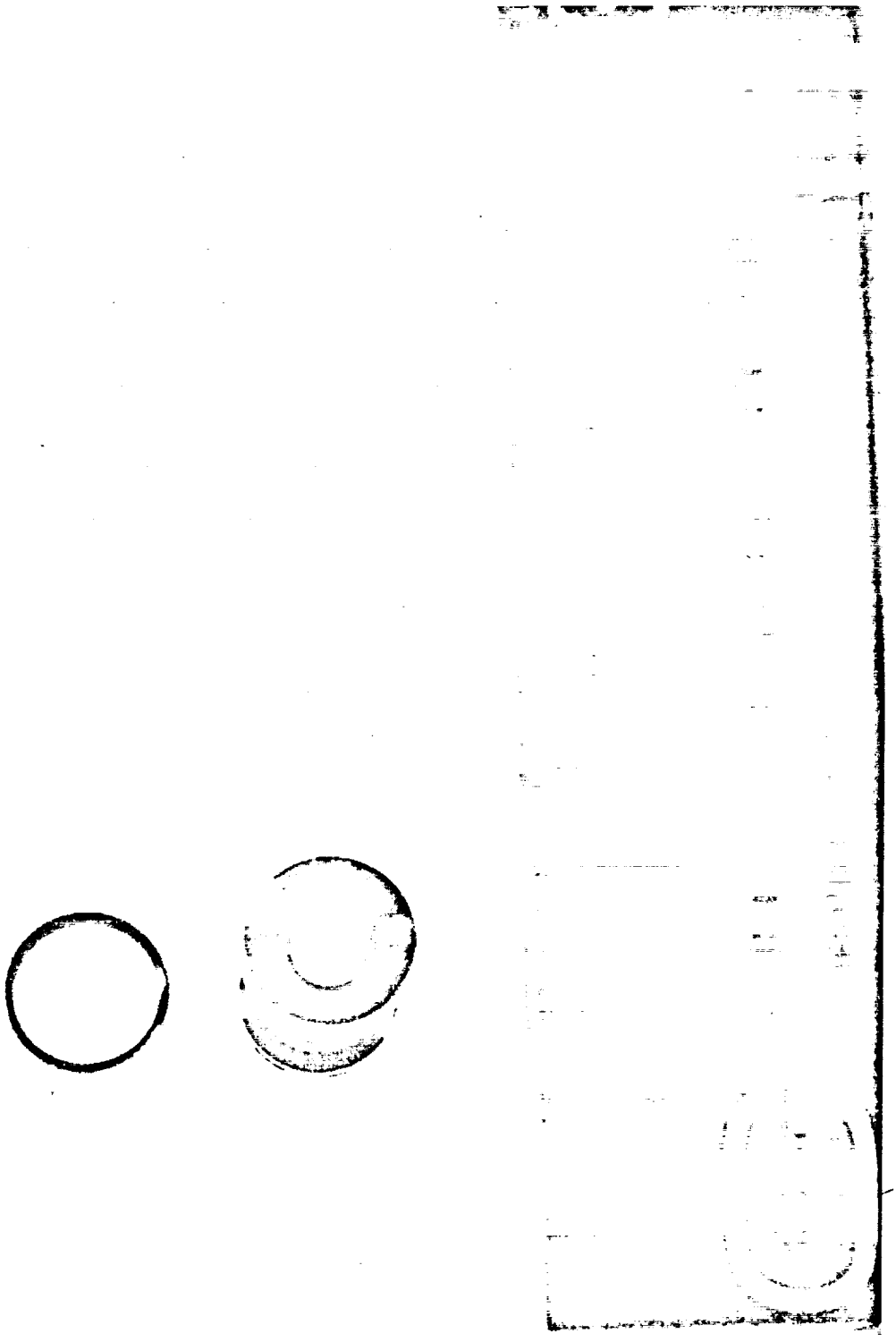

Coaxial Injector Element End

Figure 32

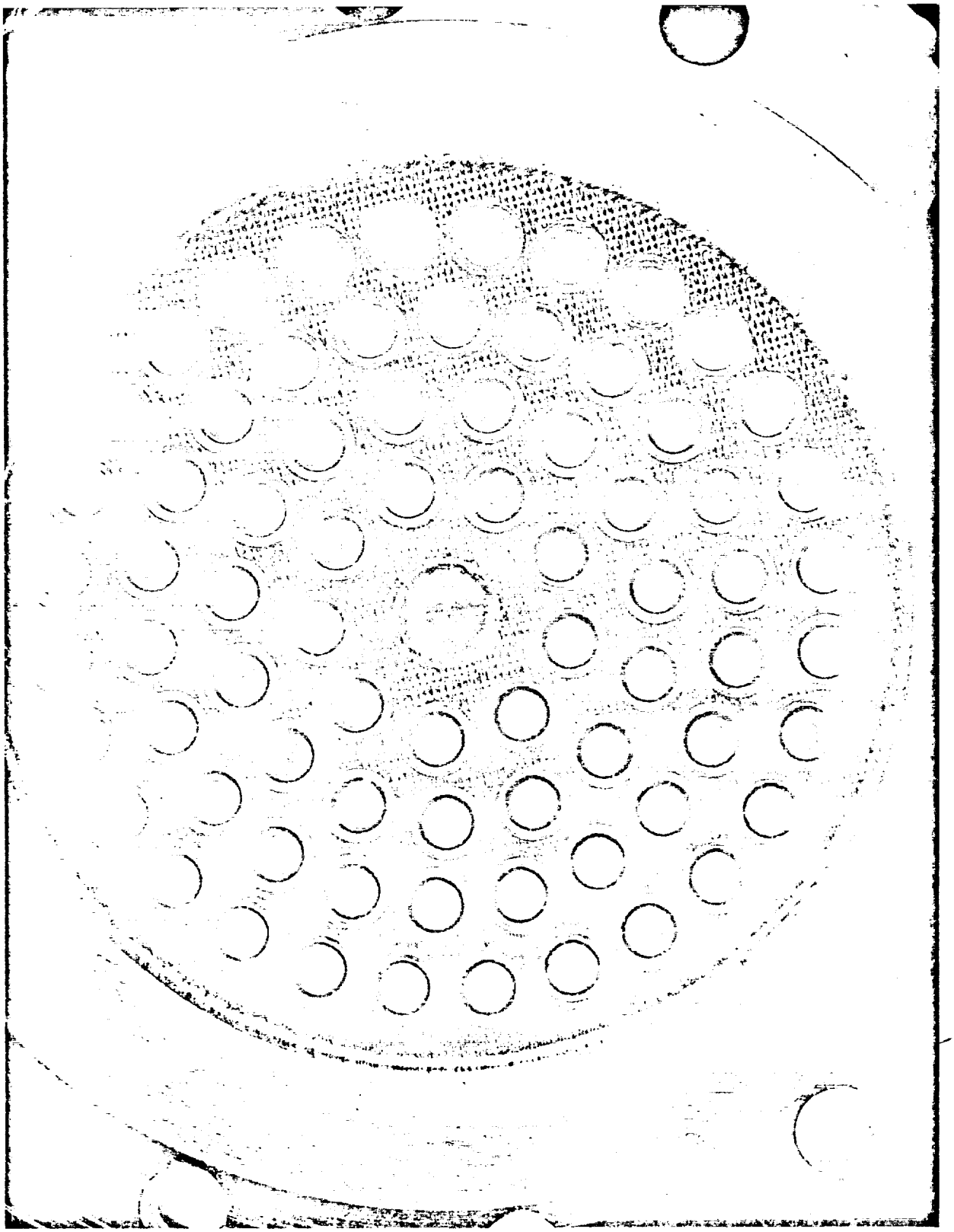

Coaxial Injector Element After Braze

Figure 33

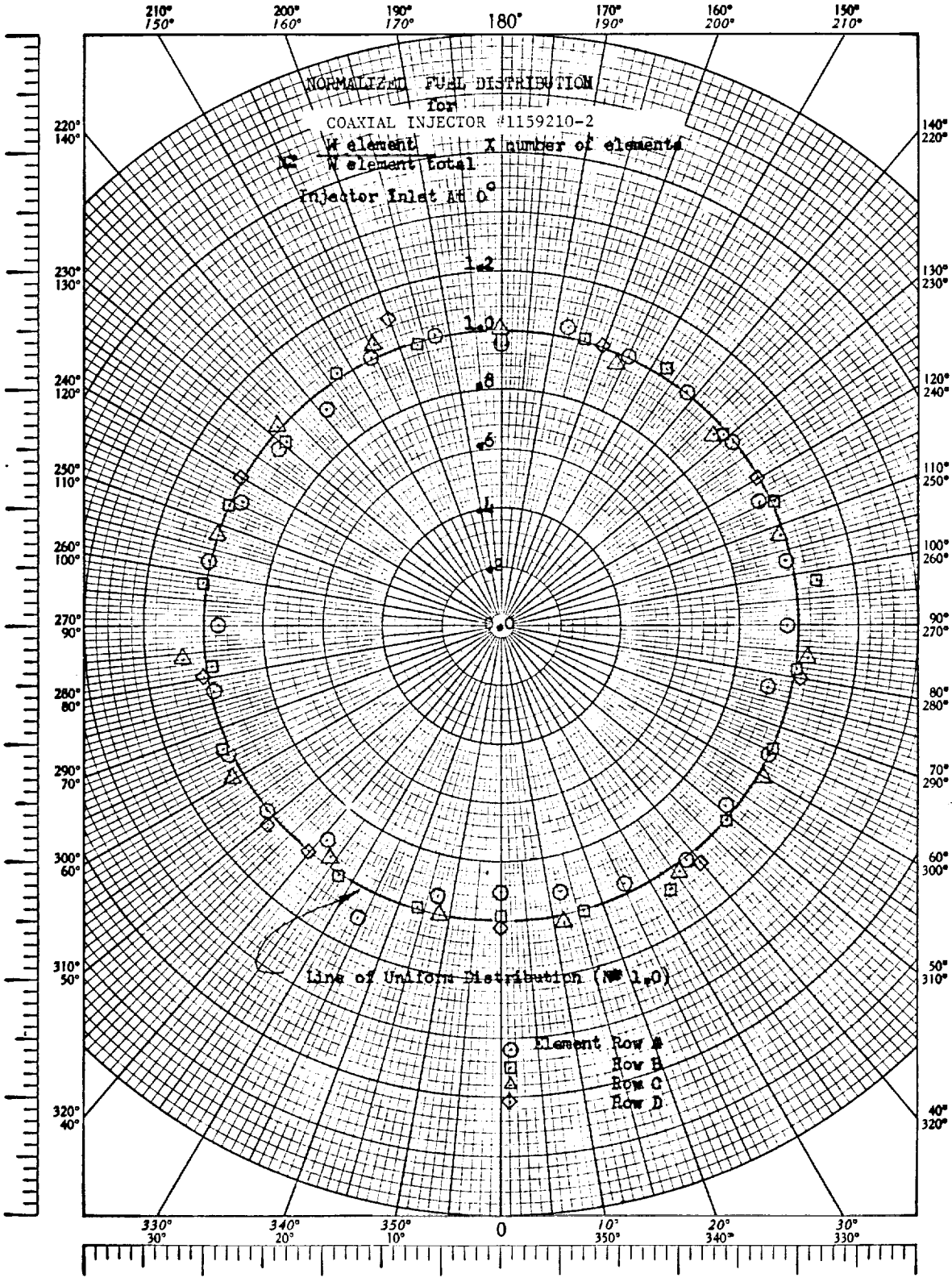

Normalized Fuel Distribution

Figure 34

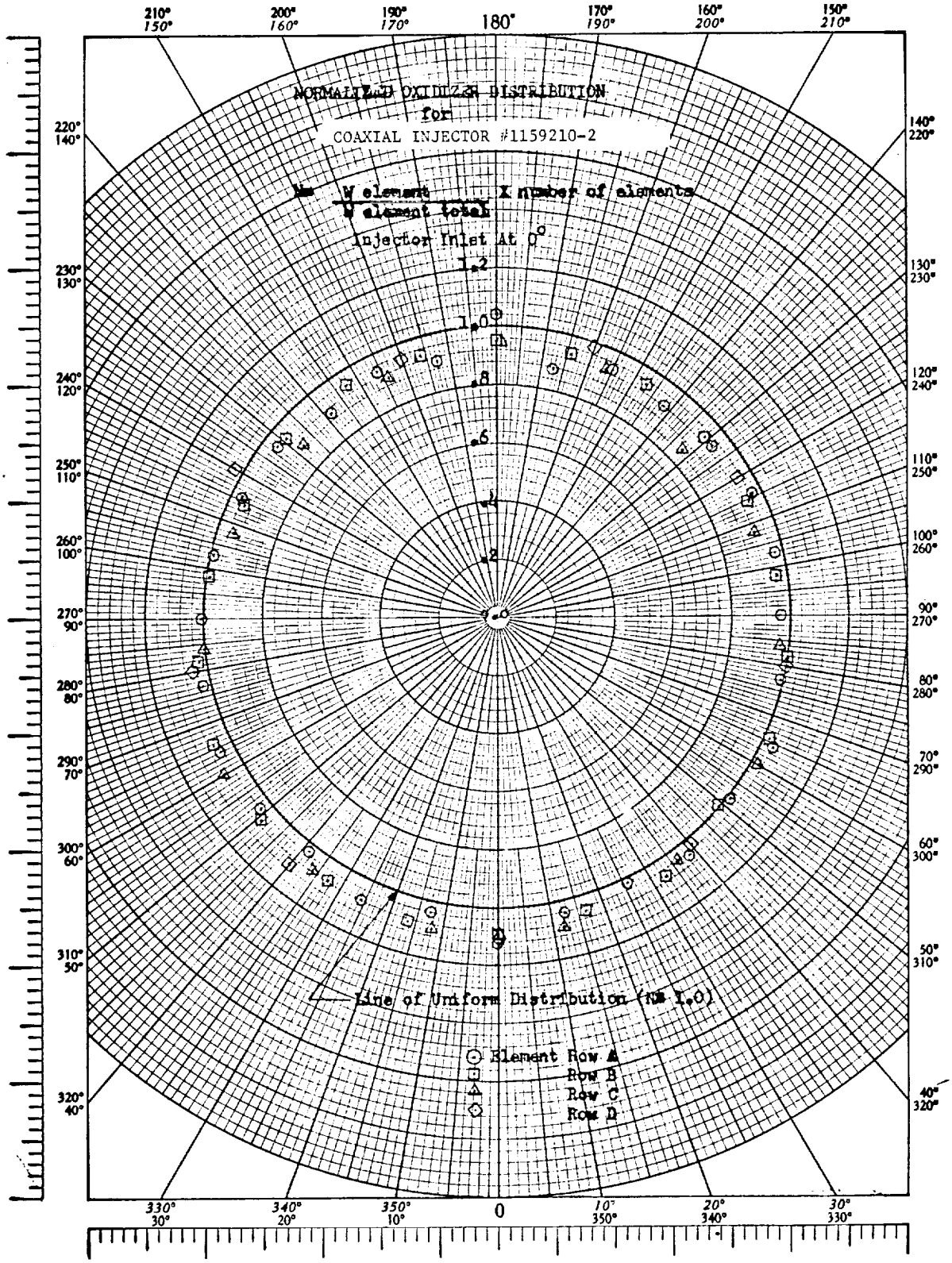

Normalized Oxidizer Distribution

Figure 35

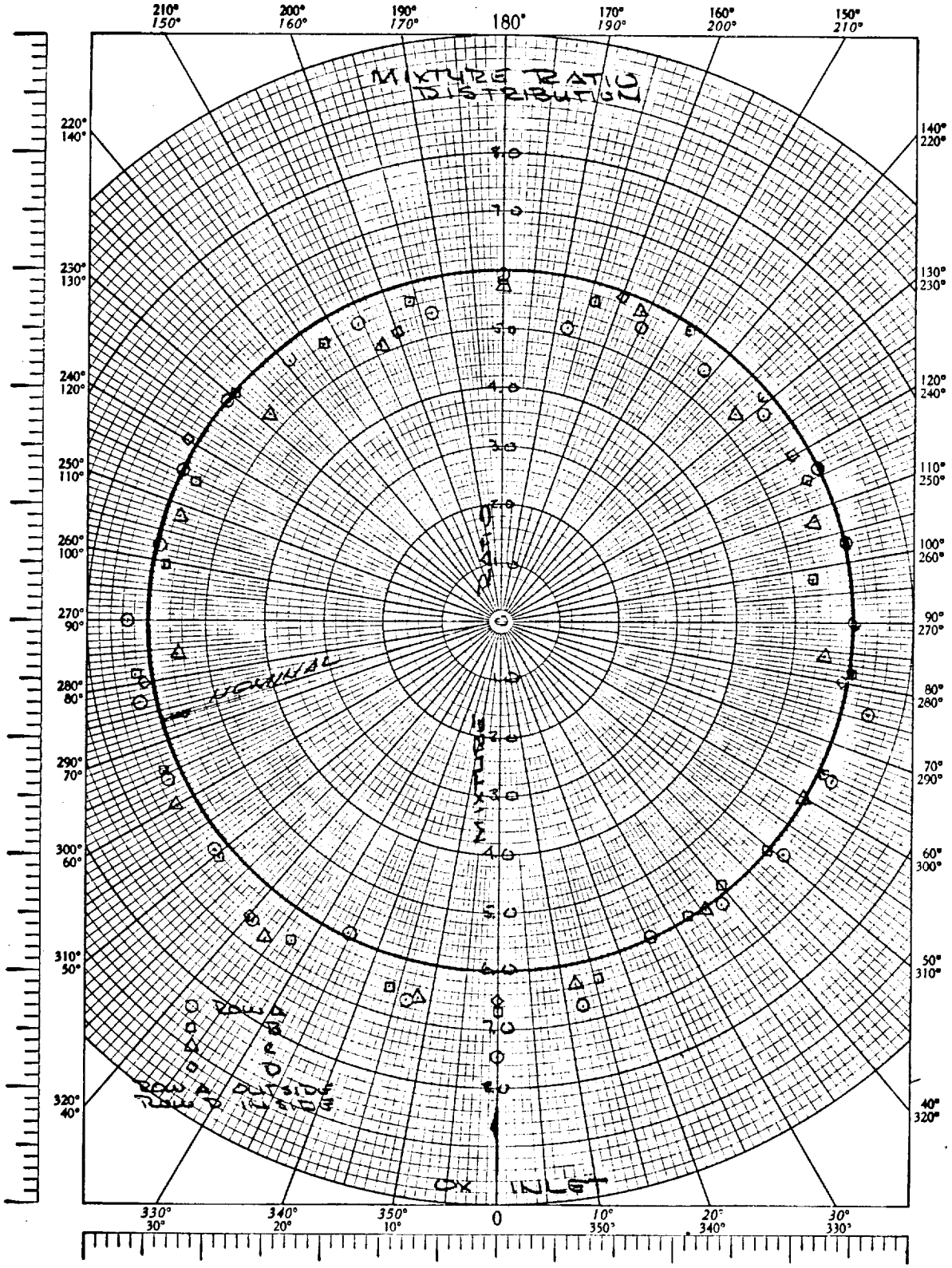

Mixture Ratio Distribution

Figure 36

$$I_{sp_{del}} \text{ at } \epsilon = I_{sp\ theo} \text{ at } \epsilon - \sum I_{sp} \text{ losses}$$

$$= I_{sp\ theo} - (ERL + MRDL + KL + DL + BL)$$

$$= I_{sp\ theo} - ERL - \underbrace{(MRDL + KL + DL + BL)}_{\text{CALCULATED}}$$

$$ERL = (I_{sp\ theo} - \text{Calculated Losses}) - I_{sp_{del}}$$

$$\% \text{ ERE} = \frac{I_{sp_{theo}} - ERL}{I_{sp_{theo}}}$$

Figure 37

% ERE Performance Derivation (As Approved by JANNAF Liquid Rocket Performance Committee)

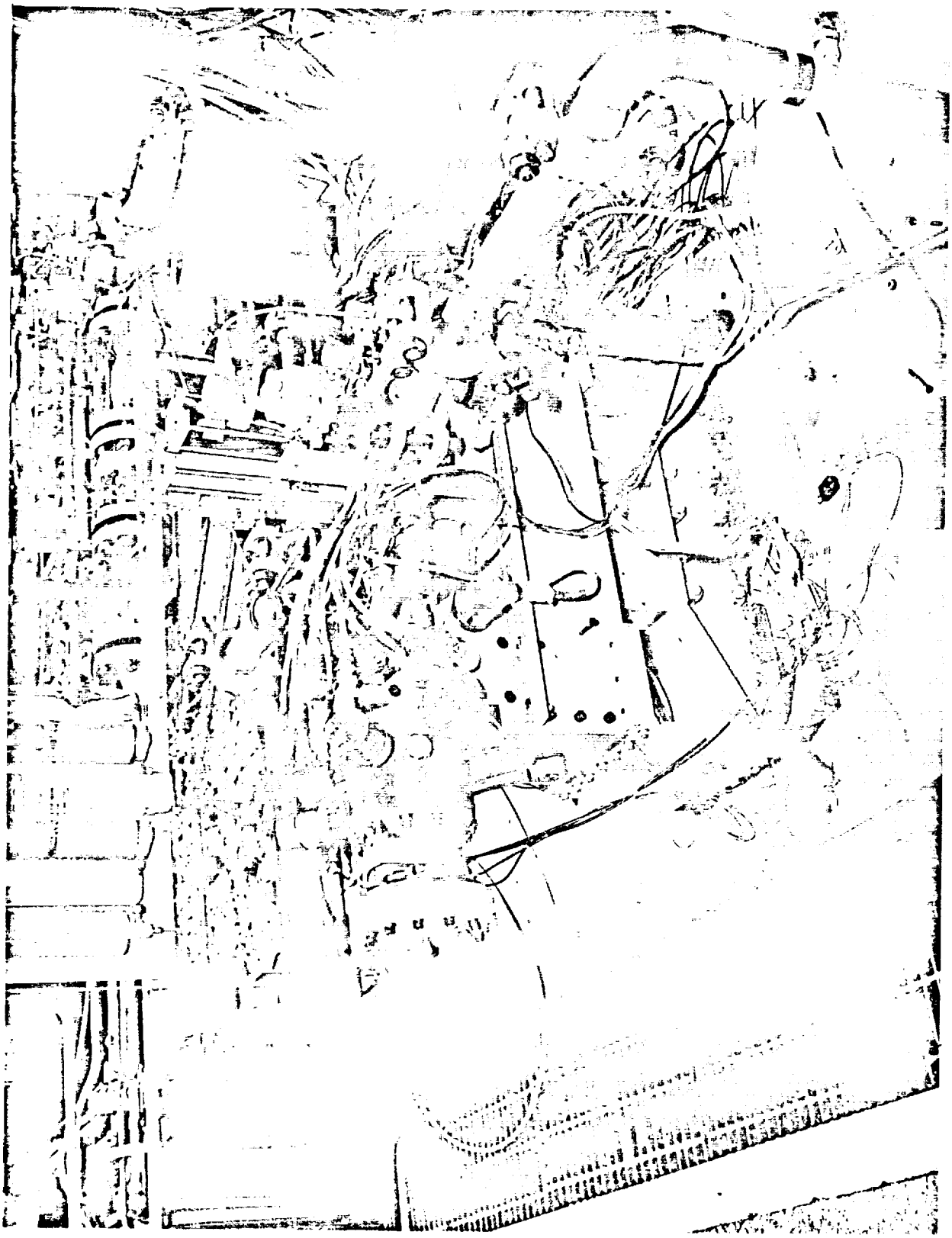

Test Stand

Figure 38

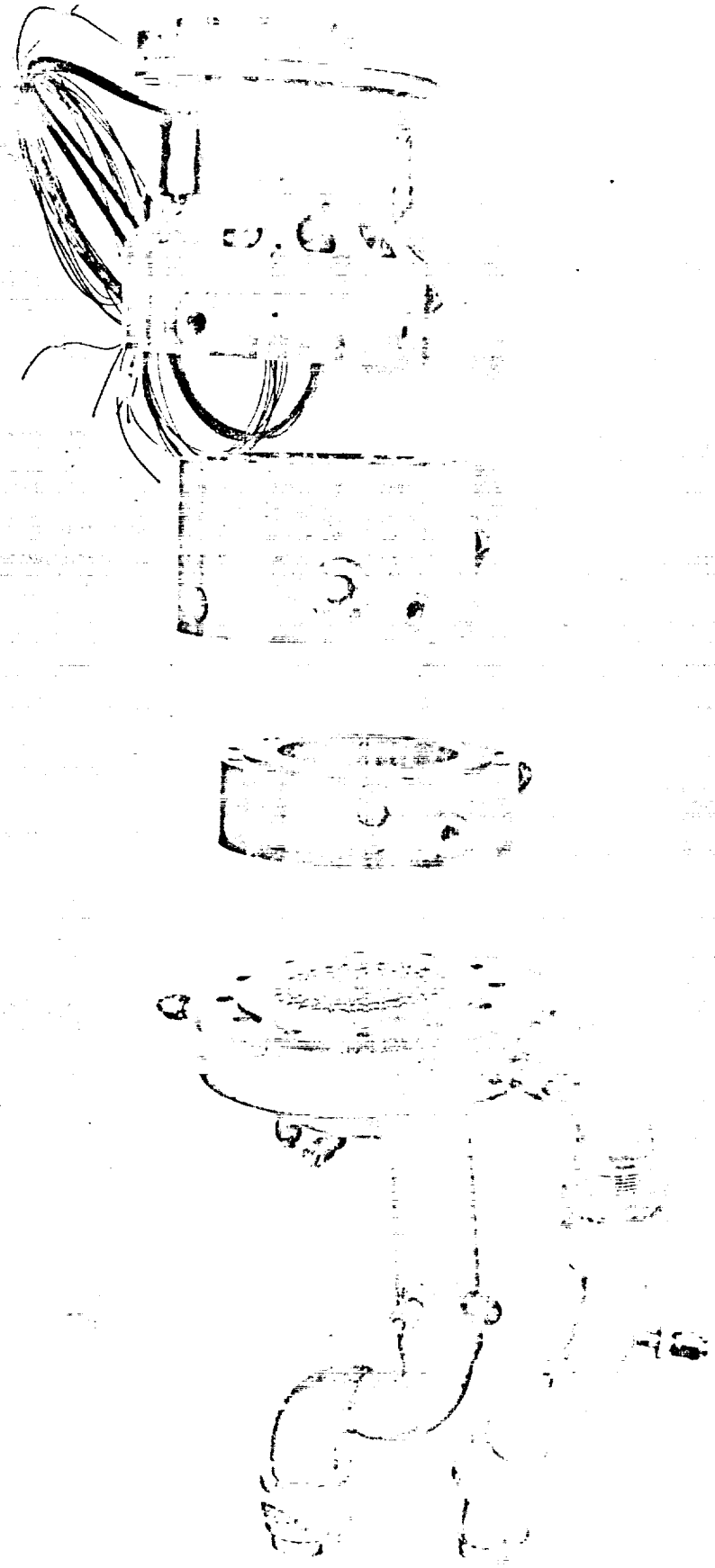

Workhorse Thrust Chamber Assembly

Figure 39

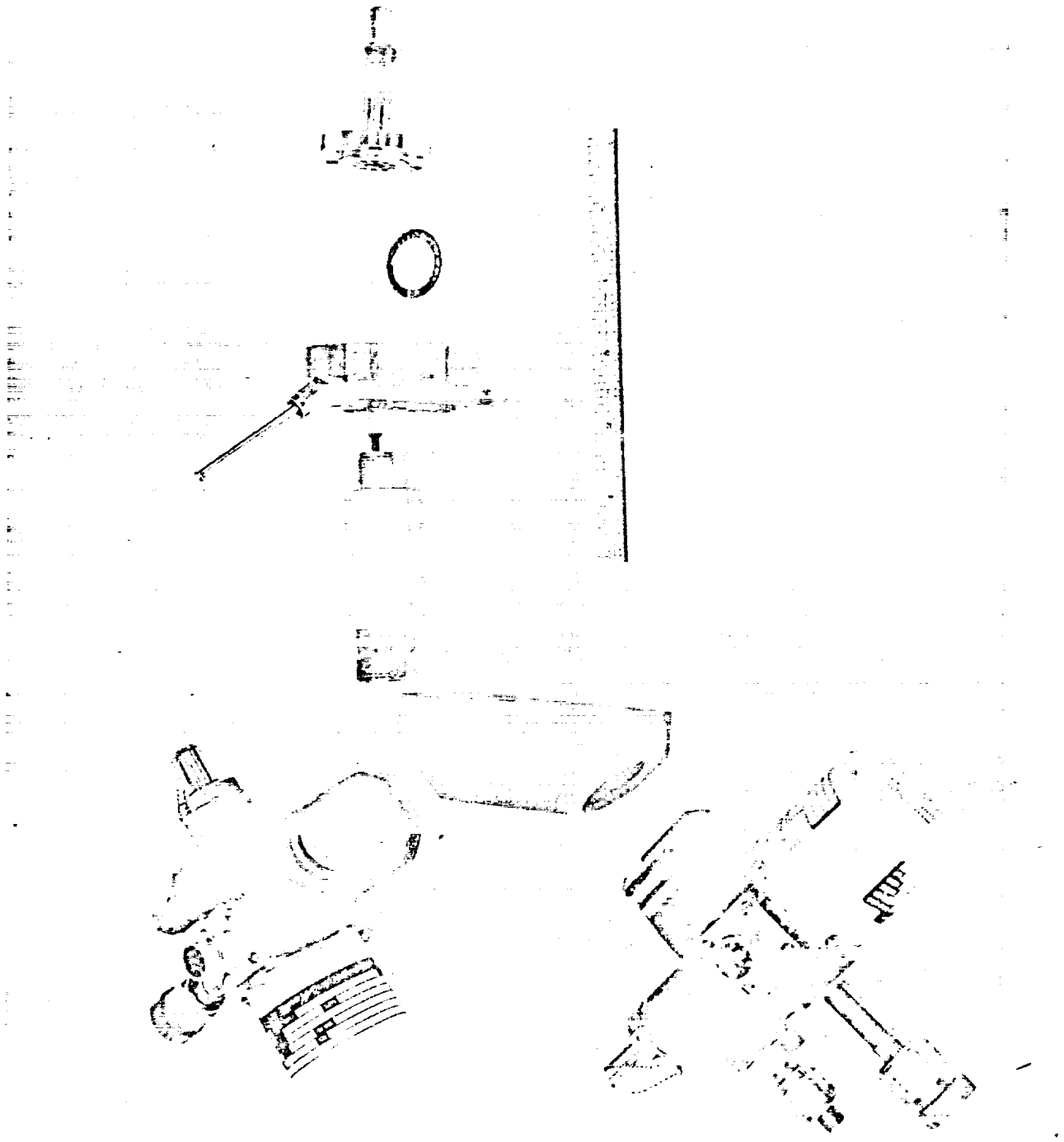

Figure 40

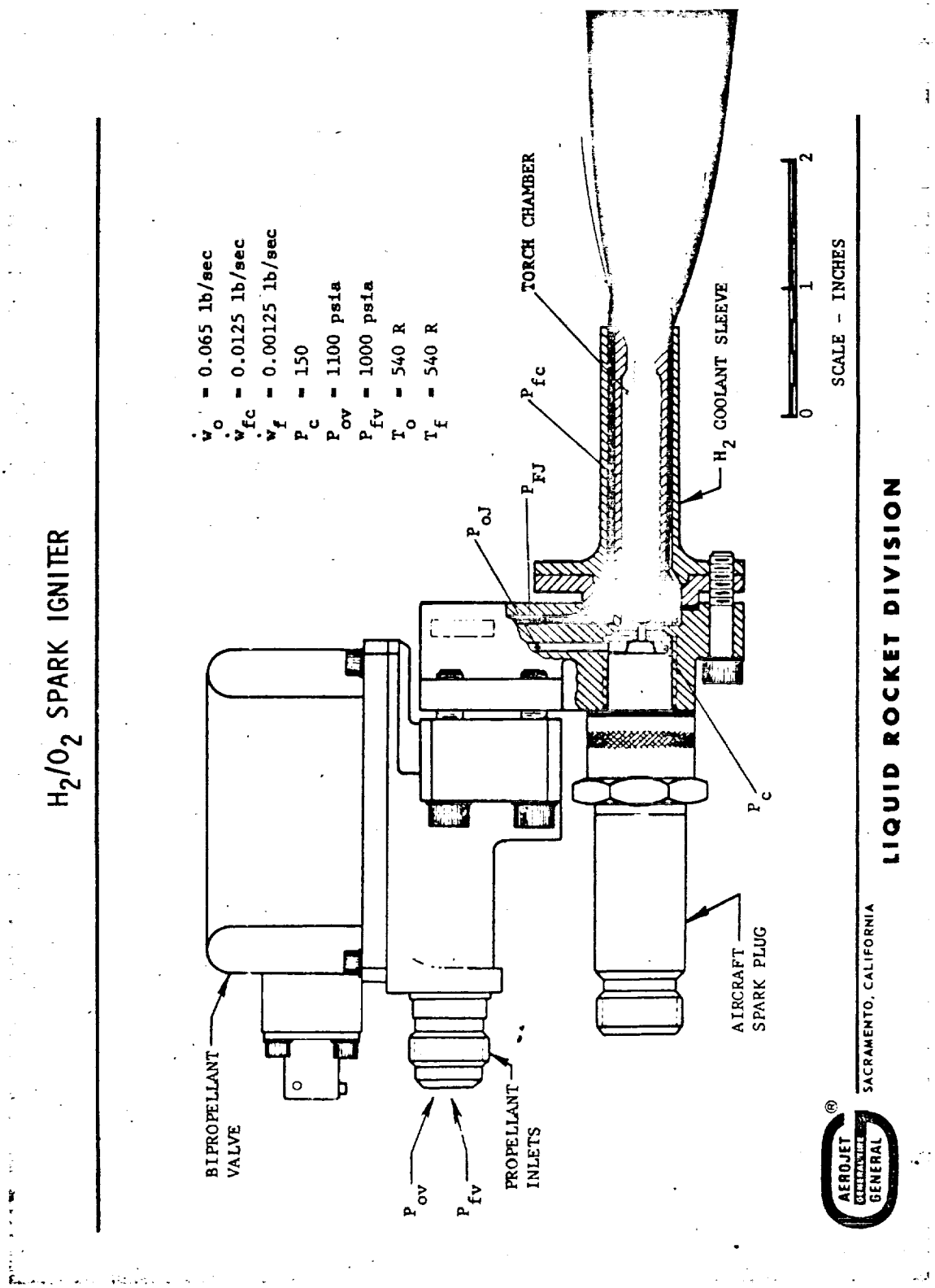

Igniter Schematic

Figure 41

Run No.	Test Date	Duration sec	P_c psia	MR O/F	I_s vac	I_s ϵ=240	ERE %	T_{ox} °R	T_F °R	L' in.	MR Ign. O/F	Remarks
101	7-2-70	0.206	419.4	5.56	333.4	421	91.40	518	551	6	5.07	800 cps at ±75 psi caused CSM shutdown. Pops indicated in igniter P_c. No hardware damage.
102	7-2-70	0.219	437.4	5.83	335.5	426	92.80	535	569	6	4.91	Same as Run No. 101.
103	7-2-70	0.180	450.4	5.93	337.2	430	93.64	532	569	6	4.90	Same as Run No. 101.
104	7-6-70	0.516	415.0	9.85	308.7	413	98.59	510	549	6	5.06	High MR test to investigate cyclic operation at 800 cps. Stable operation and no igniter pops. High performance. No hardware damage.
105	7-6-70	0.477	414.2	9.78	311.0	416	99.18	518	555	8	5.08	High MR test with 8 in. L' chamber. High performance with stable operation and no igniter Pops.
106	7-6-70	0.426	486.2	6.38	349.6	450	98.65	519	556	8	5.05	High performance and stable operation at nominal P_c and MR. Pops indicated in igniter P_c. No hardware damage.
107	7-17-70	0.489	491.8	7.13	340.3	440	98.79	512	548	8	5.16	High performance and stable operation at high MR. No igniter Pops with 1.5 x nominal igniter flow rate. Posttest analysis indicates igniter throat erosion.
108	7-17-70	0.464	494.9	7.11	341.0	441	98.87	512	550	8	5.14	Same comments as Run No. 107. Posttest inspection revealed igniter burnout. Minor erosion of injector igniter port and end of oxidizer tubes in co-axial element row adjacent to igniter.
109	7-24-70	0.490	505.4	6.05	350.2	449	97.92	515	554	8	5.41	Igniter oxidizer shut off after engine ignition to preclude burnout. Satisfactory test. No hardware damage.
110	7-24-70	0.476	524.5	5.17	362.9	455	98.38	516	555	8	5.42	Same as Run No. 109.
111	7-24-70	0.542	294.3	6.72	340.3	441	99.05	513	554	8	5.42	High MR, 300 P_c test same comments as Run No. 109.
112	7-24-70	0.542	302.1	5.90	352.2	452	99.18	523	554	8	5.24	Nominal MR, 300 P_c test same comments as Run No. 109.
113	7-24-70	0.529	309.1	4.89	364.3	455	98.90	528	554	8	5.35	Low MR, 300 P_c test minor oscillations at 740 cps for 0.10 sec at start. Same comments as Run No. 109.
114	7-24-70	0.219	293.8	3.70	354.9	424	93.20	538	560	8	5.48	3.7 MR, 300 P_c test. 800 cps ± 40 psi oscillations caused CSM shutdown. igniter Pop at igniter oxidizer shutdown. No hardware damage.
115	7-24-70	0.503	479.5	5.94	353.5	453	98.43	518	559	8	5.40	6.5 grain pulse test at nominal P_c and MR recovery in less than 6 MS from approximately 1000 psi overpressure satisfactory test. No hardware damage was noted.
116	7-29-70	0.542	499.7	6.01	353.8	454	98.67	518	559	8	5.32	Same comments as Run No. 115 except minor deformation of 6 co-axial elements from bomb fragments. Pulse testing discontinued.

OMS Injector Test Summary

Run No.	Test Date	Duration Sec.	P_c Psia	M.R. O/F	I_s Vac	I_s =240	ERE %	T_{ox} °R	T_F °R	L' in.	M.R. Ign %	REMARKS
117	8-20-70	.258	672.2	4.57	359.61	445	95.97	524	552	8	5.22	4.6 M.R., 670 P_c test. Ambient propellants 800 Cps ± 40 Psi oscillations caused CSM shutdown. Two ignitor pops. No hardware damage was noted. Ignitor oxidizer shutoff after engine ignition to preclude burnout.
118	8-20-70	.387	647.1	5.95	359.20	460	99.96	509	546	8	5.18	6.0 M.R., 650 P_c test. Ambient propellants. Satisfactory test. Stable combustion. No ignitor pops. No hardware damage. Ignitor sequence as Run No. 117.
119	8-20-70	.375	681.0	5.13	362.7	457	98.30	510	545	8	5.13	5.1 M.R., 680 P_c test. Ambient propellants. Minor intermittent oscillations at 740 Cps ± 20 Psi for .13 seconds at start. Two ignitor pops. No hardware damage. Lost thrust data, of scale. Ignitor sequence as Run No. 117.
120	8-20-70	.412	607.4	6.97	348.14	452	100.0	506	546	8	5.14	7.0 M.R., 600 P_c test. Ambient propellants. Satisfactory test. Stable combustion. One ignitor pop. No hardware damage. Ignitor sequence as Run No. 117.
121	8-24-70	.516	512.5	5.50	369.74	462	100.0	488	475	8	5.01	5.5 M.R., 500 P_c test. Cooled propellants Satisfactory test. Stable combustion. No ignitor pops. No hardware damage. Ignitor sequence as Run No. 117. Lost TOV temperature.
122	8-24-70	.542	483.9	5.58	362.60	462	100.0	490	475	8	4.97	5.6 M.R., 480 P_c test. Cooled propellants. Satisfactory test. Stable combustion. No ignitor pops. No hardware damage. Ignitor sequence as Run No. 117.
123	8-24-70	.516	453.0	6.43	349.25	456	100.0	485	464	8	5.06	6.4 M.R., 450 P_c test. Cooled propellants. Satisfactory test. Stable combustion. No ignitor pops. No hardware damage. Ignitor sequence as Run No. 117.

OMS Injector Test Summary

Figure 42. Sheet 2 of 2

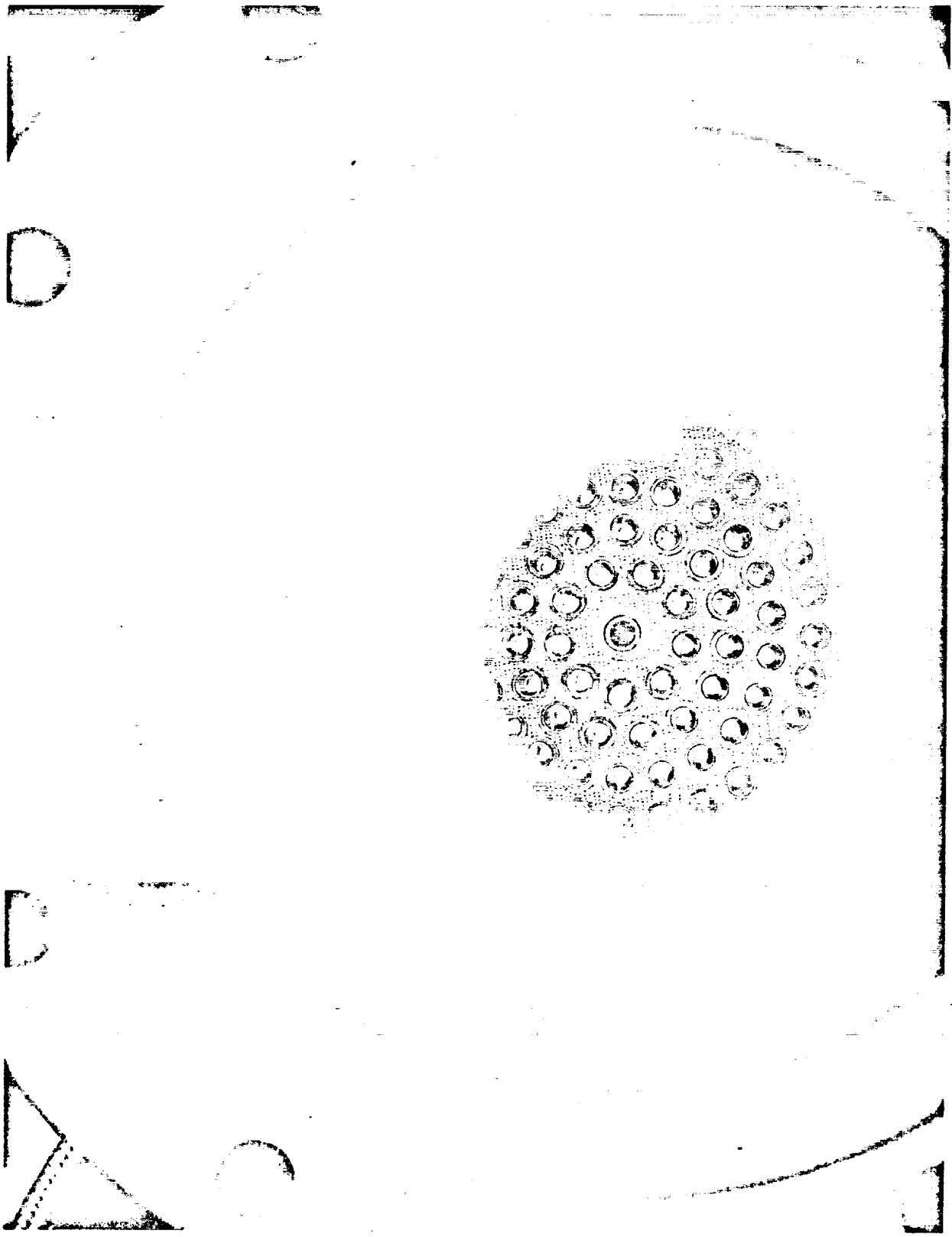

Injector Face Prefire 2K-2-108

Figure 43

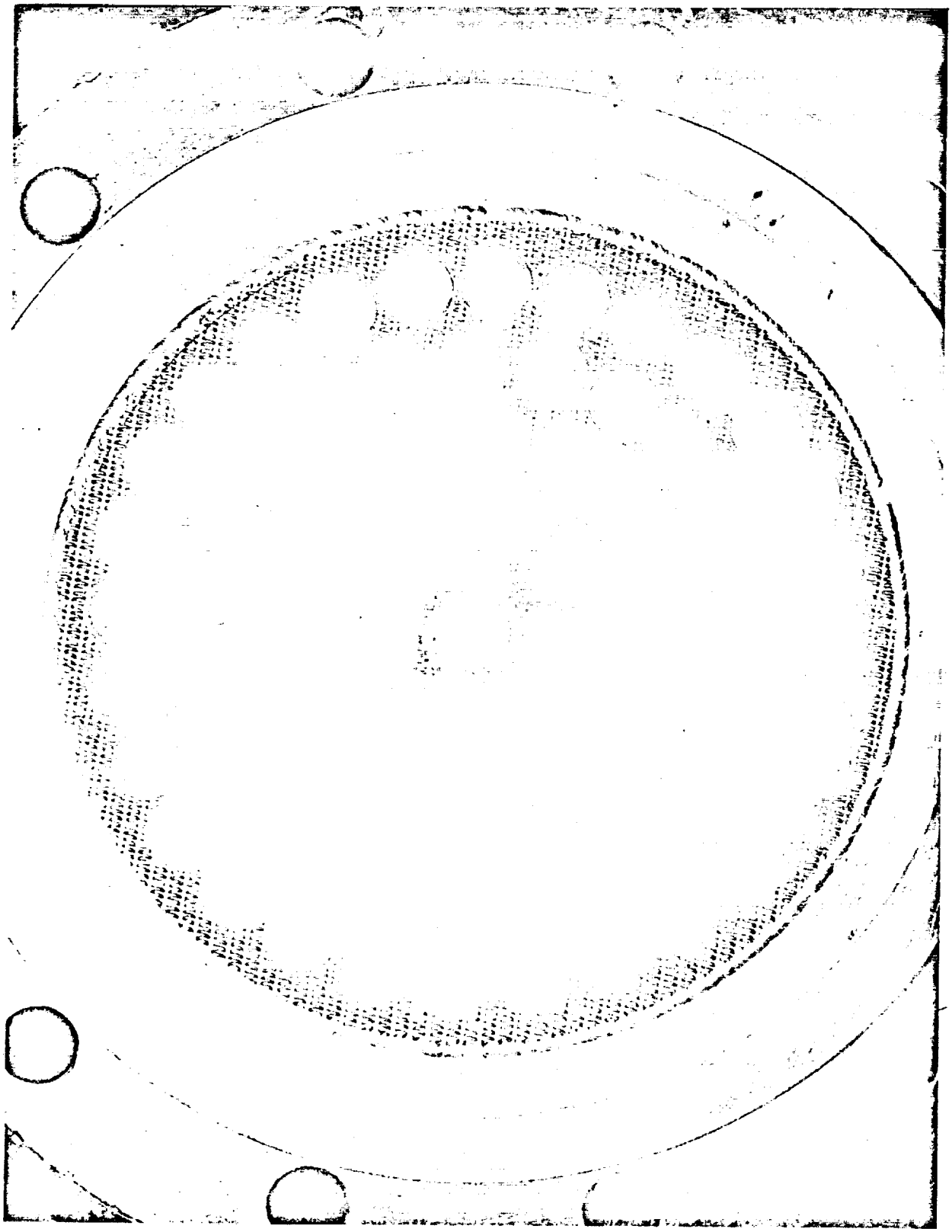

Injector Face Postfire 2K-2-108

Figure 44

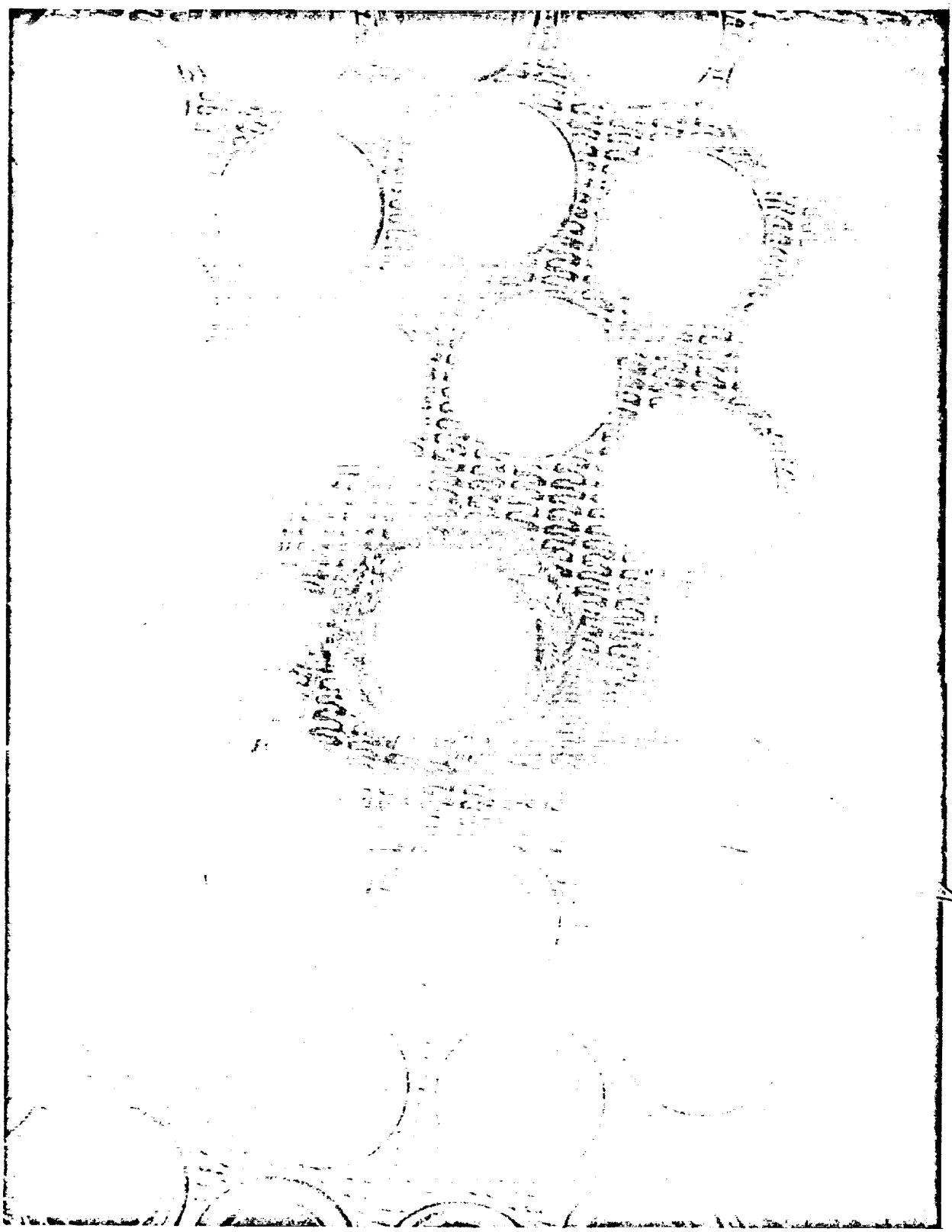

Close up of Injector Face Postfire 2K-2-108

Figure 45

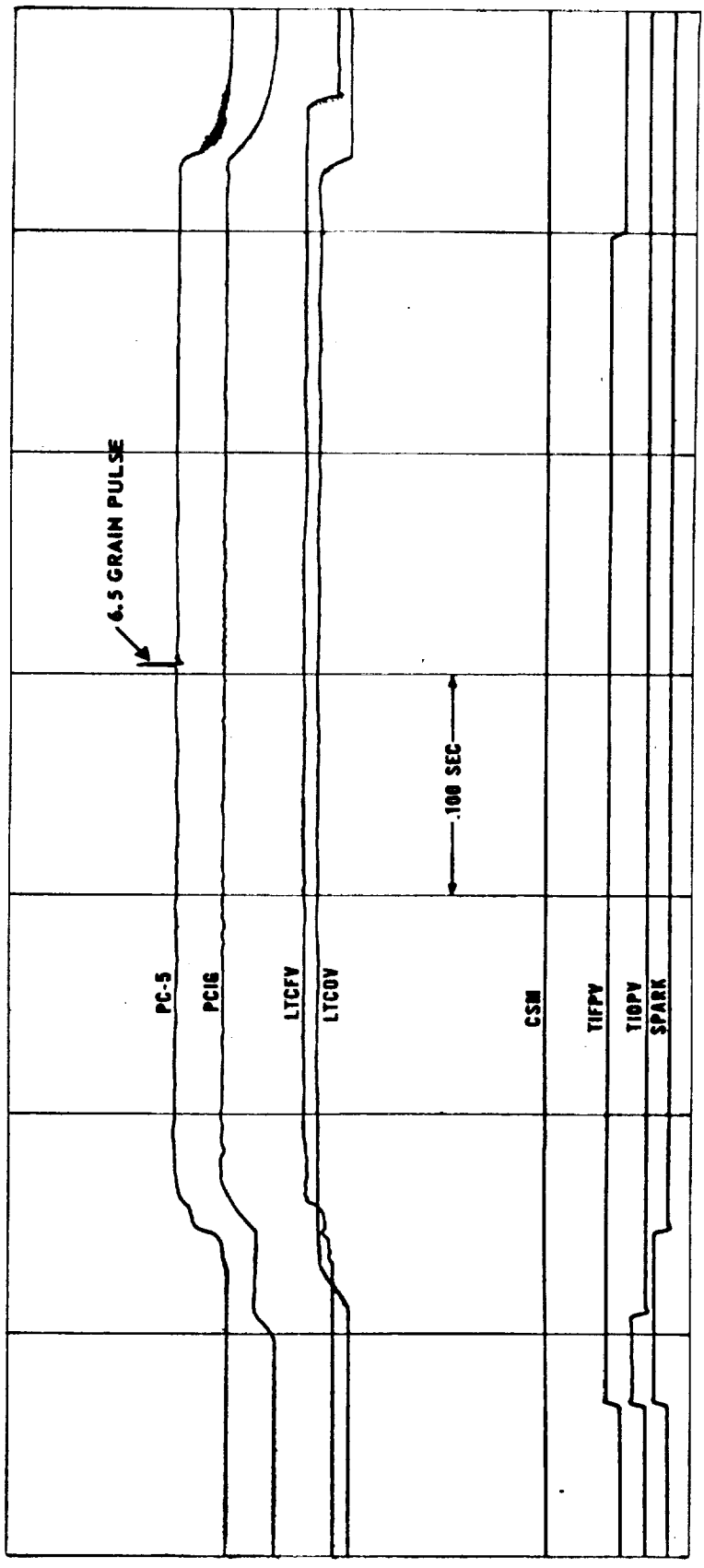

Oscillograph Record Test 115

Figure 46

115

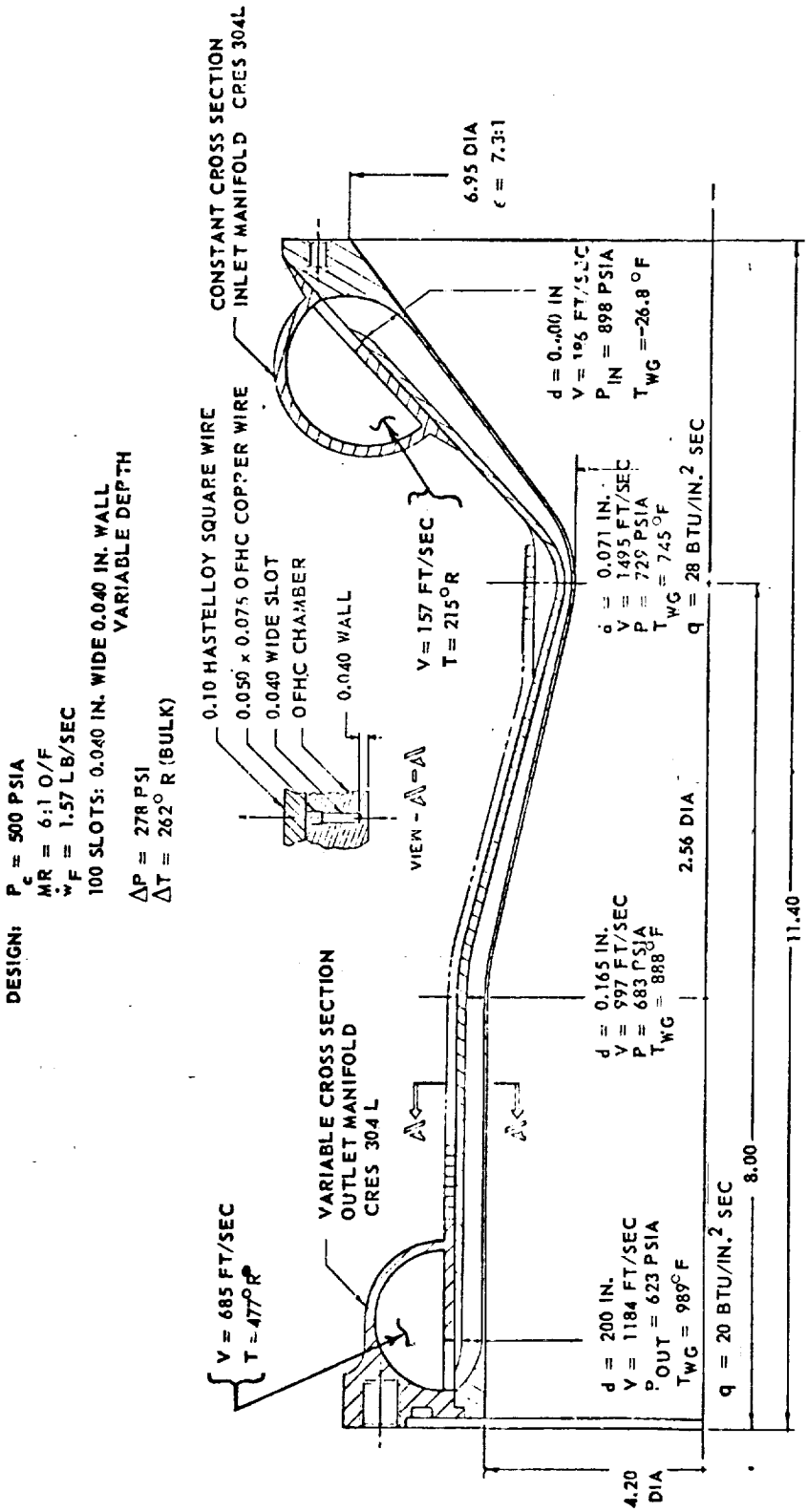

Copper Thrust Chamber

Figure 47

Inside Contour Machining

Figure 48

Inside Contour Machining

Figure 48

Coolant Passage Machining

Figure 49

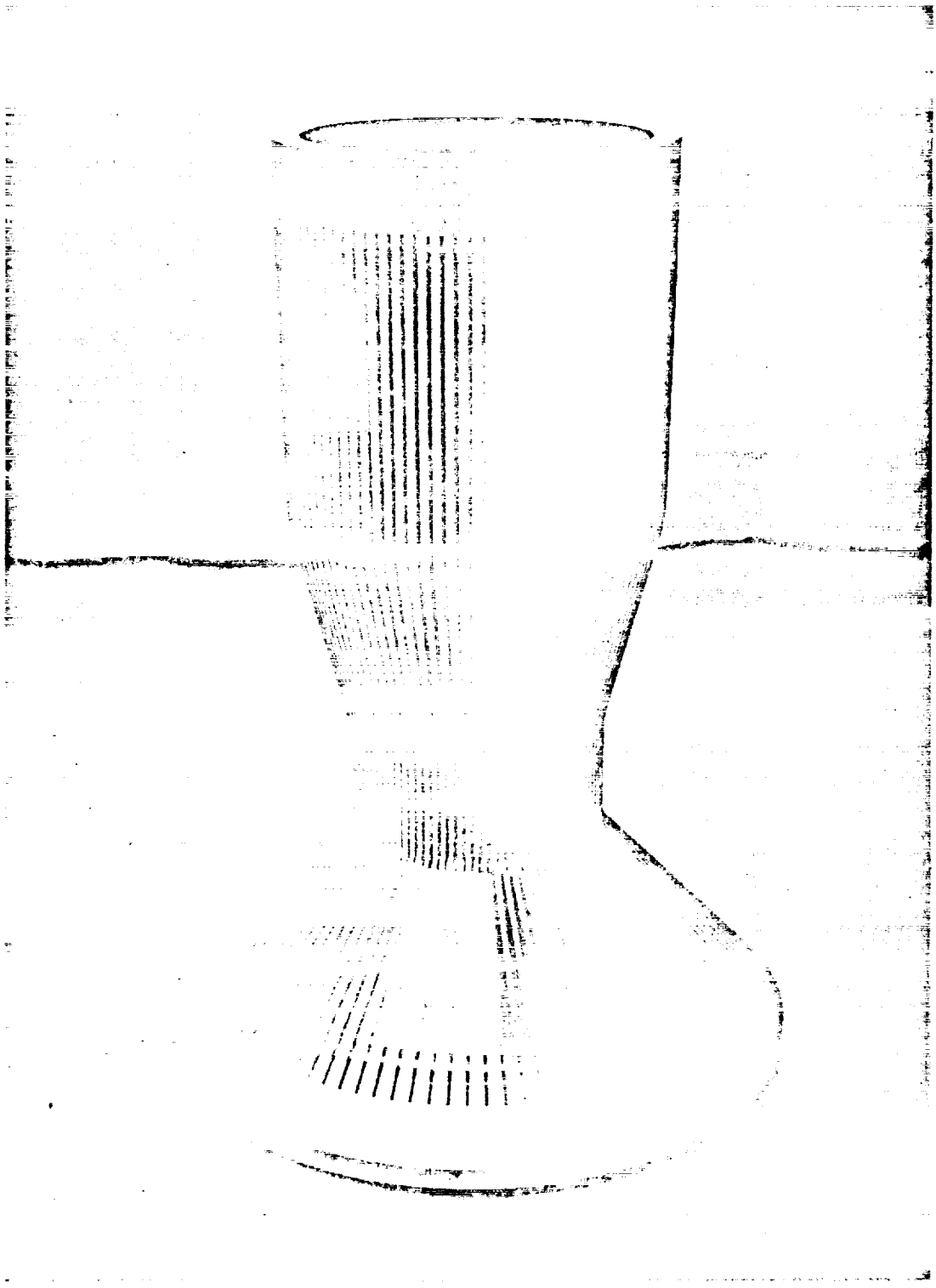

Chamber After Machining

Figure 50

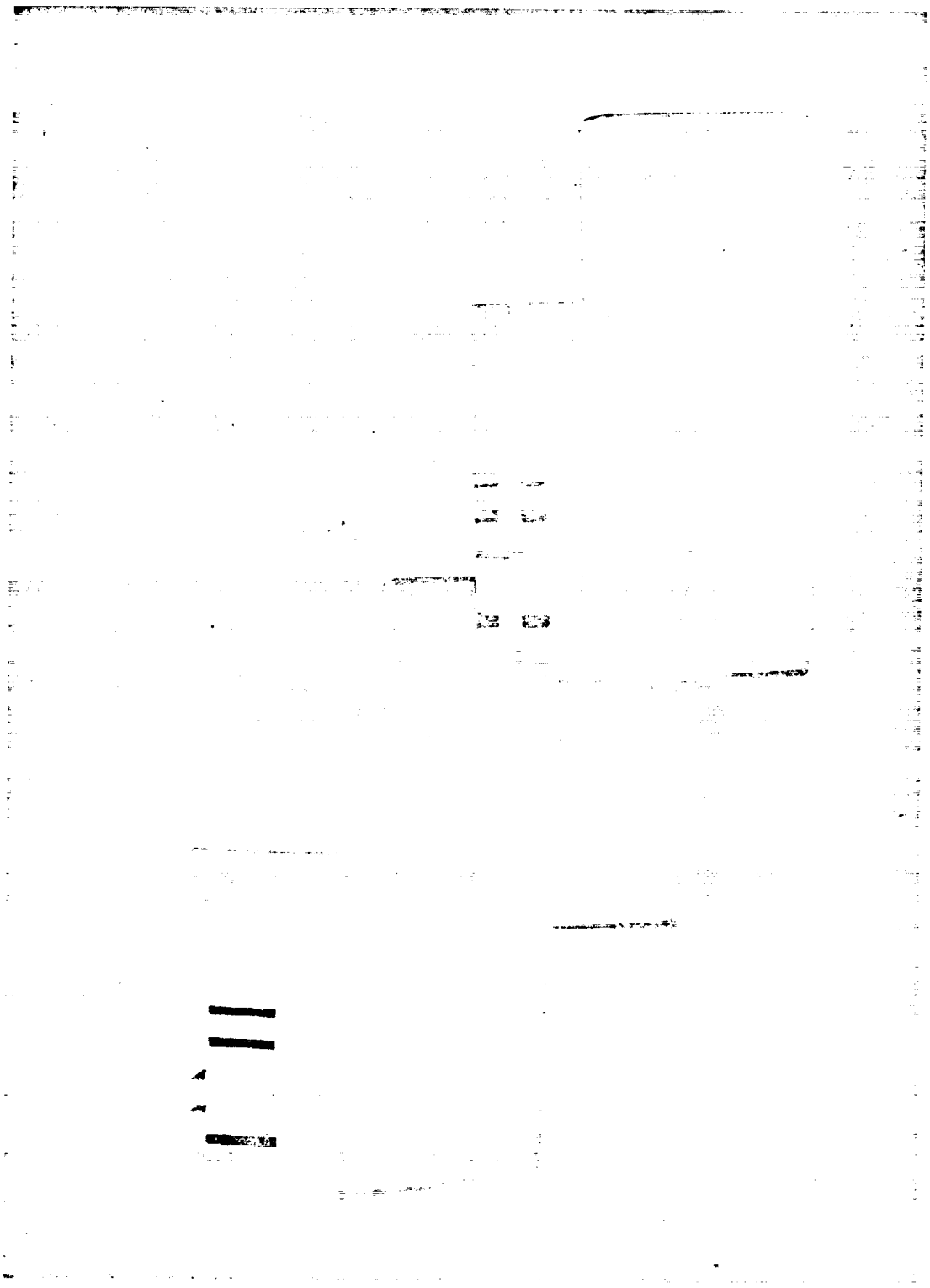

Braze Samples

Figure 51

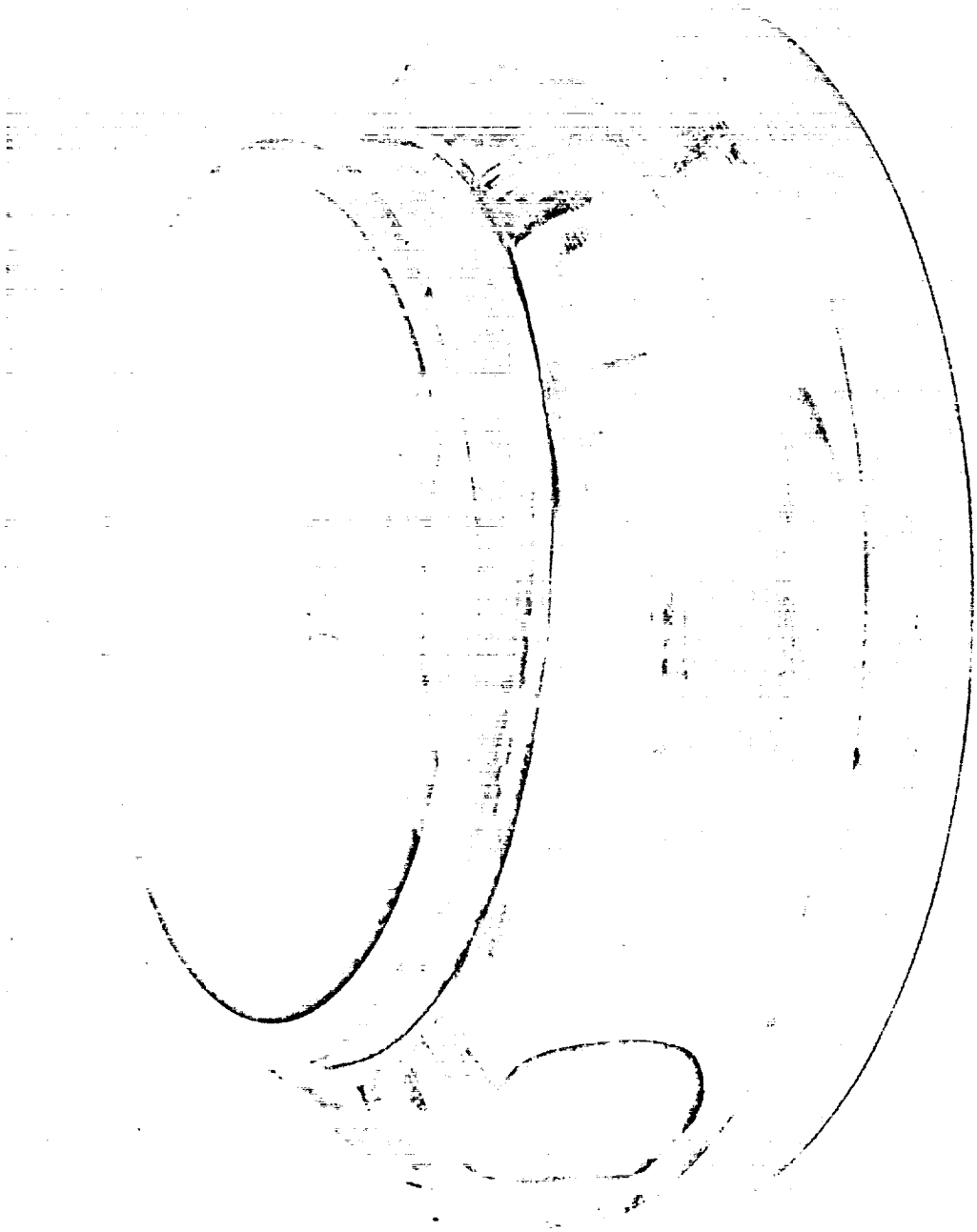

Figure 52

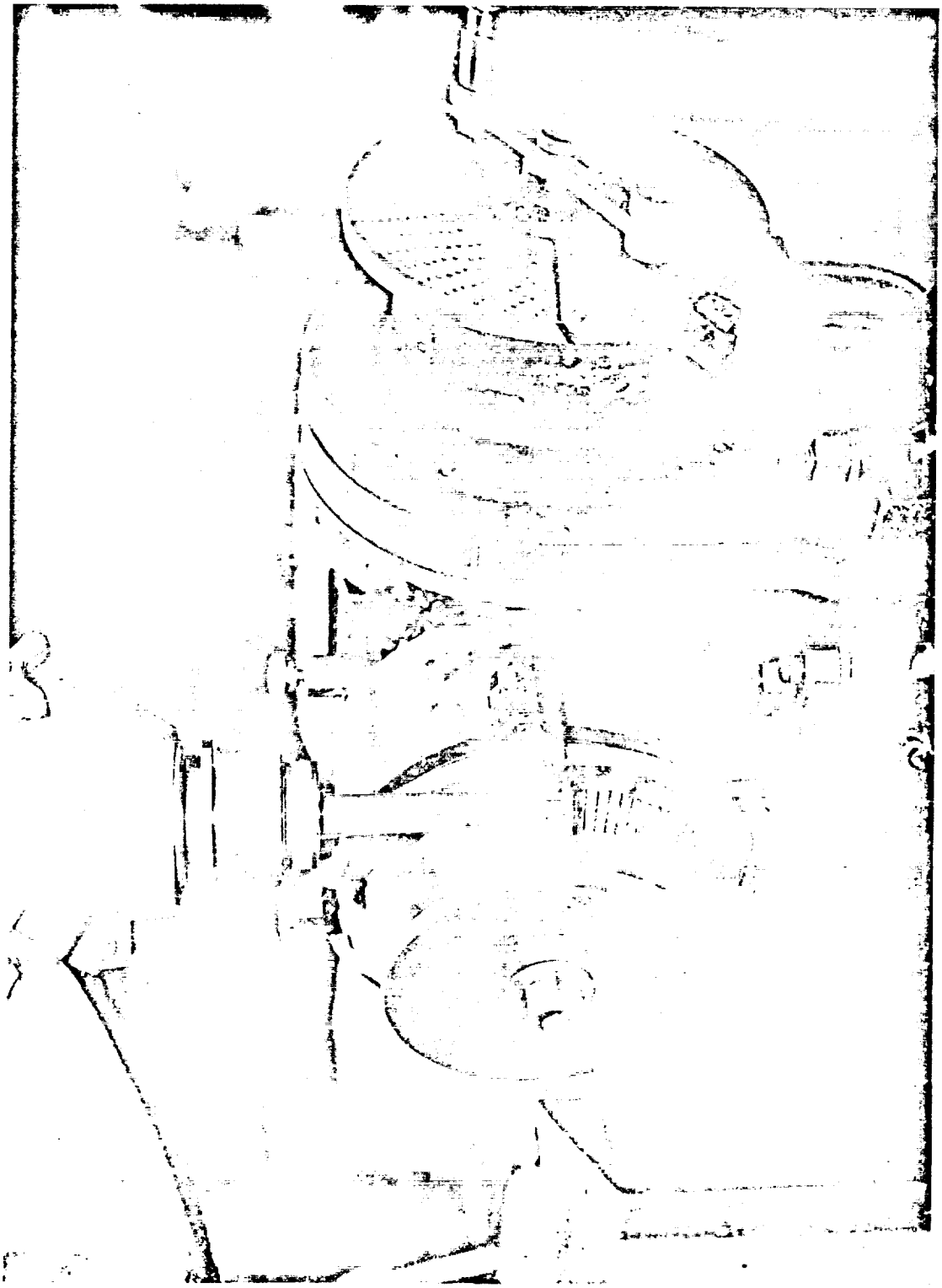

Inlet Manifold Machining

Figure 53

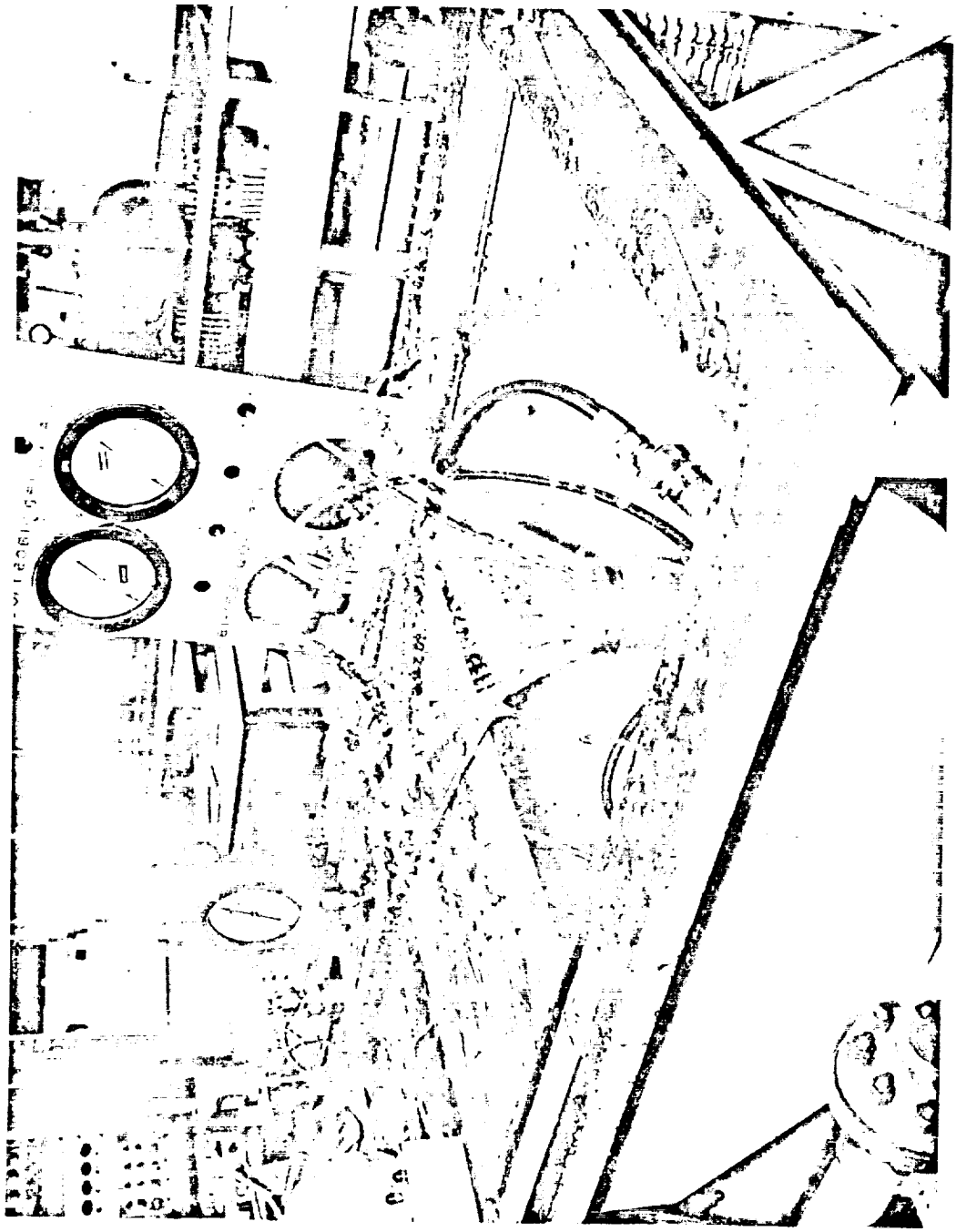

Figure 54. OME Thrust Chamber Cold Flow Test

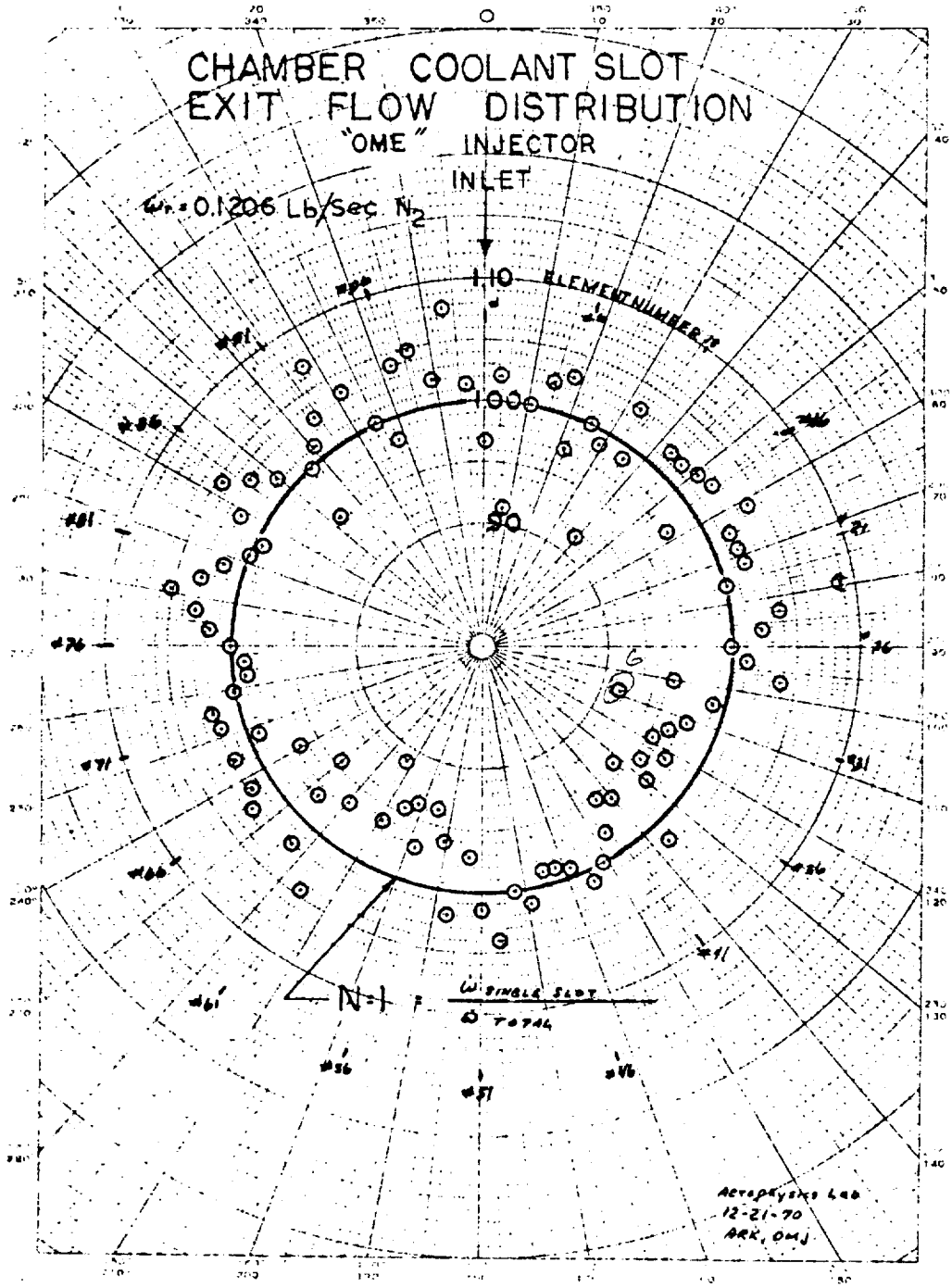

Figure 55. Results of OME Combustion Chamber Gas Flow Tests

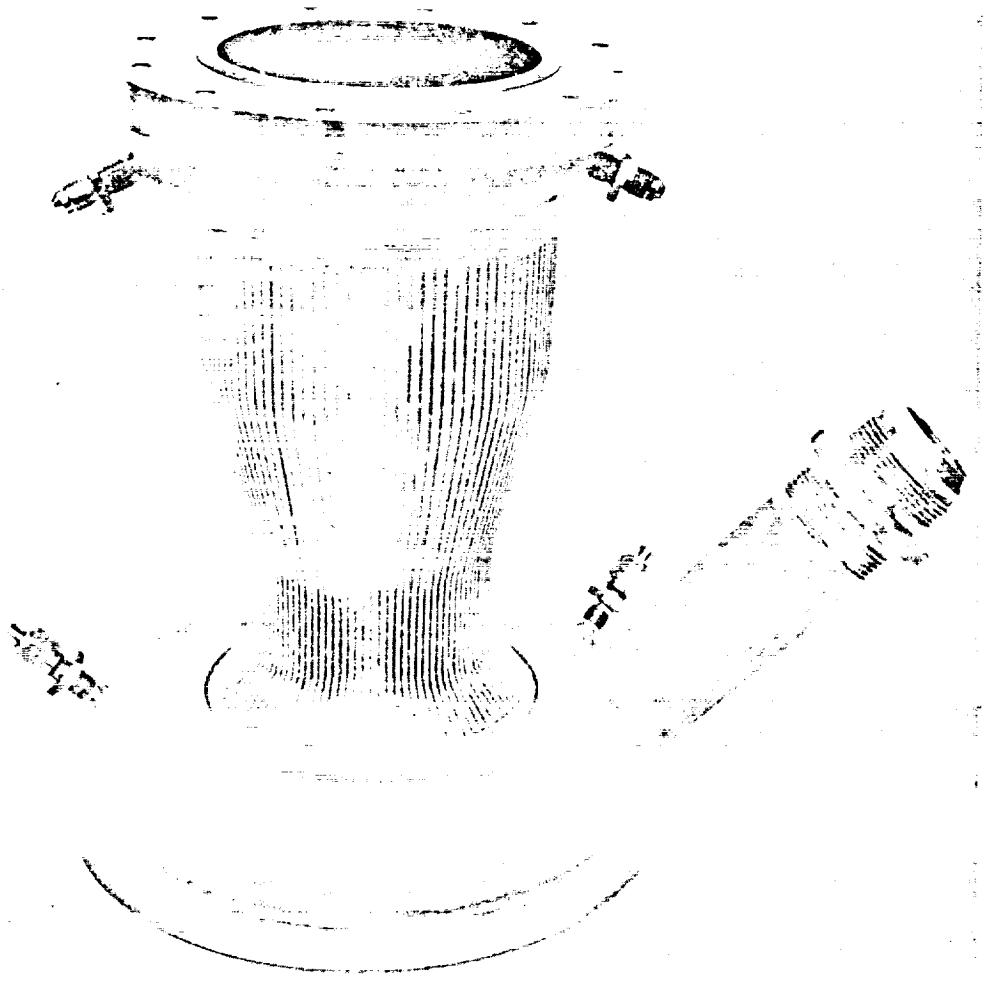

Figure 56. Combustion Chamber with Manifolds Brazed in Position

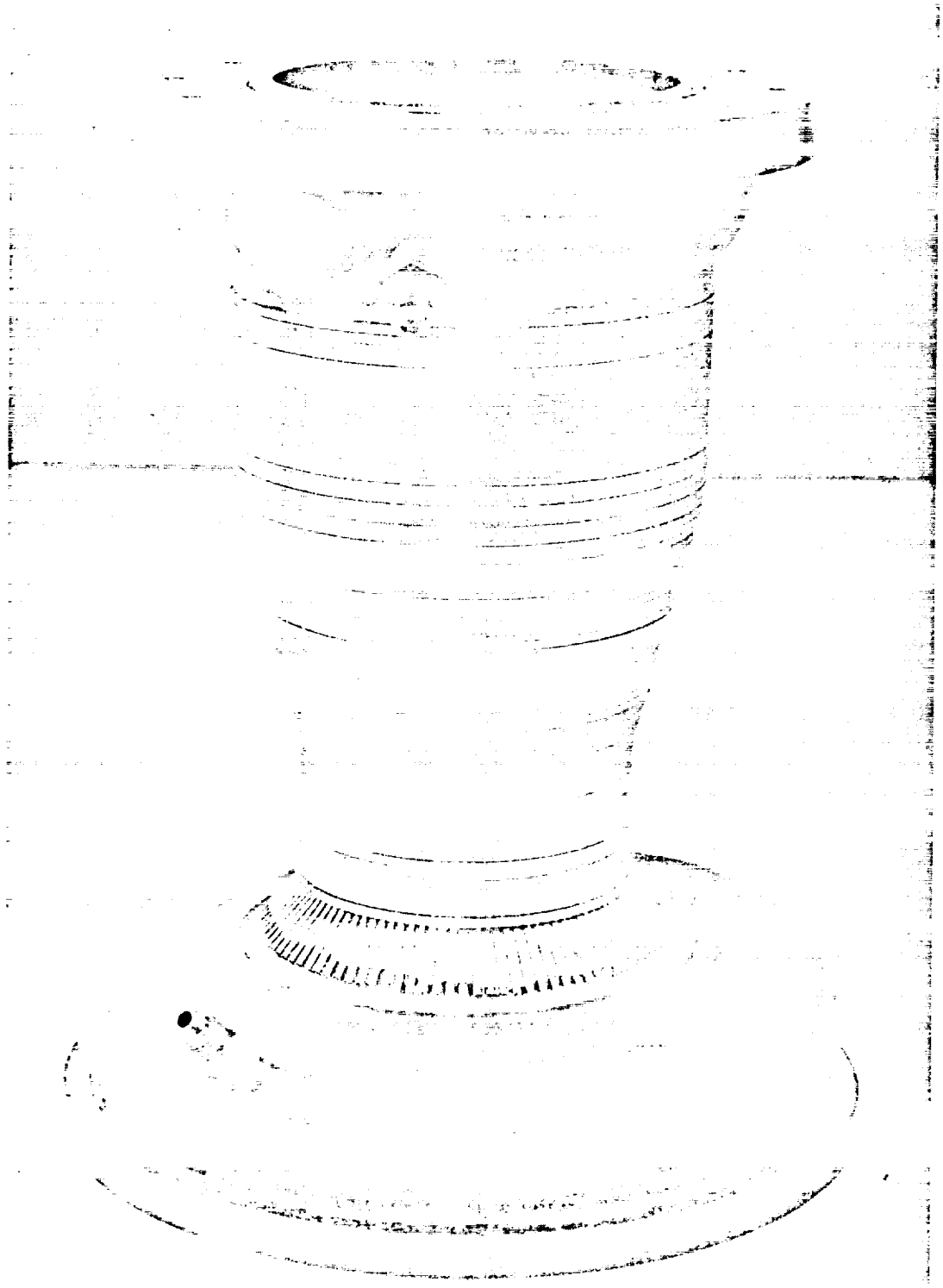

Figure 57. Combustion Chamber After Wire Wrap

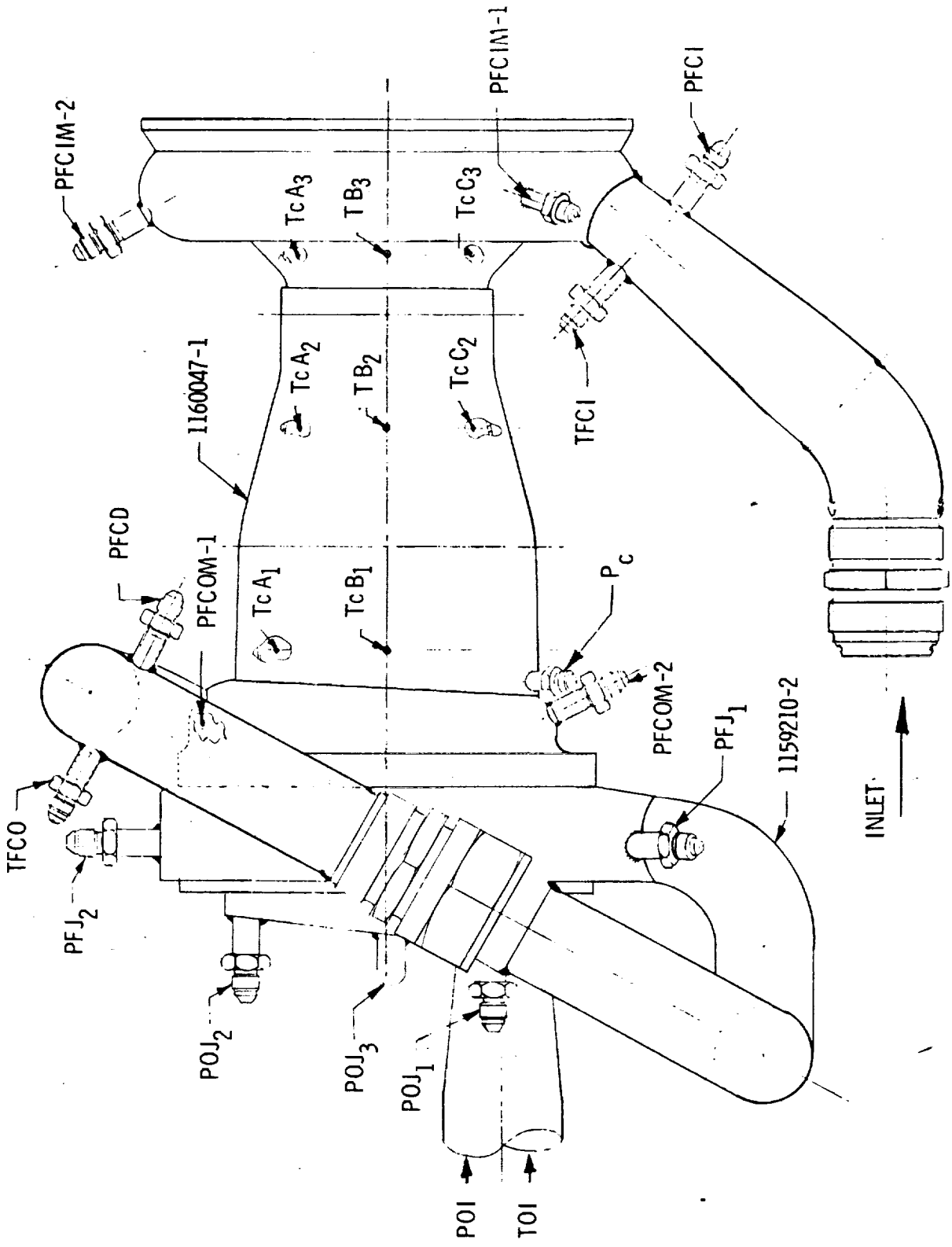

Figure 58. TCA Instrumentation Location

Parameter	Symbol	Instrument (or Equivalent)	Suggested System Range	CPS Frequency Response	Total Measurement Accuracy (1 σ)
Chamber Pressure	P_C	Taber	0-1000 psi	0-600	±0.14%
Fuel Manifold Pressure	P_{FJ}-1 and-2	Taber	0-1000 psi	0-600	±1.0%
Oxidizer Manifold Pressure	P_{OJ}-1 thru-3	Taber	0-1000 psi	0-600	±1.0%
Ambient Atmospheric Pressure	PA	Recording Barometer	28-31 in.Hg	--	±0.2%
Oxidizer Venturi Pressure	POV	Taber	0-1500 psi	0-600	±0.14%
Fuel Venturi Pressure	PFV	Taber	0-1500 psi	0-600	±0.14%
Oxidizer Venturi Temp.	TOV	CA Thermocouple	200-600°R	--	±5°F
Fuel Venturi Temp.	TFV	CA Thermocouple	200-600°R	--	±5°F
Oxidizer Flow Rate	$\dot{W}_O$	Venturi	--	--	±0.5%
Fuel Flow Rate	$\dot{W}_F$	Venturi	--	--	±0.5%
Oxidizer Temperature at Injector Inlet	TOI	CA Thermocouple	200-600°R	--	±5°F
Oxidizer Pressure at Injector Inlet	POI	Taber	0-1000 psi	0-600	±1.0%
Fuel Temperature at Injector Inlet	TFI	CA Thermocouple	200-600°R	--	±5°F
Fuel Pressure at Injector Inlet	PFI	Taber	0-1000 psi	0-600	±1.0%
Chamber Temperature	T_C-1 thru-8	CA Thermocouple	0-2000°F	--	±5°F
Fire Switch	FS	Switch Trace	--	--	--
Oxidizer Valve Trace	LTCOV	Pot Trace	--	60	±1%

Figure 59. TCA Instrumentation (Sheet 1 of 2)

Parameter	Symbol	Instrument (or Equivalent)	Suggested System Range	CPS Frequency Response	Total Measurement Accuracy (b)
Fuel Valve Trace	LTCFV	Pot Trace	--	60	±1%
Oxidizer TCV Pilot Valve Trace	TCOVPV	Switch Trace	--	60	--
Fuel TCV Pilot Valve Trace	TCFVPV	Switch Trace	--	60	--
Oxidizer Igniter Valve Trace	TIOPV	Switch Trace	--	60	--
Fuel Igniter Valve Trace	TIFPV	Switch Trace	--	60	--
Thrust	FA FB	Baldwin Baldwin	0-5K 0-5K	0-600 0-600	±0.15% ±0.15%
Chamber Pressure Igniter	P_C-I_G	Taber	0-1000 psi	0-600	±1.0%
Oxidizer Venturi Pressure Igniter	POVI	Taber	0-1500 psi	0-600	±0.14%
Fuel Venturi Pressure Igniter	PFVI	Taber	0-1500 psi	0-600	±0.14%
Oxidizer Venturi Temperature Igniter	TOVI	CA Thermocouple	200-600°R	--	±5°F
Fuel Venturi Temperature Igniter	TFVI	CA Thermocouple	200-600°R	--	±5°F
Fuel Inlet Chamber Pressure	PFCI	Taber	0-1500 psi	0-600	±.14%
Fuel Outlet Chamber Pressure	PFCO	Taber	0-1500 psi	0-600	±.14%
Fuel Inlet Chamber Temperature	TFCI	CA Thermocouple	100-300°R	--	±5°F
Fuel Outlet Chamber Temperature	TFCO	CA Thermocouple	200-600°R	--	±5°F
Fuel Inlet Chamber Manifold Pressure	PFCIM-1 -2	Taber	0-1500 psi	0-600	±.14%
Fuel Outlet Chamber Manifold Pressure	PFCOM-1 -2	Taber	0-1500 psi	0-600	±.14%

Figure 59. TCA Instrumentation (Sheet 2 of 2)

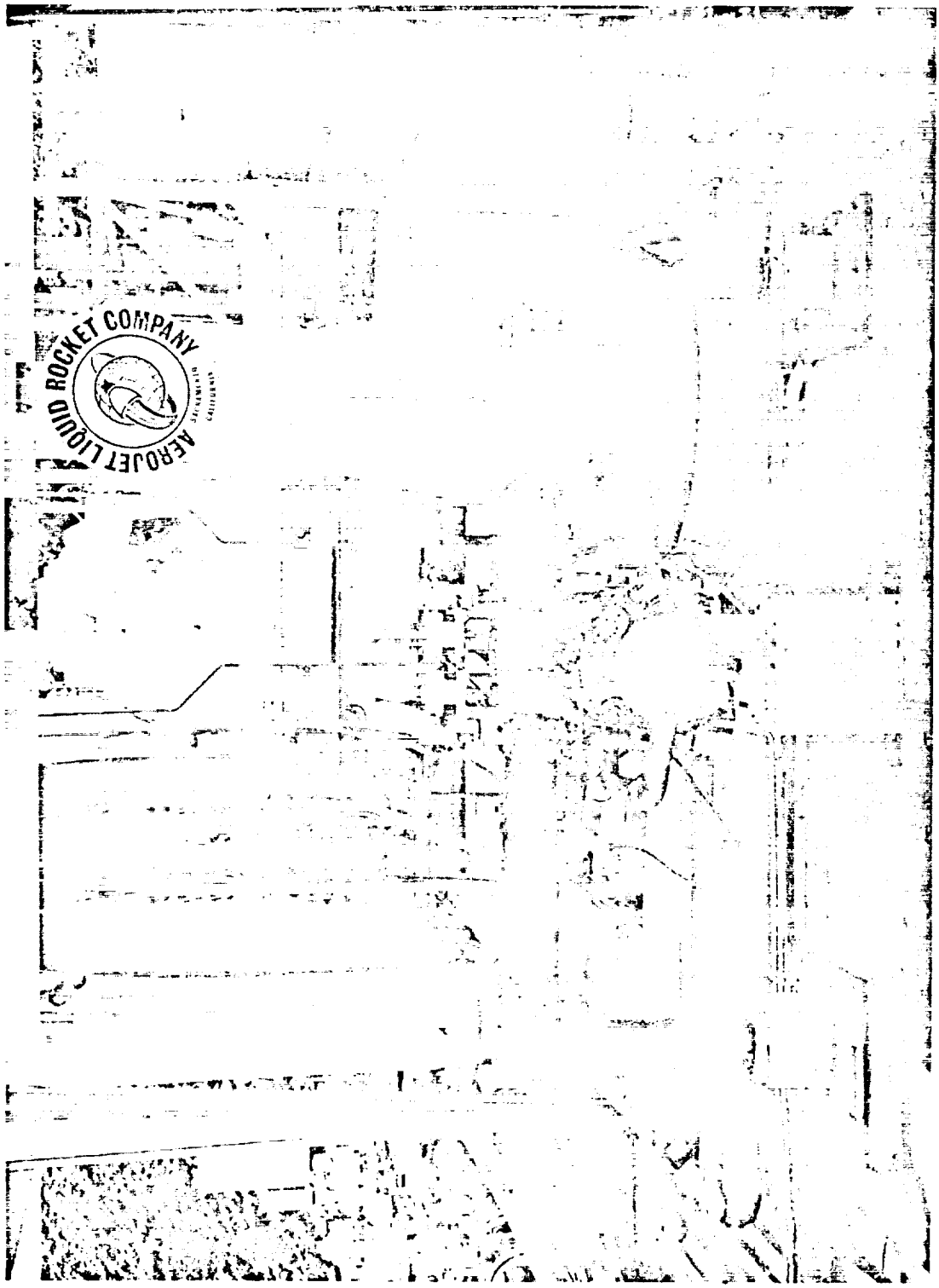

Figure 60. OME TCA on Test Stand

Figure 61. OME TCA on Test Stand

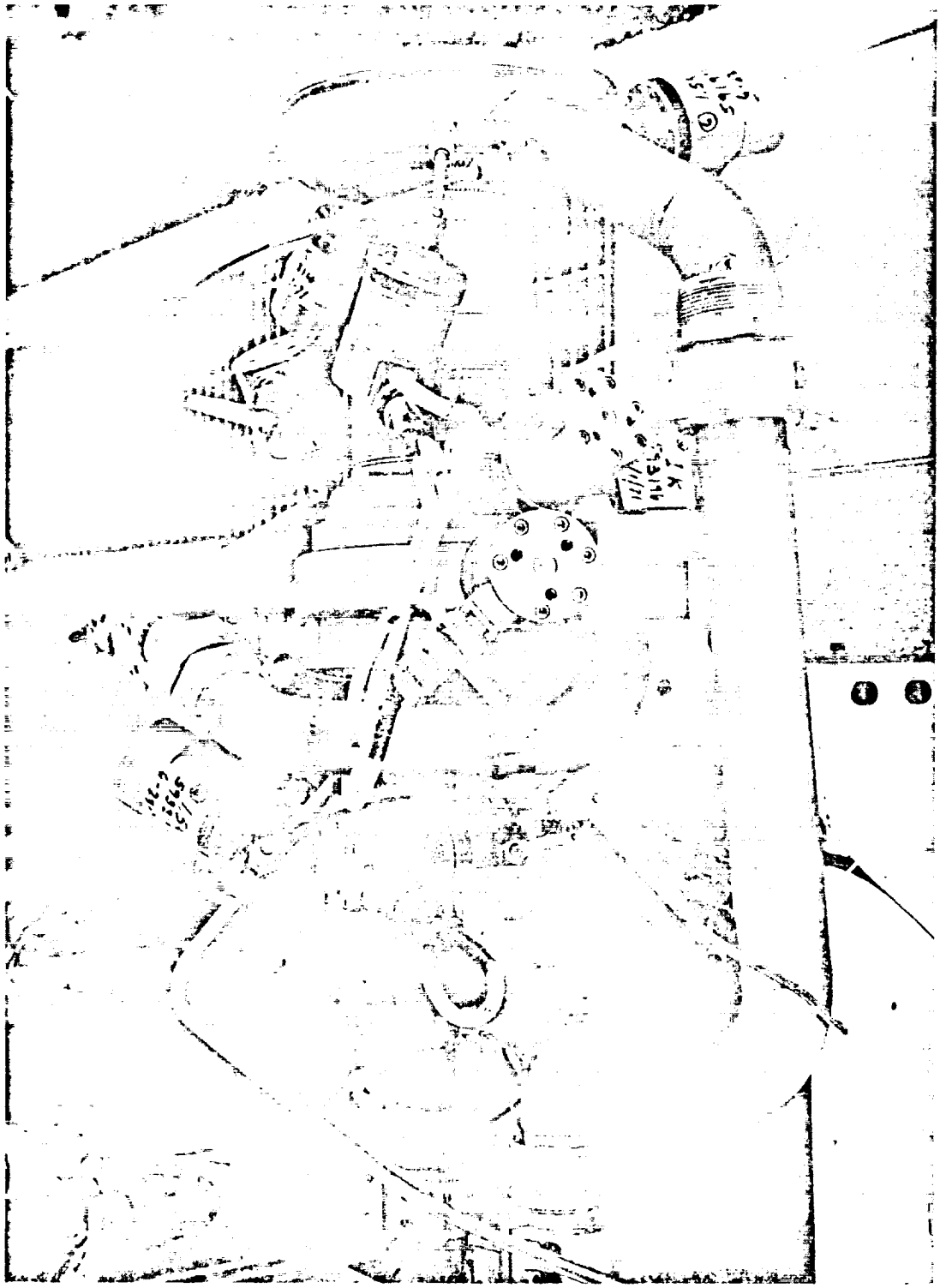

Figure 62. OME TCA on Test Stand

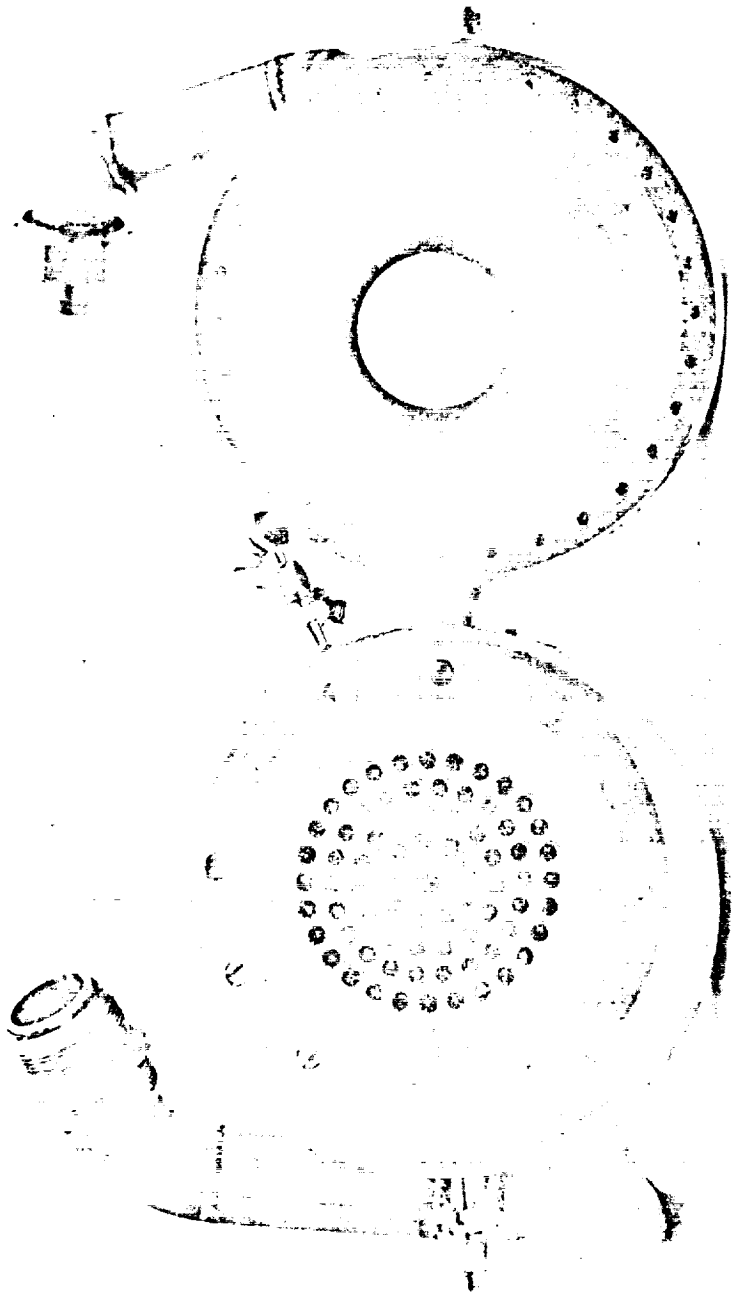

Figure 63. OMS TCA Post Fire

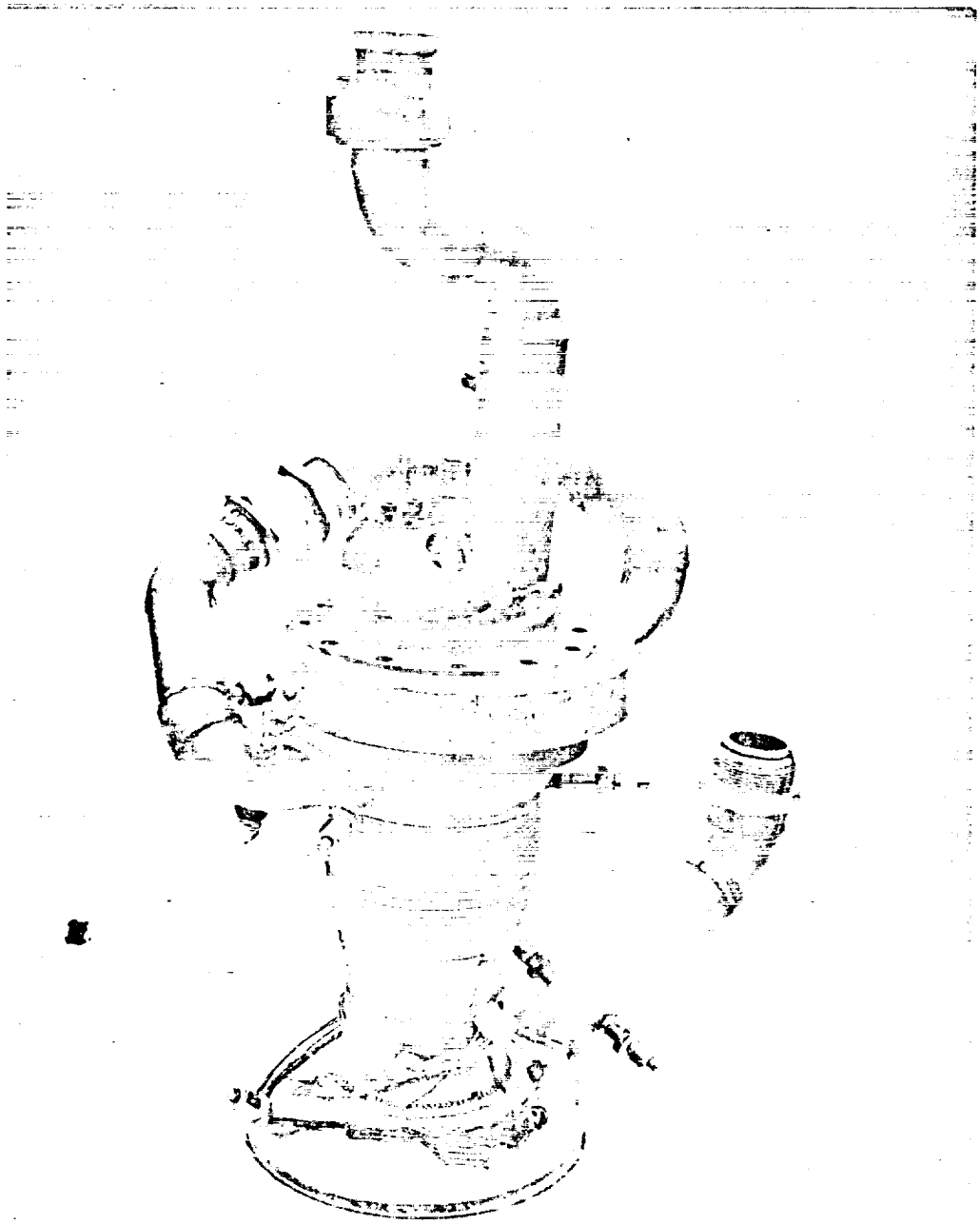

Figure 64. OMS TCA Post Fire

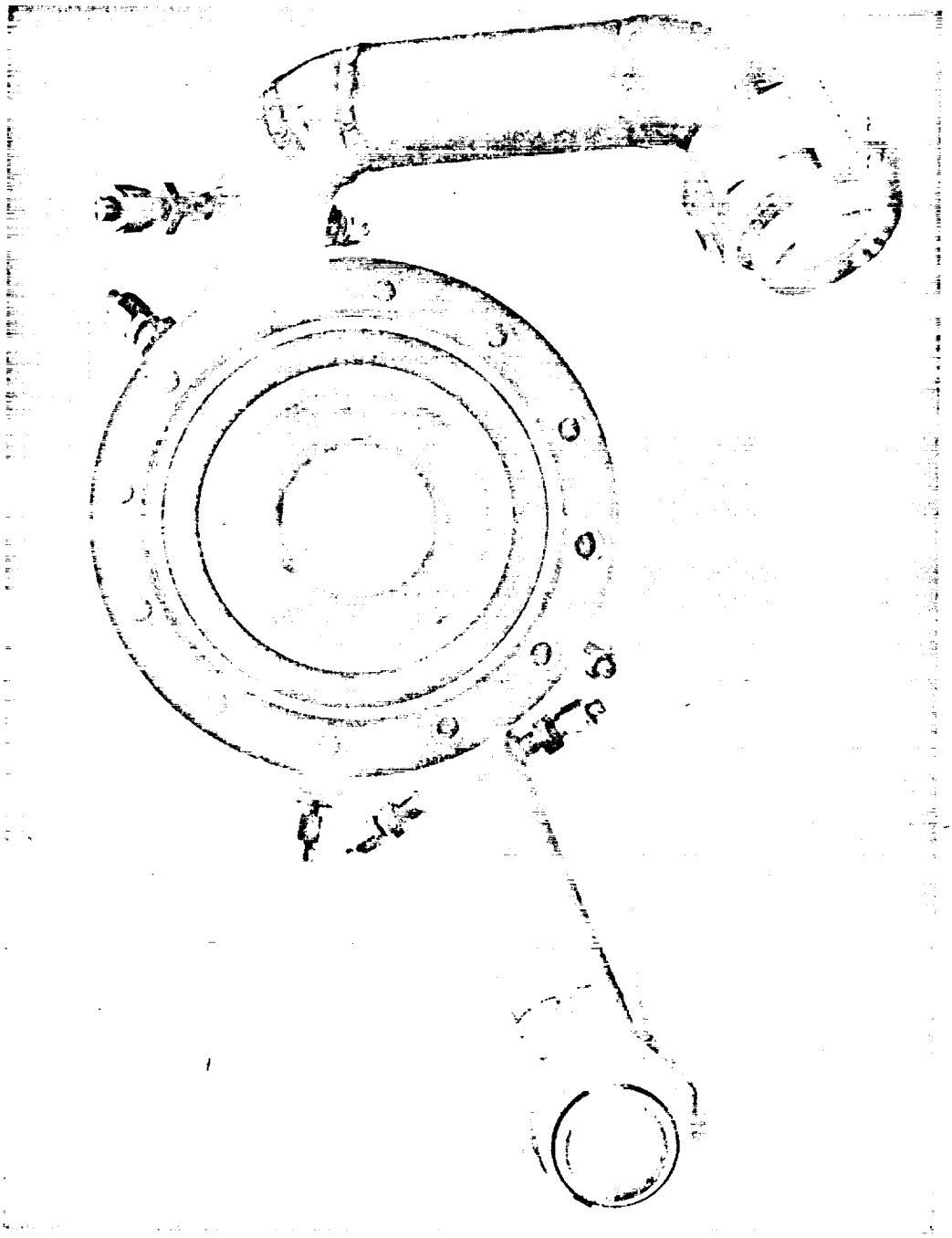

Figure 65. OMS TCA Post Fire

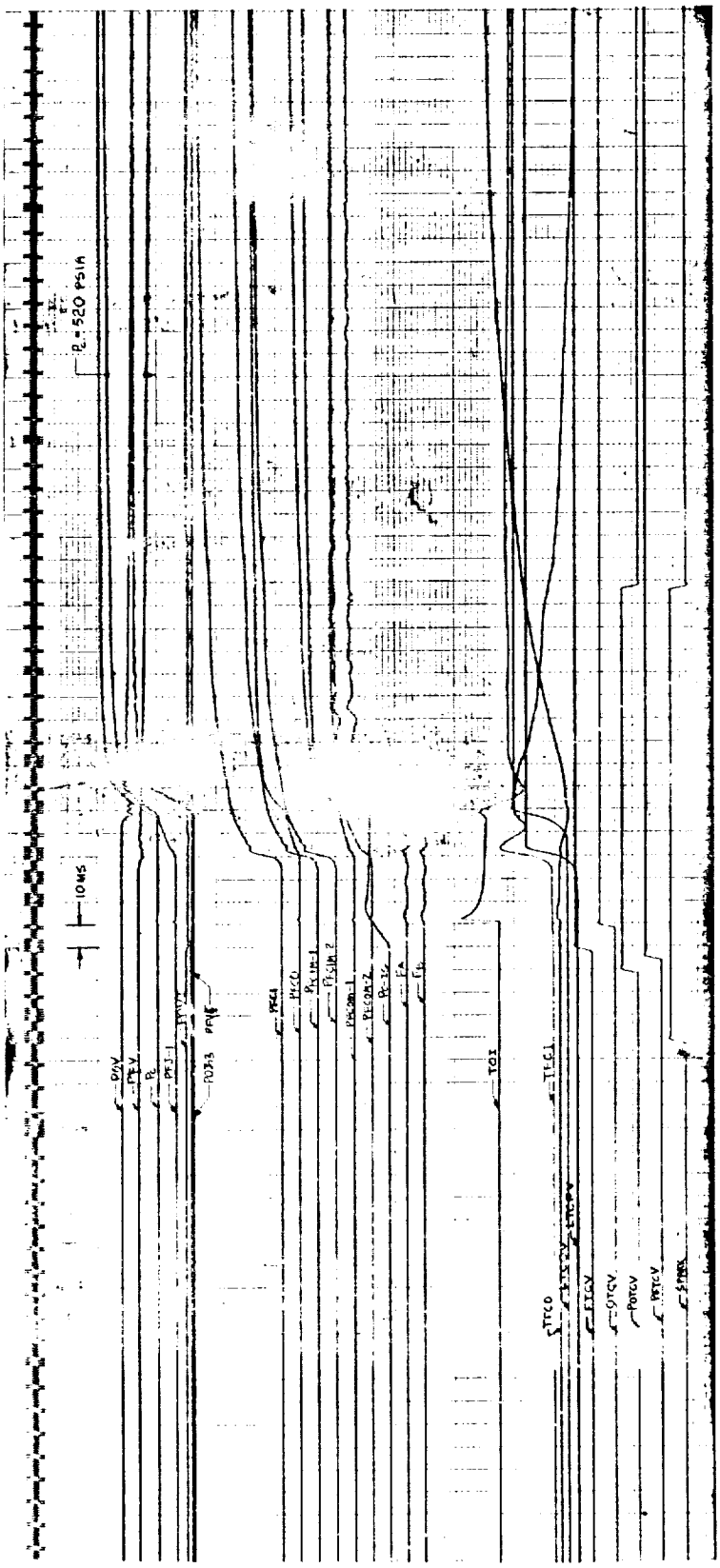

Figure 66. Oscillograph Record of Test 5K-3-102

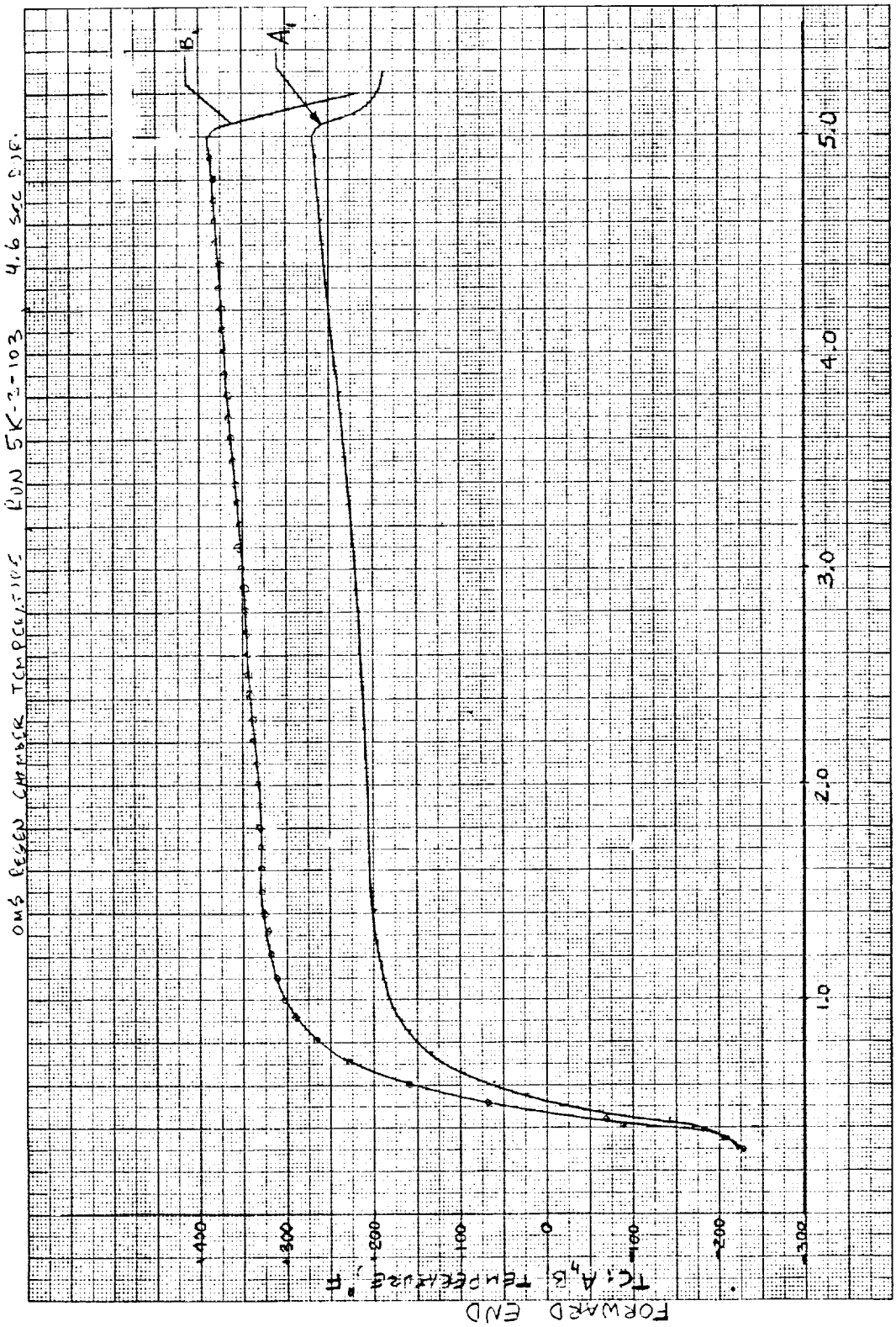

Figure 67. Test 5K-3-103 Chamber Wall Temperature vs Time (Forward Section)

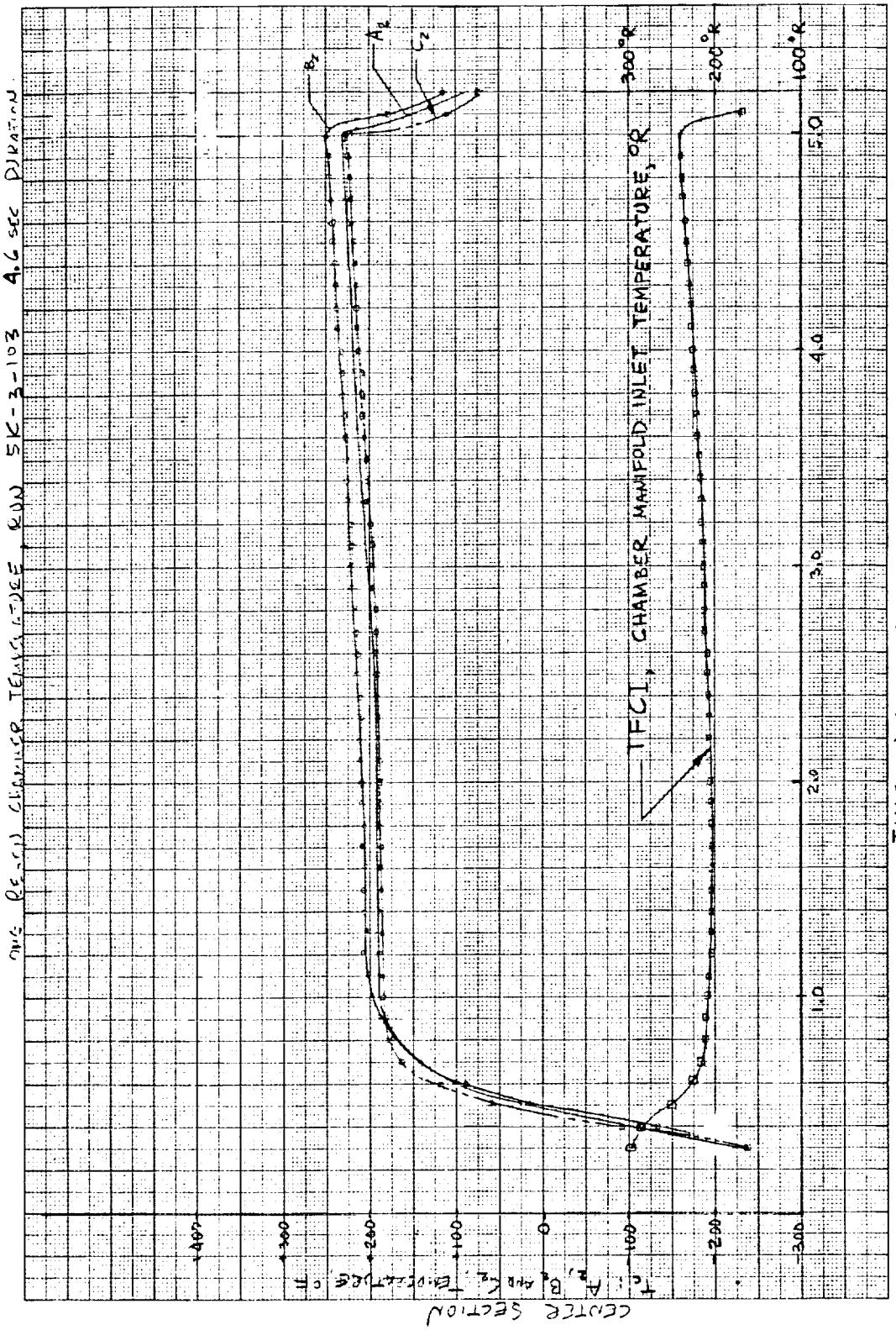

Figure 68. Test 5K-3-103 Chamber Wall Temperature vs Time (Center Section

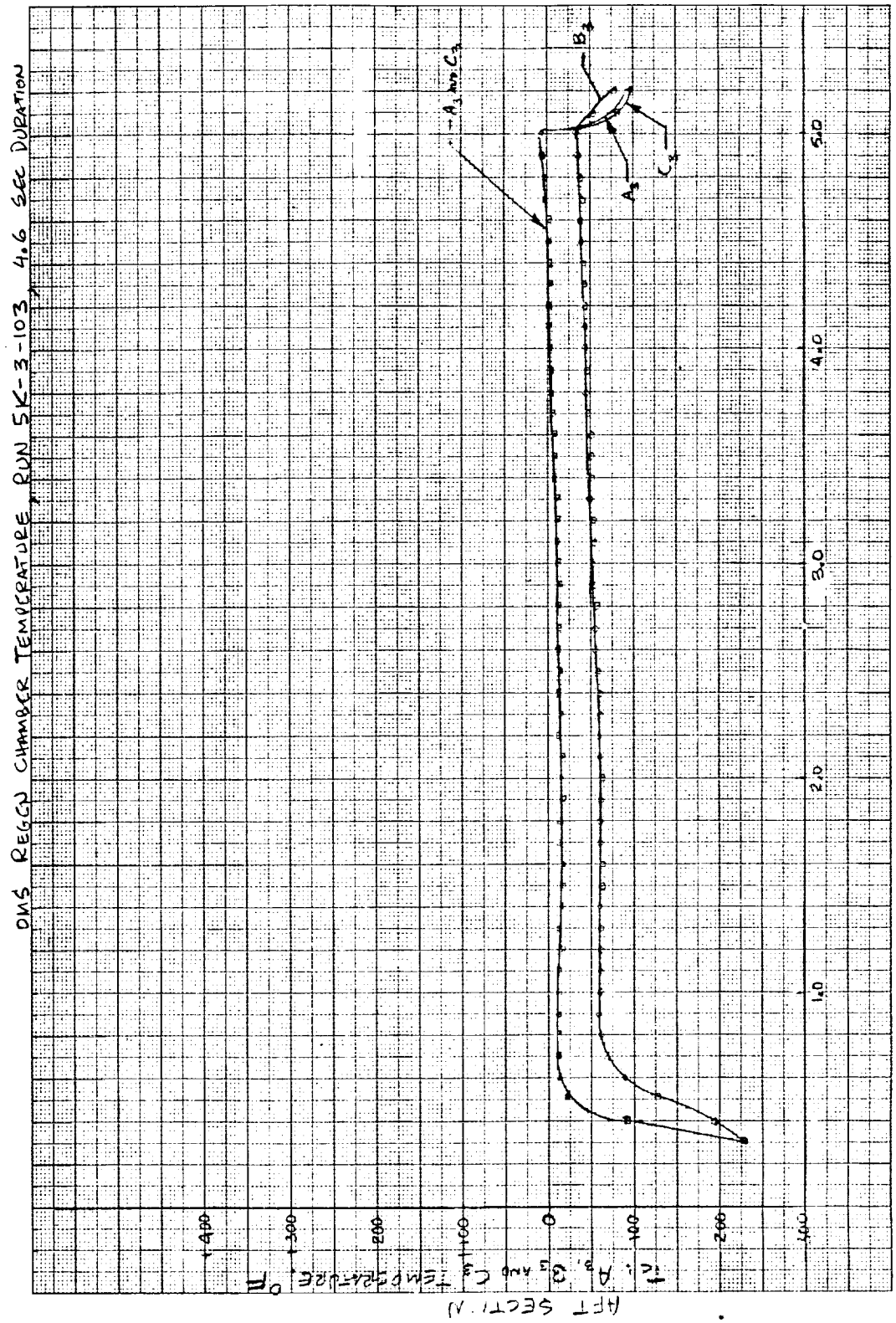

Figure 69. Test 5K-3-103 Chamber Wall Temperature vs Time (Aft Section)

Test Series	5K-3															
Run No.	101	102					103					104				
Data Summary Period, sec.	0.7-0.8	0.7-0.8	1.7-1.8	2.7-2.9	3.7-3.9	4.7-4.9	0.7-0.8	1.7-1.8	2.7-2.9	3.7-3.9	4.7-4.9	0.7-0.8	1.7-1.8	2.7-2.9	3.7-3.9	4.7-4.9
P_c, psia	528	515	518	521	522	518	512	508	502	495	485	515	512	510	500	488
$\dot{W}_o$, lbm/sec	9.362	9.469	9.330	9.288	9.241	9.135	9.463	9.301	9.248	9.178	9.055	9.492	9.279	9.210	9.041	8.834
$\dot{W}_f$, lbm/sec	1.830	1.691	1.745	1.796	1.826	1.837	1.651	1.651	1.623	1.582	1.535	1.682	1.724	1.730	1.701	1.647
$\dot{W}_{fI}$, lbm/sec	.0124	.0126	.0127	.0127	.0127	.0128	.0125	.0125	.0126	.0126	.0126	.0123	.0124	.0125	.0125	.0125
$\dot{W}_T$, lbm/sec	11.204	11.173	11.088	11.097	11.080	10.985	11.126	10.964	10.884	10.773	10.603	11.186	11.015	10.952	10.754	10.493
O/F	5.08	5.56	5.31	5.13	5.02	4.94	5.69	5.59	5.65	5.76	5.85	5.60	5.34	5.29	5.28	5.32
F_{SL}, lb_f	3502.0	3433.7	3452.4	3467.5	3466.3	3432.4	3400.5	3377.5	3344.9	3294.6	3226.5	3431.8	3404.1	3383.1	3316.6	3217.8
$P_a A_e$, lb_f	558.4	556.1					555.3					555.0				
F_{vac}, lb_f	4060.4	3989.8	4008.5	4023.6	4022.4	3988.5	3955.8	3932.8	3900.2	3849.9	3781.8	3986.8	3959.1	3938.1	3871.6	3772.8
$I_{sp, vac, del}$, sec.	362.4	357.1	361.5	362.6	363.0	363.1	355.5	358.7	358.3	357.4	356.7	356.4	359.4	359.6	360.0	359.5
$I_{sp, ODE}$, sec.	418.3	414.8	416.7	417.8	418.4	419.0	413.5	414.4	413.9	413.1	412.2	414.2	416.4	416.8	417.0	416.7
% I_{sp} (ϵ = 7.38)	86.64	86.09	86.75	86.79	86.76	86.66	85.97	86.56	86.57	86.52	86.54	86.05	86.31	86.28	86.33	86.27
$P_c g A_T/\dot{W}_T$, fps	7798	7633	7742	7780	7803	7807	7619	7669	7646	7612	7579	7631	7702	7706	7706	7696
C^*_{ODE}, fps	7850	7739	7796	7835	7860	7880	7705	7729	7716	7694	7674	7725	7787	7802	7808	7801
% C*	99.34	98.63	99.31	99.30	99.27	99.07	98.88	99.22	99.09	98.93	98.76	98.78	98.91	98.77	98.69	98.65
ΔCDL, sec.	49.2	48.3	49.0	49.1	49.2	49.2	48.1	48.5	48.4	48.3	48.2	48.2	48.7	48.7	48.7	48.7
ΔBLL, sec.	2.0	1.7	1.5	1.6	1.6	1.7	1.6	1.4	1.4	1.3	1.3	1.7	1.5	1.5	1.5	1.5
Δ KL, sec.	1.7	1.9	1.8	1.8	1.7	1.7	2.0	2.0	2.0	2.0	2.1	1.9	1.9	1.9	1.9	1.9
Δ MRMDL, sec.																
(Manifold)	0.3	0.4	0.3	0.3	0.3	0.3	0.4	0.4	0.5	0.5	0.5	0.4	0.3	0.3	0.3	0.3
(Igniter Fuel)	0.1	0.2	0.2	0.1	0.1	0.1	0.2	0.2	0.2	0.2	0.3	0.2	0.2	0.2	0.2	0.2
Δ ERL, sec.	2.6	5.2	2.4	2.3	2.5	2.9	5.7	3.2	3.2	3.4	3.1	5.6	4.4	4.6	4.4	4.6
% ERE (ϵ = 7.38)	99.38	98.75	99.42	99.45	99.40	99.31	98.62	99.23	99.23	99.18	99.25	98.65	98.94	98.90	98.94	98.90

Figure 70. OMS Cooled Chamber Performance Summary

Test Series		5K-3															
Run No.		101	102					103					104				
Data Summary Period		.7-.8	.7-.8	1.7-1.8	2.7-2.9	3.7-3.9	4.7-4.9	.7-.8	1.7-1.8	2.7-2.9	3.7-3.9	4.7-4.9	.7-.8	1.7-1.8	2.7-2.9	3.7-3.9	4.7-4.9
P_{OV}	psia	1302	1325	1311	1303	1297	1280	1324	1306	1299	1288	1270	1331	1306	1292	1270	1241
T_{OV}	°R	510	515	518	517	516	516	515	518	517	517	516	517	520	517	518	518
P_{fV}	psia	1345	1325	1295	1298	1303	1316	1302	1293	1311	1329	1346	1301	1286	1302	1320	1336
T_{fV}	°R	179	197	182	175	172	173	199	197	206	220	236	194	183	186	194	208
P_{fVI}	psia	917	937	942	946	950	955	935	939	944	948	951	925	929	934	938	942
T_{fVI}	°R	512	516	517	518	519	521	525	526	527	528	529	524	525	526	527	529
P_{fCI}	psia	1160	1115	1127	1138	1145	1145	1086	1091	1084	1072	1059	1101	1110	1110	1100	1082
P_{fCIM-1}		1157	1112	1125	1136	1142	1143	1084	1087	1080	1068	1055	1098	1107	1107	1096	1077
P_{fCIM-2}		N/A	1108	1121	1133	1139	1140	1077	1085	1078	1066	1053	1099	1106	1106	1096	1078
P_{fCOM-2}		765	734	755	763	766	763	721	732	726	717	704	731	744	744	734	717
P_{fCOM-1}		679	657	672	680	683	681	647	653	649	639	628	654	663	662	653	637
P_{fCO}		667	645	660	666	670	666	636	640	635	626	614	643	650	649	638	623
P_{fJ-2}		648	627	641	647	651	648	619	623	618	609	599	626	632	631	621	607
P_{fJ-1}		639	619	632	639	641	639	611	615	611	602	591	618	624	623	614	599
$T_{f\ CI}$	°R	196	221	193	183	178	178	215	204	211	223	238	212	196	195	202	213
$T_{f\ CO}$	°R	465	504	494	481	472	468	487	511	520	536	554	491	498	495	502	515
POI	psia	585	576	576	578	579	574	571	565	560	552	542	575	570	565	555	540
P_{OJ-3}		556	545	545	547	549	545	539	534	529	521	511	543	539	536	526	513
TOI	°R	N.G.	493	494	493	493	493	494	495	N.G.	N.G.	N.G.	494	496	496	496	495
Pø - IG	psia	537	524	529	533	534	531	520	518	513	506	496	524	523	521	512	499
TC-A1	°F	123	154	190	174	163	157	130	207	218	239	263	145	193	195	200	215
TC-A2		152	180	181	165	159	157	155	192	200	217	229	187	182	181	182	193
TC-A3		-24	+2	-25	-33	-40	-41	-11	-16	-11	-5	+4	-9	-21	-26	-24	-17
TC-B1		230	267	318	302	288	286	247	330	348	368	384	254	311	313	321	333
TC-B2		140	178	196	183	177	175	158	207	217	231	245	166	194	197	203	213
TC-B3		-82	-52	-74	-83	-88	-89	-65	-62	-55	-47	-38	-61	-72	-70	-64	-60
TC-C2		146	185	173	163	152	137	171	188	193	208	223	179	179	174	178	183
TC-C3		-28	-7	-33	-43	-51	-62	-10	-16	-12	-5	+3	-10	-24	-28	-25	-20

Figure 71. OMS Cooled Chamber Data Summary

RUN NO.	TEST DATE	DURATION SEC	P_c PSIA	MR O/F	I_s ε = 240 SEC	ERE %	T_{OI} °R	T_{FCI} °R	ΔT_F °R	ΔP PSI	BTU/SEC
101	3-9-71	0.490	528	5.08	458	99.4	-	196	269	-	1930
102	3-9-71	4.67	521	5.13	458	99.5	493	183	298	370	2060
103	3-9-71	4.67	502	5.65	456	99.2	495	211	309	352	1860
104	3-9-71	4.67	510	5.29	457	98.9	496	195	300	362	1800

Figure 72. Summary of Tests with Regeneratively Cooled Combustion Chamber

APPENDIX A

OMS INJECTOR DEVELOPMENT TEST PROCEDURE

1.0 SCOPE

1.1 This document establishes the procedures for testing the OMS Injector Assembly, Aerojet-General Corporation Drawing 1159210-2. The tests of this document comply with the requirements of Contract NAS 9-8285.

2.0 APPLICABLE DOCUMENTS

Specifications:

AFP1D 9135-7 29 September 1967	Pressurizing Agent Gaseous Nitrogen, Space Vehicle Grade
AFP1D 9135-8 4 November 1966	Liquid Oxygen, Space Vehicle Grade
MFSC 356A 27 January 1965	Hydrogen, Liquid

Drawings:

1159201	Nozzle, Heat Sink
1159196	Chamber, Non-Cooled
1159210	Injector Assembly
1159566	Igniter-Injector Assy., OMS

3.0 REQUIREMENTS

3.1 Monitoring of Tests. - Requirements of this procedure shall be monitored by the established quality control procedures to the extent specified within the contract, i.e., there shall be no quality control effort which is directly chargeable to the contract.

3.2 Data. - Test data shall be recorded as necessary for establishing and maintaining a history of the injector. Check lists shall be prepared to

include all operational steps under the procedures of this document. The completion of each step shall be verified by the test technician and/or the test engineer.

3.2.1 Proof Pressure Test. - The following data shall be recorded:

a. Proof Pressure
b. Duration of Test
c. Any Anomaly

3.2.2 External and Internal Leak Tests. - The following data shall be recorded.

a. Leak Test Pressure
b. Location and Description of Leakage

3.2.3 Rigimesh Flow Rate. - The following data shall be recorded:

a. H_2 Flow Rate
b. Inlet H_2 Pressure
c. Inlet H_2 Temperature

3.2.4 Firing Test. - The following data shall be recorded:

3.2.4.1 Motion Pictures - Motion pictures shall be taken at 400 FPS of the thrust chamber assembly (one view).

3.2.4.2 Still Photography. - Still photography shall consist of the following:

a. Close-ups of the injector, thrust chamber, igniter assembly, and TCA installation prior to test.

b. Close-ups of any chamber of injector damage.

c. Any view required by cognizant test engineer.

3.2.4.3 Original Data. - For each firing test, a single recording shall be made for barometric pressure and a single recording shall be made for free air temperature. The following parameters shall be continuously recorded.

a. Thrust
b. Fuel Flow Rate
c. Oxidizer Flow Rate
d. Chamber Pressure
e. Fuel Inlet Temperature
f. Oxidizer Inlet Temperature
g. Fuel Manifold Pressures
h. Oxidizer Manifold Pressures
i. Thrust Chamber Temperatures
j. Igniter Fuel Flow Rate
k. Igniter Oxidizer Flow Rate
l. Chamber Pressure-Igniter

3.2.4.4 Reduced and Derived Data. - For each run the following reduced and derived data shall be presented for the period FS_2 - 0.10 seconds to FS_2.

a. Thrust, F: Average Measured Thrust of FA and FB, lb.
b. Fuel Flow Rate, $\dot{W}_F$: Actual Measured, lb/sec
c. Oxidizer Flow Rate, $\dot{W}_O$: Actual Measured, lb/sec
d. Igniter Fuel Flow Rate, $\dot{W}_{FI}$: Actual Measured, lb/sec
e. Igniter Oxidizer Flow Rate, $\dot{W}_{OI}$: Actual Measured, lb/sec
f. Mixture Ratio, MR: Calculated MR = $\dot{W}_O/\dot{W}_F$
g. Igniter Mixture Ratio, MR_I: Calculated MR = $\dot{W}_{OI}/\dot{W}_{FI}$

h. TCA Mixture Ratio, MR_{TCA}: Calculated $MR_{TCA} = \frac{\dot{W}_O + \dot{W}_{OI}}{\dot{W}_F + \dot{W}_{FI}}$

i. Chamber Pressure, P_C: Average Measured Pressure of:

(1) Pc1 and Pc2 for Chamber Configuration A

(2) Pc3 and Pc4 for Chamber Configuration B

(3) Pc5 and Pc6 for Chamber Configuration C

j. Injector Face Characteristic Exhaust Velocity, c*: ft/sec

$$c^* = \frac{P_C A_T G}{\dot{W}_T}$$

where:

$\dot{W}_T$ = Total Propellant Flow Rate, lb/sec,

$(\dot{W}_O + \dot{W}_{OI} + \dot{W}_F + \dot{W}_{FI})$

P_C = Chamber Pressure from (i) above

A_T = Chamber Throat Area - $in.^2$ determined before test

G = 32.174 ft/sec^2

k. Measured Specific Impulse

$$I_{sp} \text{ Measured} = \frac{F_{AVE}}{\dot{W}_T}$$

l. Chamber Exit Area, A_E determined prior to test.

m. Pulse Charge Size and Ignition Time if applicable.

3.2.4.5 Mechanical Data. -

3.2.4.5.1 Thrust Chamber Data. - The chamber throat area and exit area shall be determined and recorded prior to the first firing and

at intervals comprising 4 or 5 tests. The chamber shall be at ambient temperature and a minimum of eight (8) micrometer readings shall be taken of the respective diameters.

3.3 Facilities and Equipment

3.3.1 All Tests. - After completion of fabrication, the use of Freon only is permitted for cleaning or flushing of injector internal passages.

3.3.2 Proof Pressure Test. - The following facilities shall be required:

a. The injector proof pressure test shall be conducted in conjunction with the proof test of the hot fire TCA installation. A suitable back pressure pot or plate shall be provided.

3.3.3 External Leak Test. - The following facilities shall be required:

a. The injector external leak test shall be conducted immediately following the proof test and in conjunction with the leak test of the hot fire installation. A suitable leak solution detection technique shall be employed. No visible external leakage is allowed.

3.3.4 Interchannel Leak Test. - The following facilities shall be required:

a. The interchannel leak test shall be conducted during the fabrication sequence immediately following the brazing of the 74 co-axial elements to the injector body. The following equipment is required:

(1) A filtered gaseous N_2 pressurization system.
(2) A suitable injector face pressure pot.
(3) Visual pressure gages as required.
(4) Seventy-four (74) suitable plugs for sealing the oxidizer tubes of the co-axial elements on the injector face side.

3.3.5 Rigimesh Flow Rate Test. - The following facilities shall be required:

a. The rigimesh flow rate test shall be conducted utilizing a sample from the rigimesh sheet stock utilized for injector fabrication. The following equipment is required:

(1) A filtered gaseous H_2 pressurization system
(2) A suitable rigimesh fixture
(3) Pressure monitoring system
(4) Flow rate measuring system
(5) Valves and tubing as required

3.3.6 Backflush. - The following facilities shall be required:

a. A filtered gaseous N_2 pressurization system
b. A suitable injector face pressure pot
c. Visual gages as required

3.3.7 Firing Test. - Facilities for the hot firing tests shall consist of an open reinforced concrete test stand, necessary control and safety systems and provisions to supply pressurized propellants to the injector.

3.3.7.1 Igniter Valves. - A solenoid operated igniter valve shall be used in each igniter propellant system and shall be located immediately upstream and as close to the injector as practical to minimize fill volumes. Igniter sequence shall be as follows:

a. Ignition spark shall be initiated simultaneous with the electrical signal to the igniter propellant valves. Igniter valve opening shall be simultaneous with a fuel valve lead of 5 M.S. permissible. Total opening and closing times shall not exceed 30 M.S. maximum. Ignition spark shall be terminated 60 $\pm$ 10 M.S. after spark initiation.

3.3.7.2 Workhorse Main Propellant Valves. - Workhorse propellant valves shall be used in each propellant line and shall be located

immediately upstream and as close to the injector as practical to minimize fill volumes. Main propellant valve sequence shall be as follows:

a. Main valve opening shall be simultaneous with a fuel valve lead of 20 M.S. permissible. Valve opening shall be initiated 20 $\pm$ 10 M.S. after initiation of igniter spark. Valve opening time shall be 150 $\pm$ 30 M.S.

b. Main valve closing shall be simultaneous $\pm$ 20 M.S. and the closing time of each valve shall be within 20 M.S. of each other. Closing time shall be 100 $\pm$ 40 M.S. Signal for main propellant valve closure shall be initiated 80 $\pm$ 10 M.S. prior to signal of igniter valve closure.

3.3.7.3 Test Support Equipment. - The following components and equipment shall be required:

a. TCA and system leak test fixture

b. Tubing, fittings, bolts, nuts, washers, and miscellaneous items required for TCA buildup.

3.3.7.4 Propellants and Pressurants

3.3.7.4.1 Oxidizer. - The oxidizer used for test firings shall be oxygen (O_2), conforming with specification AFP1D 9135-8, dated 4 November 1966.

3.3.7.4.2 Fuel. - The fuel used for test firings shall be hydrogen (H_2), conforming with Specification MFSC 356A, dated 27 January 1965.

3.3.7.4.3 Propellant Pressurant. - The propellant feed system shall be self pressurized, i.e., the oxidizer and fuel shall serve as their respective pressurants.

3.4 **Instrumentation. -**

3.4.1 Non-Firing Tests. - Parameters to be measured and instruments to be used for each measurement shall be in accordance with Table IA.

3.4.2 Firing Tests. - Parameters to be measured and the instruments to be used for each measurement shall be as specified by Table IB. The schematic location of each measurement shall be as shown in Figure 1 or 2.

3.4.3 Instrumentation Calibration. - The calibration of equipment and instruments specified herein shall meet the requirements of specification MIL-C-45662. The appropriate plant measurements standards instruction manual shall establish the detail requirements and calibration intervals in accordance with Specification MIL-C-45662.

3.5 Test Conditions. -

3.5.1 Non-Firing Tests. - Proof pressure, external leak, interchannel leak, backflush and rigimesh flow rate tests shall be conducted at ambient temperature and pressure.

3.5.2 Firing Test

3.5.2.1 Atmospheric Conditions. - The firing tests shall be conducted at ambient temperature and pressure.

3.5.2.2 Propellant Inlet Temperatures. - The fuel and oxidizer inlet temperatures for each test shall be as specified in Test Plan OMS-100.

3.5.2.3 Shutdown Criteria

3.5.2.3.1 Combustion Stability Monitor (CSM). - A combustion stability monitor shall be installed to monitor combustion chamber (P_C) output. The test shall be terminated automatically by the CSM unit if the amplitude at frequencies above 1000 CPS exceeds 50 psi peak-to-peak for 40 $\pm$ 10 M.S.

3.5.2.3.2 Combustion Chamber Throat Temperature. - The test shall be terminated if combustion chamber throat temperature exceeds 1200°F.

4.0 PROCEDURES

4.1 General

4.1.1 Order of Performance. - Unless otherwise specified, the following tests shall be performed in the order listed. In addition, the steps in each firing test buildup or firing test phase may be varied to best meet the total firing test or setup requirements.

4.1.2 Prevention of Contamination. - All ports and the injector face shall be covered during all processing with appropriate closures or fittings except when removal is required for testing.

4.2 Interchannel Leak Test. - The interchannel leak test shall be performed as follows, immediately following the brazing of the co-axial elements to the injector body.

a. Plug the oxidizer tube of each of the 74 co-axial elements on the face side of the injector. See 3.3.4 - Facilities.

b. Install injector face plate and cap off fuel manifold inlet and fittings.

c. Connect face plate inlet fitting to GN_2 source and submerge injector in Freon backside up.

d. Pressurize to 50 ± 10 psig and observe for leakage around each element at backside interface. Document leakage location if applicable. No interchannel leakage allowed.

e. Gas purge injector dry after test completion.

4.3 Proof Pressure Test. - The proof pressure test shall be conducted as follows:

a. Install injector and thrust chamber in test stand with all instrumentation attachments in functional condition.

b. Install suitable chamber exit pressure plate or pot.

c. Proof pressure test TCA assembly and test installation downstream of main propellant valves. Maintain proof test pressure of 900 ± 25 psi for a minimum of five minutes using gaseous O_2 as the pressurant.

4.4 External Leak Test. - The leak pressure test shall be conducted immediately following the above proof pressure test as follows:

a. Establish leak test pressure of 400 ± 25 psi.

b. Leak test all fittings and joints utilizing Leak Tec method. No leakage allowed upstream of exit pressure plate and main propellant valves. No leakage allowed.

4.5 Backflush. - Backflush shall be conducted after completion of fabrication and prior to fire test as follows:

a. Install suitable face plate or pressure pot to injector face.

b. With all injector inlet fittings open (including instrumentation bosses) backflush using gaseous N_2 for a minimum of five minutes with a face pressure of 50 $\pm$ 10 psig.

4.6 Rigimesh Flow Rate Test. - The rigimesh flow rate test shall be conducted utilizing a sample contained in a suitable fixture as follows:

a. Install fixture containing rigimesh in flow system capable of monitoring H_2 flow rate and maintaining designated upstream and downstream pressures.

b. Measure H_2 flow rate at ambient temperature (record H_2 temperature) at the following pressure conditions:

Pressure Upstream of Rigimesh = 565 $\pm$ 5 psig
Pressure Downstream of Rigimesh = 485 $\pm$ 5 psig

4.7 Firing Test

4.7.1 Buildup. - Assembly of the injector and heat sink combustion chamber shall be accomplished utilizing the appropriate attaching hardware and seals according to the configuration specified in Test Plan IOS-100. The chamber configurations to be tested, A, B, and C, are shown in Figures 1 and 2 and are described as follows:

Designation	Configuration	$*A_T$, in.^{2}	L', in.
A	P/N 1159201-1	5.70	4.0
B	P/N 1159201-1 with P/N 1159196-1 L' Section	5.70	6.0
C	P/N 1159201-1 with P/N 1159196-2 L' Section	5.70	8.0

4.7.2 Prefire Leak Check. - A prefire leak check shall be conducted after each chamber buildup and/or as deemed necessary by the test conductor according to Paragraph 4.4 of this procedure.

4.7.3 Hardware Temperature Conditioning. - For all tests using temperature conditioned propellants, the test hardware shall be temperature conditioned by alternately flowing the conditioned oxidizer and fuel through the injector. A thermocouple shall be installed on each of the propellant inlet lines approximately 4 inches upstream of the injector to monitor hardware temperature. The temperature indicated at these locations immediately prior to test, shall be within 10°F of the propellant run temperature specified in Test Plan OMS-100.

4.7.4 Test Firings. - The test firings shall be conducted at the conditions specified in Test Plan OMS-100.

4.7.4.1 Pulse Tests. - Tests requiring pulses or bombs are designated in Test Plan OMS-100. For each pulse test, a 6.5 grain pulse charge shall be installed in the thrust chamber pulse port, see Figures 1 and 2. A dummy pulse shall be installed in this port for all tests not requiring pulses. A suitable pulse ignition system shall be provided with appropriate timing device.

*Design throat area, actual to be determined by measurement.

TABLE IA

INSTRUMENTATION

Parameter	Symbol	Instrument (or Equivalent)	Suggested System Range	CPS Frequency Response	Total Measurement Accuracy (1σ)
Chamber Pressure	P_C-1 thru -6	Taber	0-1000 psi	0-600	±0.14%
Chamber Pressure	P_C-P-1 thru -6	Photocon	0-1000 psi	0-10,000	±5.0%
Fuel Manifold Pressure	P_{FJ}-1 and -2	Taber	0-1000 psi	0-600	±1.0%
Oxidizer Manifold Pressure	P_{OJ}-1 thru -3	Taber	0-1000 psi	0-600	± 1.0%
Ambient Atmospheric Pressure	PA	Recording Barometer	28-31 in.Hg	--	±0.2%
Oxidizer Venturi Pressure	POV	Taber	0-1500 psi	0-600	±0.14%
Fuel Venturi Pressure	PFV	Taber	0-1500 psi	0-600	±0.14%
Oxidizer Venturi Temp.	TOV	CA Thermocouple	200-600°R	--	±5°F
Fuel Venturi Temp.	TFV	CA Thermocouple	200-600°R	--	±5°F
Oxidizer Flow Rate	$\dot{W}_O$	Venturi	--	--	±0.5%
Fuel Flow Rate	$\dot{W}_F$	Venturi	--	--	±0.5%
Oxidizer Temperature at Injector Inlet	TOI	CA Thermocouple	200-600°R	--	±5°F
Oxidizer Pressure at Injector Inlet	POI	Taber	0-1000 psi	0-600	±1.0%
Fuel Temperature at Injector Inlet	TFI	CA Thermocouple	200-600°R	--	±5°F
Fuel Pressure at Injector Inlet	PFI	Taber	0-1000 psi	0-600	±1.0%
Chamber Temperature	T_C-1 thru -16	CA Thermocouple	0-2000°F	--	±5°F
Stability Monitor	CSM	Switch Trace	--	--	--
Fire Switch	FS	Switch Trace	--	--	--
Oxidizer Valve Trace	LTCOV	Pot Trace	--	60	±1%

TABLE IA (cont.)

Parameter	Symbol	Instrument (or Equivalent)	Suggested System Range	CPS Frequency Response	Total Measurement Accuracy(1σ)
Fuel Valve Trace	LTCFV	Pot Trace	--	60	±1%
Oxidizer TCV Pilot Valve Trace	TCOVPV	Switch Trace	--	60	--
Fuel TCV Pilot Valve Trace	TCFVPV	Switch Trace	--	60	--
Oxidizer Igniter Valve Trace	TIOPV	Switch Trace	--	60	--
Fuel Igniter Valve Trace	TIFPV	Switch Trace	--	60	--
Thrust	FA	Baldwin	0-5K	0-600	±0.15%
	FB	Baldwin	0-5K	0-600	±0.15%
Chamber Pressure Igniter	P_C-I_G	Taber	0-1000 psi	0-600	±1.0%
Oxidizer Venturi Pressure Igniter	POVI	Taber	0-1500 psi	0-600	±0.14%
Fuel Venturi Pressure Igniter	PFVI	Taber	0-1500 psi	0-600	±0.14%
Oxidizer Venturi Temperature Igniter	TOVI	CA Thermocouple	200-600°R	--	±5°F
Fuel Venturi Temperature Igniter	TFVI	CA Thermocouple	200-600°R	--	±5°F

TABLE IB

INSTRUMENTATION

Parameter	Symbol	Strip Chart	ADC (Digital)	OSC	Tape
Chamber Pressure	P_C-1 thru -6	X	Rapid Sample	X	X
Chamber Pressure	P_C-P-1 thru -6				
Fuel Manifold Pressure	P_{Fj}-1 and -2		X	X	
Oxidizer Manifold Pressure	P_{Oj}-1 thru -3		X	X	
Oxidizer Venturi Pressure	POV		X		X
Fuel Venturi Pressure	PFV		X		X
Oxidizer Venturi Temperature	TOV		X	X	
Fuel Venturi Temperature	TFV		X	X	
Oxidizer Inlet Pressure	POI		X	X	
Oxidizer Inlet Temperature	TOI	X	X	X	
Fuel Inlet Pressure	PFI		X	X	
Fuel Inlet Temperature	TFI	X	X		
Chamber Temperatures	TC-1 thru -16		X	X	
Stability Monitor	CSM			X	X
Fire Switch	FS	X	X	X	X
Oxidizer Valve Trace	LTCOV			X	
Fuel Valve Trace	LTCFV			X	
Oxidizer TCV Pilot Valve Trace	TCOVPV			X	
Fuel TCV Pilot Valve Trace	TCFVPV			X	
Oxidizer Igniter Valve Trace	TIOPV			X	
Thrust	FA, FB	X	Rapid Sample	X	
Chamber Pressure (Igniter)	Pc-IG	X	X	X	X
Oxidizer Venturi Pressure (Igniter)	POVI		X	X	
Fuel Venturi Pressure (Igniter)	PFVI		X	X	
Oxidizer Venturi Temp. (Igniter)	TOVI		X	X	
Fuel Venturi Temp. (Igniter)	TFVI		X	X	

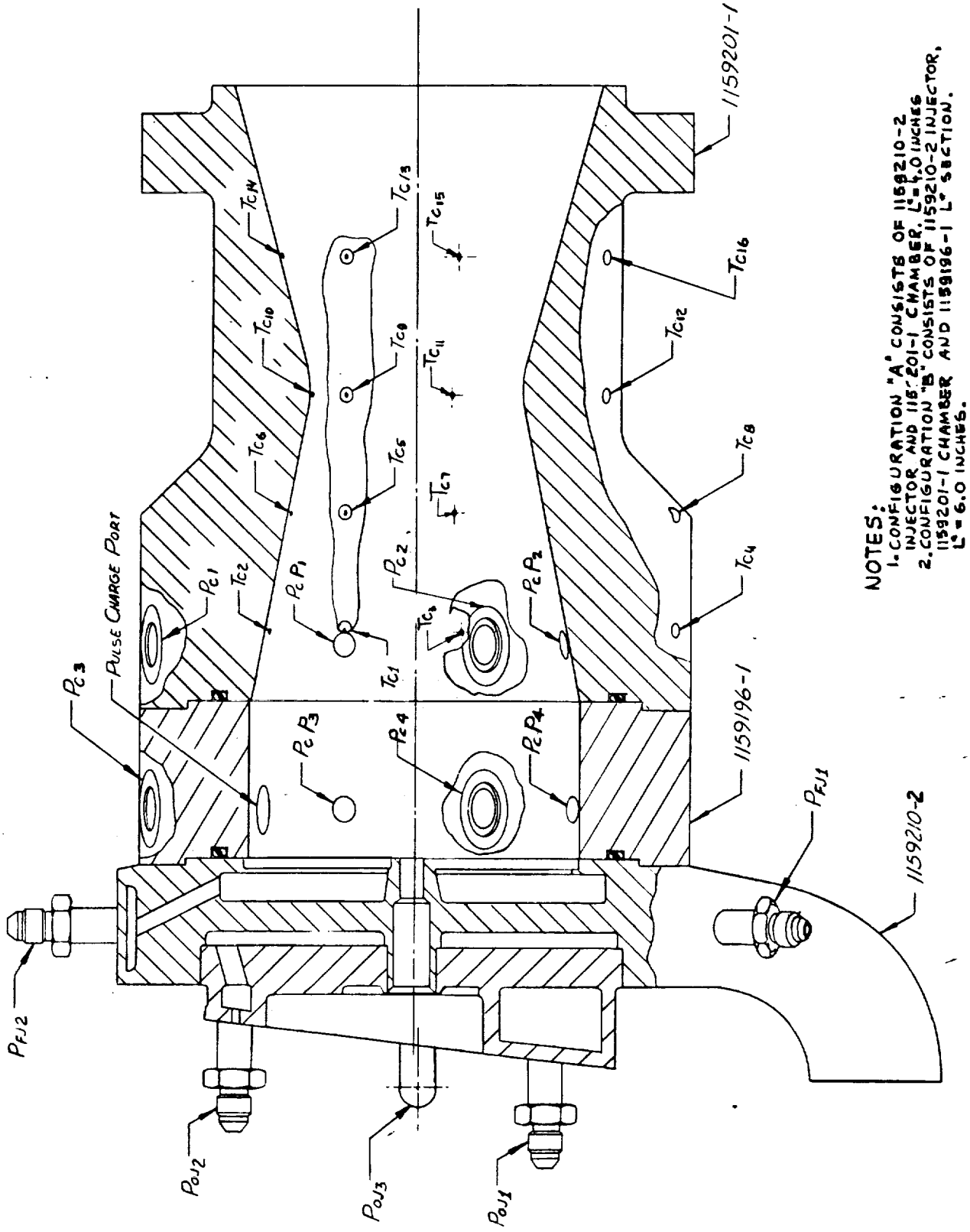

TCA Instrumentation Configurations A and B

Figure 1

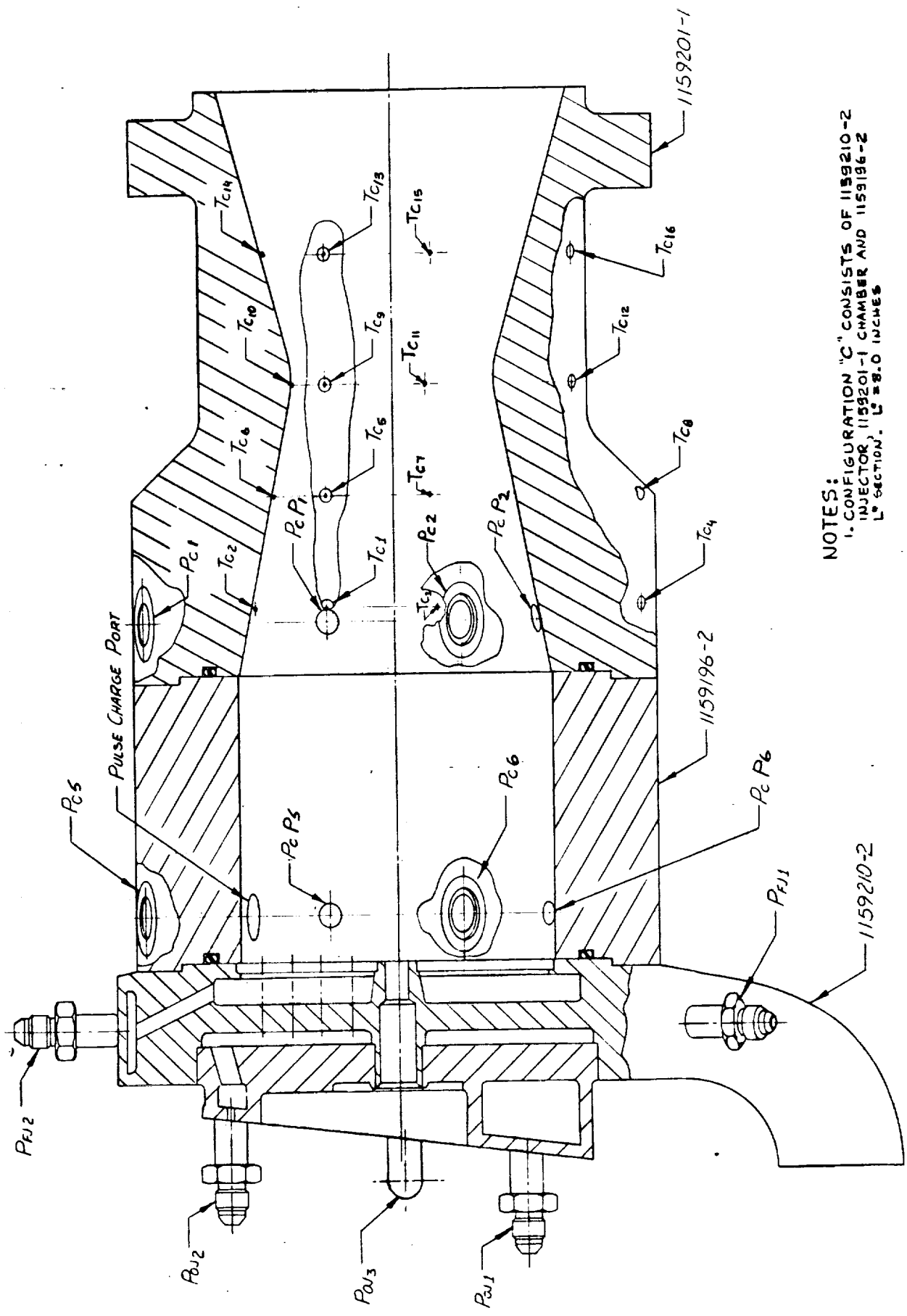

TCA Instrumentation Configuration C

Figure 2